SCHOOL OF
CIVIL ENGINEERING

INDIANA
DEPARTMENT OF HIGHWAYS

JOINT HIGHWAY RESEARCH PROJECT

JHRP-84-8

STABILIZATION OF SLOPES USING PILES

FINAL REPORT

S. Hassiotis and J. L. Chameau

PURDUE UNIVERSITY

JOINT HIGHWAY RESEARCH PROJECT

JHRP-84-8

STABILIZATION OF SLOPES USING PILES

FINAL REPORT

S. Hassiotis and J. L. Chameau

Interim Report

Stabilization of Slopes Using Piles

To: H.L. Michael, Director
Joint Highway Research Project

May 1, 1984

Project: 6-36-360

From: J.L. Chameau, Research Associate
Joint Highway Research Project

File: 6-14-15

Attached is an Interim Report on the HPR Part II study titled "Design of Laterally Loaded Drilled-In-Piers for Landslide Correction Anchored Within Sedimentary Rocks". The report is entitled "Stabilization of Slopes Using Piles". It is authored by S. Hassiotis and J.L. Chameau of our staff.

The report presents a methodology for the design of piles or piers used to improve the stability of a slope. A step-by-step procedure is proposed to select design parameters such as pile diameter, spacing, and location which will provide an appropriate factor of safety for the slope and insure the integrity of the piles. Two computer programs are provided to perform the necessary operations. The first computer program calculates the factor of safety of the reinforced slope; the second program determines shear force, bending moment, and displacement profiles along the pile. These programs can be used iteratively to achieve an optimum design solution.

The report is submitted as partial fulfillment of the objectives of the study.

Respectfully submitted,

J. L. Chameau

J.L. Chameau
Research Associate

cc:

A.G. Altschaeffl	W.H. Goetz	C.F. Scholer
J.M. Bell	G.K. Hallock	R.M. Shanteau
W.F. Chen	J.F. McLaughlin	K.C. Sinha
W.L. Dolch	R.D. Miles	C.A. Venable
R.L. Eskew	P.L. Owens	L.E. Wood
J.D. Fricker	B.K. Partridge	S.R. Yoder
G.D. Gibson	G.T. Satterly	

Interim Report

Stabilization of Slopes Using Piles

by

S. Hassiotis
and
J.L. Chameau

Joint Highway Research Project

Project No.: 6-36-360

File No.: 6-14-15

Prepared as Part of an Investigation

Conducted by

Joint Highway Research Project
Engineering Experiment Station

Purdue University
in cooperation with the

Indiana Department of Highways

and the

U.S. Department of Transportation
Federal Highway Administration

Purdue University
West Lafayette, Indiana
May 1, 1984

TECHNICAL REPORT STANDARD TITLE PAGE

1. Report No.	2. Government Accession No.	3. Recipient's Catalog No.
FHWA/IN/JHRP-84/8		

4. Title and Subtitle	5. Report Date
Stabilization of Slopes Using Piles	May 1, 1984
	6. Performing Organization Code

7. Author(s)	8. Performing Organization Report No.
S. Hassiotis and J. L. Chameau	JHRP-84-8

9. Performing Organization Name and Address	10. Work Unit No.
Joint Highway Research Project Civil Engineering Building Purdue University West Lafayette, IN 47907	11. Contract or Grant No. HPR-1(21) Part II
12. Sponsoring Agency Name and Address	13. Type of Report and Period Covered
Indiana Department of Highways State Office Building 100 North Senate Avenue Indianapolis, IN 46204	Interim Report
	14. Sponsoring Agency Code CA 359

15. Supplementary Notes

Conducted in cooperation with U.S. Department of Transportation, Federal Highway Administration under a research study entitled, "Design of Laterally Loaded Drilled-In-Piers for Landslide Correction Anchored Within Sedimentary Rocks"

16. Abstract

This study is part of a project undertaken at Purdue University to develop a methodology for the design and analysis of slopes stabilized with piles. Different aspects of this problem are considered: (1) the determination of the force exerted on the piles by the slope; (2) the effect of a row of piles on the stability of a slope; and (3) simultaneous slope stability analysis and pile design to meet minimum safety requirements for both the slope and the piles.

It is suggested to compute the force exerted by the piles on the slope by dividing the maximum value calculated using the theory of plastic deformation by the factor of safety of the slope. The Friction Circle Method is extended to incorporate the reaction force provided by the piles and calculate the safety factor of the reinforced slope. The displacement, bending moment, and shear force profiles along the piles are also determined. A step-by-step procedure is proposed to select the pile dimensions and reinforcement which will provide an appropriate factor of safety for the slope and insure the integrity of the piles.

These results are incorporated in two computer programs which can be used iteratively to provide an optimum design solution.

17. Key Words	18. Distribution Statement
Slope Stability, Pile, Pier , Factor of Safety, Stabilization, Reinforcement	No restrictions. This document is available to the public through the National Technical Information Service, Springfield, VA 22161

19. Security Classif. (of this report)	20. Security Classif. (of this page)	21. No. of Pages	22. Price
Unclassified	Unclassified	181	

Form DOT F 1700.7 (8-69)

ACKNOWLEDGEMENTS

The financial support for this research was provided by the Indiana Department of Highways and the Federal Highway Administration. The research was administered through the Joint Highway Research Project, Purdue University, West Lafayette, Indiana.

Special thanks are extended to Ms. Cathy Ralston for typing this report. The help and recommendations provided by Messrs. Mike Oakland and Frank Adams are greatly appreciated.

TABLE OF CONTENTS

LIST OF TABLES

LIST OF FIGURES

Appendix Figure

LIST OF ABBREVIATIONS AND SYMBOLS

A	——	dimensionless coefficient depending on the density of sand
$\overline{AB}$	——	chord length
AB	——	arc length
a_o, a_1, a_2, a_3	——	constants of integration
b	——	pile diameter
BC	——	boundary condition
BD	——	distance that the pile penetrates into the bedrock
c	——	cohesion intercept
c_a	——	available unit cohesion
CE	——	length of the pile from the ground surface to the critical surface
CEO	——	angle between F_p and the horizontal
c_r	——	unit cohesion required for equilibrium
C_r	——	resistance due to cohesion
C_1, C_2, C_3, C_4	——	constants of integration
D	——	distance in the direction of the pile row
D_1	——	center to center distance between the piles
D_2	——	clear distance between the piles

E_d —— modulus of elasticity as given by the pressuremeter

EB —— length of the pile between the critical surface and the bedrock

ED —— length of the pile below the critical surface

EI —— pile stiffness

E_R —— insitu modulus of elasticity of rock

E_S —— modulus of elasticity for sand

E_{t50} —— characteristic modulus of intact rock

f'_c —— concrete strength

F_c —— factor of safety with respect to cohesion

F_ϕ —— factor of safety with respect to friction

F_p —— unit reaction force provided to the slope by the piles

F_t —— total force exerted on the passive piles

FS —— safety factor of the slope

f_1, f_2 —— constants that define the pressure q

H —— slope height

i —— slope angle

K —— elastic constant

K_S —— coefficient of subgrade reaction of the first layer below the critical surface

K_R —— coefficient of subgrade reaction of the second layer below the critical surface

K_{SO} —— coefficient of subgrade reaction at the critical surface

K_{SL} —— coefficient of subgrade reaction at the end of the first layer

K_{RO} —— coefficient of subgrade reaction at the beginning of the second layer

K_{RL} —— coefficient of subgrade reaction at end of the second layer

K_{SL} —— coefficient of vertical subgrade reaction of a 1-ft plate

M —— bending moment on the pile

MT —— total number of equally spaced intervals

m_v —— modulus of volume decrease

n, n_1, n_2 —— empirical indexes equal to or greater than zero

OG —— moment arm of F_p

P —— resultant of normal frictional forces

p —— intensity of loading, proportional to deflection of the beam

q_1 —— force per unit length on the pile at the ground surface

q_2 —— force per unit length on the pile at the critical surface

q —— intensity of distributed load applied on the beam

R —— radius of the critical circle

S —— horizontal distance from the toe of the slope to the pile row

V —— shear force on the pile

V_c —— shear strength provided by the concrete

W —— weight of the critical mass

x,y —— angles that define the critical surface

y_m —— pile deflection at point m

y —— horizontal displacement of the pile at depth z

y_s —— horizontal displacement that the soil would undergo without the piles

y_1 —— pile deflection above the critical surface

y_2 —— pile deflection below the critical surface without the piles

$\bar{z}$ —— depth along the pile measured from the ground surface

z —— depth along the pile measured from the critical surface

α —— $\pi/4 + \phi/2$

γ —— unit weight of the soil

θ —— slope of the pile

λ —— length of the intervals in the discretized pile

μ_s —— Poisson's ratio

σ_a —— normal stress at the surface perpendicular to the x-axis

σ_n —— normal stress at the failure surface

σ_x —— normal stress at the surface inclined an angle α from the x-axis

ϕ —— angle of internal friction of the soil

ϕ_a —— available friction angle

ϕ_r —— friction angle required for equilibrium

HIGHLIGHT SUMMARY

Drilled piers or bored piles can be an efficient means to control slope movements where other corrective measures fail to insure stability or when their use is prohibited due to space limitations. A design methodology is proposed herein to assess both the forces acting on the piles (or piers) and the influence of the pile row on the stability of the slope. The forces acting on the pile sections above and below the critical surface are calculated using the theories of plastic deformation and subgrade reaction, respectively.

The theory of plastic deformation is based on the assumption that the soil surrounding the piles is in a state of plastic equilibrium. Under this assumption, the force acting on the passive piles is expressed as a function of the soil strength parameters and of the pile diameter, spacing and position. The actual reaction force exerted by the piles on the slope is assumed to be a fraction of the force corresponding to the plastic state condition. The Friction Circle Method of

slope stability analysis is extended to incorporate the reaction force and determine the critical surface and safety factor of the reinforced slope. A computer program is also developed to obtain the displacement, bending moment, and shear force profiles along the piles. A step-by-step procedure is proposed to achieve an optimum design solution which provides a required factor of safety for the slope and insures the integrity of the piles.

CHAPTER I. INTRODUCTION

Insuring the stability of both natural and man-made slopes continues to be an important problem in geotechnical engineering. Slides account for many civil engineering failures and often result in extensive property damage and sometimes loss of human life. There is no universally accepted method for the prevention and/or correction of landslides. Each slide is unique and should be considered on the basis of its own individual characteristics. Avoidance of a potential slide area can be a primary consideration when selecting a new site. Otherwise, corrective measures can be taken which include: (1) improving the slope geometry by changing the slope angle, excavating the soil at the head, or increasing the load at the toe; (2) constructing a compound slope; and (3) providing surface and subsurface drainage. However, where such corrective measures fail to insure stability or when their use is prohibited due to space limitations, retaining structures may be necessary. Piles carried across the active or potential failure surface can be used

efficiently as the retaining element, since they can often be installed without disturbing significantly the equilibrium of the slope.

The analysis of a slope/pile system requires that the soil pressure acting on the piles, and the subsequent reaction that the piles provide to the slope, be known. There are several techniques which are currently used to estimate the pressures that act on active or passive piles. They include the coefficient of subgrade reaction method, methods based on the assumption of elastic soils and other empirical methods. Most of these techniques either consider the solution of a single pile and introduce corrective factors to analyze the row of piles, or treat the row of piles as a retaining wall. The first approach can lead to inaccurate answers in case of passive piles, while the second approach provides very conservative answers. Moreover, very limited research has been done to determine the growth mechanism of the lateral force acting on a pile embedded in a slope and the increase in the factor of safety of the slope due to the presence of the piles. In addition, a design methodology is required to assist in selecting design parameters, such as pile diameter, spacing, and location that will insure the stability of both the slope and the pile.

In this report, the pressure acting on the piles is calculated using the theory of plastic deformation developed by Ito and Matsui (1975). The major assumption in this theory is that the soil in the area surrounding the piles is in a state of plastic equilibrium. With this assumption, the force acting on the piles can be expressed as a function of the soil strength, and the pile diameter, spacing and location. The safety factor of the slope after the placement of the piles is calculated assuming that a portion of that force is counteracting the driving forces of the slope. Finally, a step-by-step procedure is proposed to select design parameters, which will achieve the stability of the slope and adequate dimensioning of the piles.

The concepts and methods presented herein are incorporated in two computer programs, which should provide efficient design tools to practicing engineers. The first computer program calculates the safety factor of the reinforced slope as a function of pile diameter, location and spacing. The second program calculates the shear force, bending moment and displacement along the length of the pile as a function of the soil pressure, and the pile diameter, stiffness, location, spacing, and boundary conditions. These programs can be used iteratively to provide an optimum design solution.

CHAPTER II. SLOPE REINFORCEMENT

Soil reinforcement techniques such as reinforced earth, stone columns, soil anchors, and piles and piers can be used to stabilize slopes and highway embankments. When properly designed and constructed, reinforcing elements can be appropriate to solve stability problems, particularly where space is restricted, and they can provide cost-effective solutions to many transportation design and construction problems.

Piles, carried across an active or potential failure surface and aligned to form a cantilever wall, have been used in the past, although early uses of such walls have resulted in some failures (Baker and Marshall,1958; Root,1958; Broms,1969). Merriam (1960) described the unsuccessful attempt to stabilize the Portuguese Bend slide of the Palos Verdes peninsula in Los Angeles County, where an ancient slide mass had been reactivated by a new housing development in the area. Movements at the rate of 1.25 in. per day were observed. In order to stabilize the slide, 25 4-ft diameter concrete caissons were installed in separate

groups of 2 or 3. Initially the soil flowed around the caissons, but these were eventually broken by the mass movement. Since the original slide had remolded the soil to its residual strength, the small relative increase in shear strength provided by the caissons had an insignificant effect on the slope stability.

Since then, more effective walls have been constructed. Shallow slides, up to 20-ft deep, have been stabilized by the use of sheet piling (Toms and Bartlett, 1962) and closely spaced driven cantilever piles (Zaruba and Mencl,1967). A root pile wall was used to correct a landslide near Monessen, Pennsylvania (Dash and Jovino,1980). Stone columns have been used effectively in Europe (Goughnour and DiMaggio,1978). Drilled cantilever pier walls have been used successfully in the Ohio River Valley (Nethero,1982). Satisfactory results were achieved with 18-in. to 30-in. diameter piers spaced 5 to 7-ft on center. Actual installations of such piers include the use of cast-in-place concrete cylindrical columns in an effort to stop soil movements, which had been sufficient to cause closing of a roadway. In a different application, piers placed at the toe of a slope stopped a slide which had been triggered by an unbraced cut.

Deep-seated slides have also been stabilized successfully by large diameter cylinder piles, anchored

sheet pile walls, or rock anchored cylinder piles. Some of these cases will be discussed below.

Large diameter cast-in-place concrete cylinders were used for a sidehill stabilization during the construction of the Seattle freeway in Washington (Andrews and Klassel,1964). During excavation for the footing of a bridge structure, a large deep-seated slide started to develop, immediately adjacent to a seven-story apartment building. A retaining wall, which had been planned between the bridge footing excavation and the building, could not be built because further excavation for the wall would cause the slide to progress and endanger the building. To avoid this, cast-in-place cylinder piles were used to form the wall. To develop the resistance required to withstand the assumed loads, the design called for 4.75 ft cylinders on 6-ft centers. The cylinders were designed to penetrate the slip plane and other potential sliding planes. Welded steel beams were employed to reinforce the concrete cylinders.

A sheet pile wall anchored with pre-tensioned soil anchors helped to stabilize a potentially dangerous slope during construction in the Ohio River valley. According to D'Appolonia et al. (1967), the wall provided short term stability by preventing progressive failure, while drainage assured long-term atability.

Cylinder piles were used in an effort to stop movement during construction for the freeway on Potrero Hill in San Francisco (Nicoletti and Keith,1969). A rock bolted retaining wall was installed to restrain an unbraced cut. The top of a railroad tunnel was located 25-ft below the freeway and near the top of the wall. The overall stability of the tunnel, wall, and the slope rising above it, had been unbalanced by the cut. Towards the end of the construction, large lateral movements were observed in the tunnel. In order to stop the movements, a wall was constructed of a series of heavy steel piles, placed in drilled holes on each side of the tunnel, and connected by steel struts across the top of the tunnel. This technique proved to be efficient in preventing further movement.

A double row of anchored piles became necessary during railroad work in Belgium (DeBeer and Wallays,1970). In order to enlarge the railroad bed, an existing slope, nearly at its equilibrium, was cut back, maintaining the original angle. The excavations reactivated slips which had previously occurred in a crushed schist mass, and a series of retrogressive slips was initiated. Since the slope was located in a city, only limited flattening was possible.

Hence, the stability was insured by the resistance provided by 3.5 to 5-ft diameter piles spaced 6.5 to 10-ft on centers.

An anchored cylinder pile wall was installed during construction of interchanges to connect I-471 with local traffic arteries in Cincinnati, Ohio (Offenberger, 1981). Excavations on the southwest side of Mt. Adams triggered large ground movements in an area known to have experienced small movements in the past. Data from slope indicators showed that the earth movement was in a deep seated weak clay layer near the rock surface, and well below the elevation of retaining wall footings. A cantilever wall was determined to be inappropriate, because considerable embedment into the rock would be necessary. In addition, undesirable downslope displacement would be needed to develop the required lateral resistance. Thus, a cylinder pile wall with tie-back tendons was recommended. The cylinder piles were drilled through 50 ft of overburden and socketed into shale and limestone.

Recent applications of slope stabilization using steel piles have been described by Ito and Matsui (1981). Several landslides have been stabilized in Japan using such piles. In the United States, piers with tie-back rock anchors were drilled through a landslide and embedded in an unweathered schist during

construction at the Geyser Power Plant in California (Hovland et al., 1982).

These case histories indicate that the use of piles for stabilizing slopes is becoming more common. However, little information is currently available regarding (1) the pile behavior under lateral loading induced by the movement of the slide and (2) the effect of the pile row on the overall stability of the reinforced slope. The research reported herein is a step towards solving these two problems and developing a methodology for the analysis and design of the slope/pile system.

CHAPTER III. SLOPE STABILIZATION USING PILES

The analysis of a slope reinforced with piles requires that the force applied to the piles by the failing mass, and in turn the reaction from the piles to the slope, be known. In addition, a slope stability analysis that takes into account the reaction force is necessary. In this chapter, a theoretical method for the calculation of pressures acting on passive piles (piles subjected to lateral loading by horizontal movements of the surrounding soil) is discussed. Then, the resulting pile reaction is incorporated into a slope stability analysis to determine the factor of safety of a slope reinforced with a row of piles. Finally, parametric studies are performed to assess the influence of the location and spacing of the piles on the stability of the slope.

PILES IN SOIL UNDERGOING LATERAL MOVEMENT

The problems of active piles (piles subjected to a horizontal load at the head and transmitting this load to the soil) embedded in clay or sand and subjected to horizontal static loads of short or long duration have been treated by several authors (Matlock and Reese, 1960; Davisson and Gill, 1963; Broms, 1964; Vesic, 1965; Davisson, 1970; Poulos, 1973; Jamiolkowski and Garassino, 1977; Kishida and Nakai, 1977; Coyle et al., 1983). By making simplifying assumptions with regard to the deformation characteristics of the soil layer surrounding the piles, these authors arrived at acceptable solutions of piles subjected to horizontal loads at the top. In most cases, the problem of a single pile has been solved, and some correction factors for group effects have been introduced.

For the case of passive piles (piles subjected to lateral soil movements), the problems are more complicated because the lateral forces acting on the piles are now dependent on the soil movements, and these are in turn affected by the presence of the piles. For example, it is possible for a pile group to stop these movements, creating a completely different situation than that for a single pile. Hence, the solution for a single pile cannot be easily adapted for the situation

of a pile group, although several authors have suggested such an approach (Poulos,1973; Baguelin et al.,1976; Viggiani,1981). Other researchers have considered the problem from the fundamental standpoint of group (row) action (Ito and Matsui, 1975; Winter et al., 1983). Several theoretical approaches for the calculation of pressures on piles placed in deforming soils will be presented here.

Theoretical Solutions

Analytical models that have been used to obtain a theoretical solution for piles placed in deforming soils include: 1) a soil characterized by a modulus of subgrade reaction; 2) a soil considered to be an elastic-plastic material; 3) the finite element method used with bilinear or hyperbolic approximations of the soil behavior; and 4) other approaches.

Subgrade Reaction Method

In the modulus of subgrade reaction method, the pile is considered to be a beam on an elastic foundation, and the equilibrium equation is written as:

$$EI \frac{d^4 y_p}{dz^4} = K_s (y_p - y_s) \qquad (3\text{-}1)$$

where EI = pile stiffness

y_p = horizontal displacement of the pile at depth z

y_s = horizontal displacement the soil would undergo without the pile

K_s = subgrade reaction modulus, function of z and $(y_p - y_s)$

Computer programs are available to solve this equation (Baguelin et.al., 1976), but problems exist in the evaluation of y_s. When measured values of y_s are introduced, the solution of this equation agrees well with experimental results. When theoretical values of y_s are introduced, the solution of the equation is unrealistic (Theoretical values of y_s are discussed by Poulos, 1967 and Canizo and Merino, 1977; Tables can be used to determine the horizontal displacements of an elastic layer subjected to various vertical load conditions). In addition, the applicability of the solution to a row of piles is uncertain because the group action modifies the initial soil deformation values that are used in the calculations (DeBeer, 1977).

Other researchers have used the subgrade reaction concept for the calculation of the horizontal force. Fukuoka (1977) studied the pile-soil interaction in slopes subject to creep by means of a Winkler type model. He assumed that the unbalanced force that

causes the creep is a function of the velocity of the creeping mass. Measurements are needed along the length of the pile for the determination of such a velocity, and in turn, for the calculation of the unbalanced force. A reaction force provided by the piles and equal to the unbalanced force should be adequate to stop the landslide. To calculate the lateral resistance of the piles against the landslide, Fukuoka utilized the modulus of subgrade reaction method, and gave equations for the calculation of the deflection curve of the pile and for the bending moments and horizontal reactions. However, when the soil is moving, it is very difficult to define a coefficient of subgrade reaction to be used in the equations (DeBeer, 1977).

Viggiani (1981) used the subgrade reaction theory to analyze the interaction between a sliding mass and a stabilizing pile. His approach is based on concepts developed by Broms (1964) who evaluated the ultimate capacity of a vertical pile acted upon by a horizontal load, using an estimated subgrade reaction coefficient. Viggiani evaluated the maximum shear force that a pile can receive from the sliding mass and transmit to the underlying soil, by analyzing six possible failure mechanisms for the pile. This theory can be used for the design of the piles against an ultimate pressure.

However, it does not provide a way to calculate a value of the pressure at the initial stage of the landslide, which could be used to determine the effect of the piles on the factor of safety of the slope.

Elastic-Plastic Material

Calculations based on the assumption of an elastic-plastic material are described by Poulos (1973). The solution of the problem is obtained by imposing compatibility of displacements between the pile and the adjacent soil. The pile displacement is evaluated from the bending equation of a thin strip. The soil displacement is evaluated from the Mindlin equation (Mindlin, 1936) for horizontal displacement caused by horizontal loads within a semi-infinite mass. By solving a system of equations, the displacement and horizontal pressure on the pile can be evaluated. This method is applicable only when dealing with an ideal soil and a single pile.

More recently, Oteo (1977) refers to a method applied by Begemann-DeLeeuw (1972). The method has been derived for the analysis of pressures on piles when the surrounding soil undergoes horizontal displacement due to a surficial surcharge in the vicinity. It considers the soil to be a linearly elastic material and is based on stress and displacement fields given by

the Boussinesq theory. This technique is only applicable to the case of a known surcharge applied to the slope.

Finite Element Method

The applicability of finite-element techniques to the analysis of slope stabilization has been discussed by Rowe and Poulos (1979). They employed a two-dimensional finite element model for soil-structure interaction proposed earlier by Rowe et al.(1978). It is recognized that a finite element analysis of the stabilization problem should make allowance for the soil-structure interaction effects, but also for three-dimensional effects such as arching between piers. A computer program which can model these effects is being developed at Purdue University (Oakland and Chameau, 1983). The program can also evaluate the influence of piles position, size, spacing and stiffness on slope movements. When completed, this program will be added to the design methodology proposed herein to form a complete design-analysis package.

Other Approaches

Several other methods have also been used in the past. Baker and Yonder (1958) suggested calculating the thrust against the piles by the procedure of slices

and considering the piles as cantilever beams, provided that they penetrate into a stable soil layer for one third of their total length. Andrews and Klassel (1964) and Nethero (1982) calculated the pressure on the pile by using the concept of passive and active pressures assuming that the piles form a cantilever wall. However, analyzing the pile group as a retaining wall can lead to very conservative designs, since the soil arching between the piles is not taken into account.

DeBeer and Wallays (1970) reported a method for determining the forces and bending moments on a pile in the case of an unsymmetrical surcharge placed around the pile. The method is based on concepts introduced by Brinch Hansen (1961) on the ultimate resistance of rigid piles against transverse forces.

Wang et.al. (1979) proposed a semi-empirical technique to calculate the pressure on piles embedded in deforming soils using inclinometers to determine the soil movements. The soil pressures required to cause those movements where then estimated using the modulus of subgrade reaction theory.

Winter et.al.(1983) described a method for slope stabilization using piles based on the viscosity law of cohesive soils. It uses a solution derived for the

horizontal pressure against piles in viscous soils. Two requirements, a desired reduction of the sliding velocity and a safe maximum bending moment on the piles, are satisfied by the correct choice of pile spacing and pile diameter. This method is only applicable for the case of a clay mass subject to creep.

The Theory of Plastic Deformation

In most of the methods discussed so far, a theoretical solution for the passive piles was obtained by either solving the problem of a single pile or by analyzing the pile group as a retaining wall. The method proposed by Winter et.al.(1983) considers the solution of piles placed in a row and takes into account the spacing between the piles at the beginning of the analysis. However, this method can only be used in purely cohesive slopes undergoing creep. A theoretical method has been proposed by Ito and Matsui (1975) to analyze the growth mechanism of lateral forces acting on stabilizing piles when the soil is forced to squeeze between the piles. In this analysis, the plastic state which satisfies the Mohr-Coulomb yield criterion is assumed to occur in the soil just around the piles. The method was developed specifically to calculate pressures that act on passive piles in a row. The assumptions of the theory of plastic deformation are

given in the next section. Then, a derivation of its application to piles used in slope stabilization is presented. Finally, the validity of the theory is discussed.

Assumptions

It is assumed that the piles placed in plastically deforming ground, such as a landslide, can prevent further plastic deformations. In order to design the piles, the lateral forces need to be estimated as accurately as possible. These forces, however, are a function of the movement of the sliding mass. They may vary from zero, in case of no movement, to an ultimate value, in case of large movements. Ito and Matsui (1975) developed the theory of plastic deformation to estimate a value of the lateral force between these two extremes, assuming that no reduction in shear resistance along the sliding surface has taken place due to strain-softening caused by the movement of the landslide. For that reason, only the soil around the piles (Figure 1) is assumed to be in a state of plastic equilibrium, satisfying the Mohr-Coulomb yield criterion. Hence, the lateral load acting on the piles can be estimated regardless of the state of equilibrium of the slope.

The theory of plastic deformation is based on the

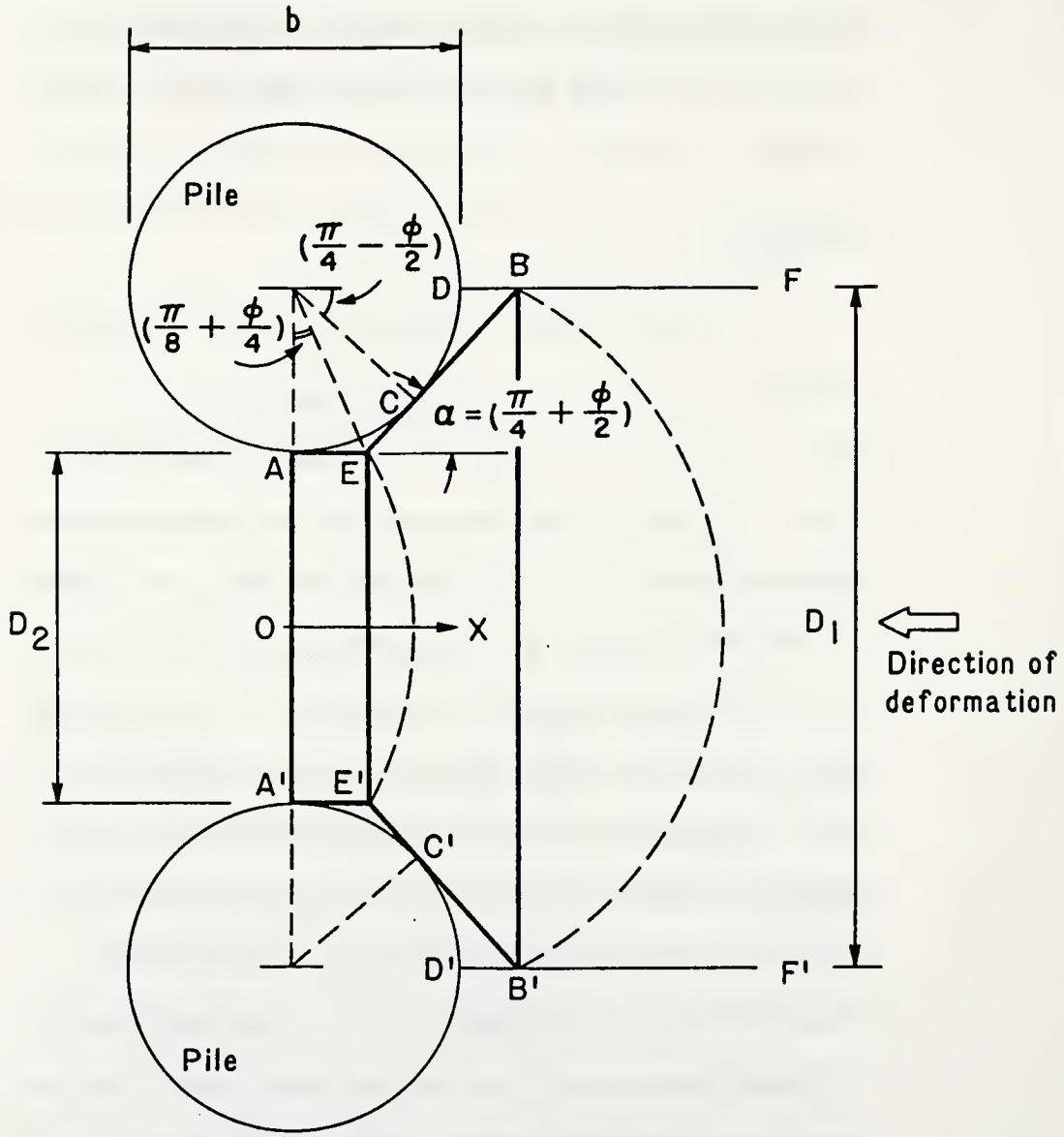

Figure 1 Plastically Deforming Ground Around Stabilizing Piles (After Ito and Matsui, 1975).

following assumptions:

1) When the soil layer deforms, two sliding surfaces, AEB and A′E′B′, occur, making an angle of $(\pi/4 + \phi/2)$ with the x-axis (Figure 1);
2) The soil is in a state of plastic equilibrium only in the area AEBB′E′A′ where the Mohr-Coulomb yield criterion applies;
3) The active earth pressure acts on plane AA′;
4) Plane strain conditions exist with respect to depth;
5) The piles are rigid elements;
6) The frictional forces on surfaces AEB and A′E′B′ are neglected when the stress distribution in the soil AEBB′E′A′ is considered.

The last assumption has been a point of controversy in the past, because it seems to indicate that the stresses acting on surfaces AEB and A′E′B′ are principal stresses. This, however, is not true (Ito and Matsui, 1978); Let us consider two small elements within the plastic region (Figure 2), element I in the center of this region, and element II on the edge. The stresses shown in element I, σ_{aI} and σ_{xI}, are principal stresses, and the Mohr's circles for that element are shown in Figures 3a and 3b for purely cohesionless and cohesive soils, respectively. It is expected that the Mohr circles will move to the right as different ele-

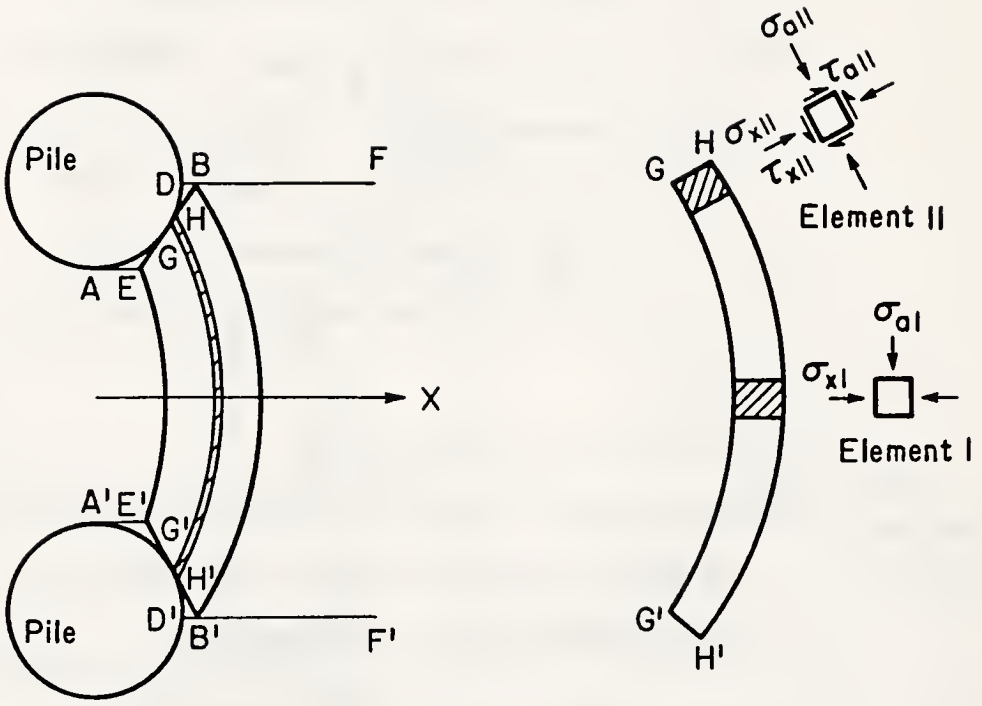

Figure 2 Stresses Acting On Elements in Plastically Deforming Ground (After Ito and Matsui, 1975).

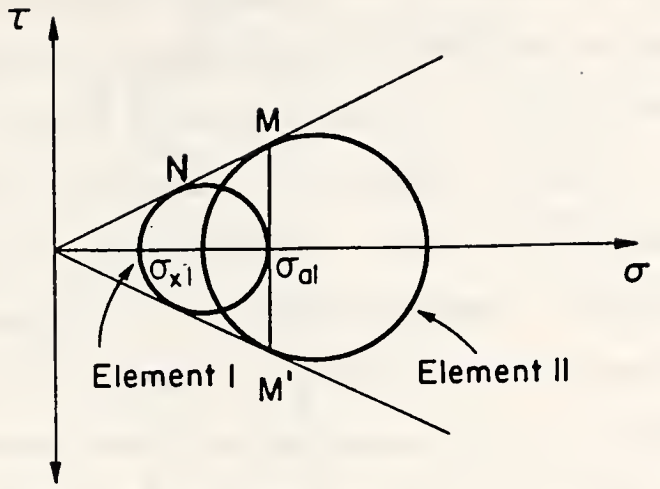

(a) Cohesionless Soil

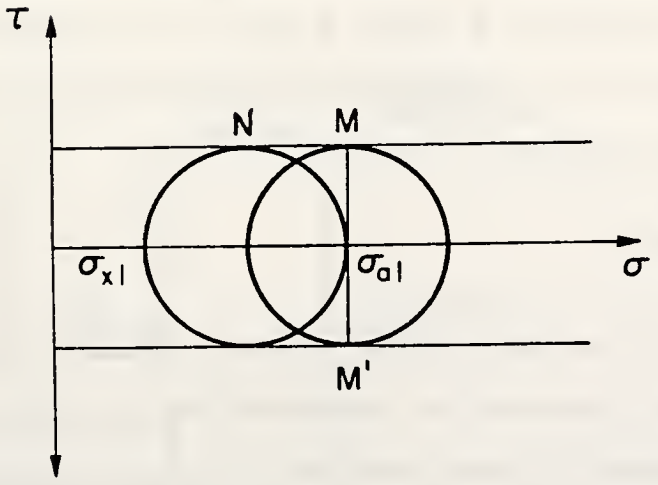

(b) Frictionless Soil

Figure 3 Mohr Circles of Elements in Plastically Deforming Ground (After Ito and Matsui, 1979).

ments are considered, advancing from the center towards the edge of area GHH'G' (i.e., in Figure 3, point N will move along the failure envelope to point M). However, it would be difficult to analyze such a complex distribution of stresses. For simplicity, every point on area GHH'G', except planes GH and G'H', is assumed to be under the same stresses as element I. For planes GH and G'H', it is assumed that the normal stress acting on element II, σ_{aII}, is equal to the normal stress acting on element I, σ_{aI} (Figure 3). It is clear that the assumption of a uniform stress distribution for AEBB'E'A' does not consider planes EB and E'B' to be principal planes. The stresses acting on those planes are represented by points M and M', and are taken into account in the equilibrium equations written for area GHH'G' (Equation 3-2 below).

Derivation

The successive steps necessary to derive the force acting on the pile per unit depth are presented herein. Expressions of this force are given for c-ϕ, ϕ, and c materials.

First, the equilibrium of the differential element GHH'G' surrounded by solid lines in Figure 4a is considered. Summation of forces in the x direction gives:

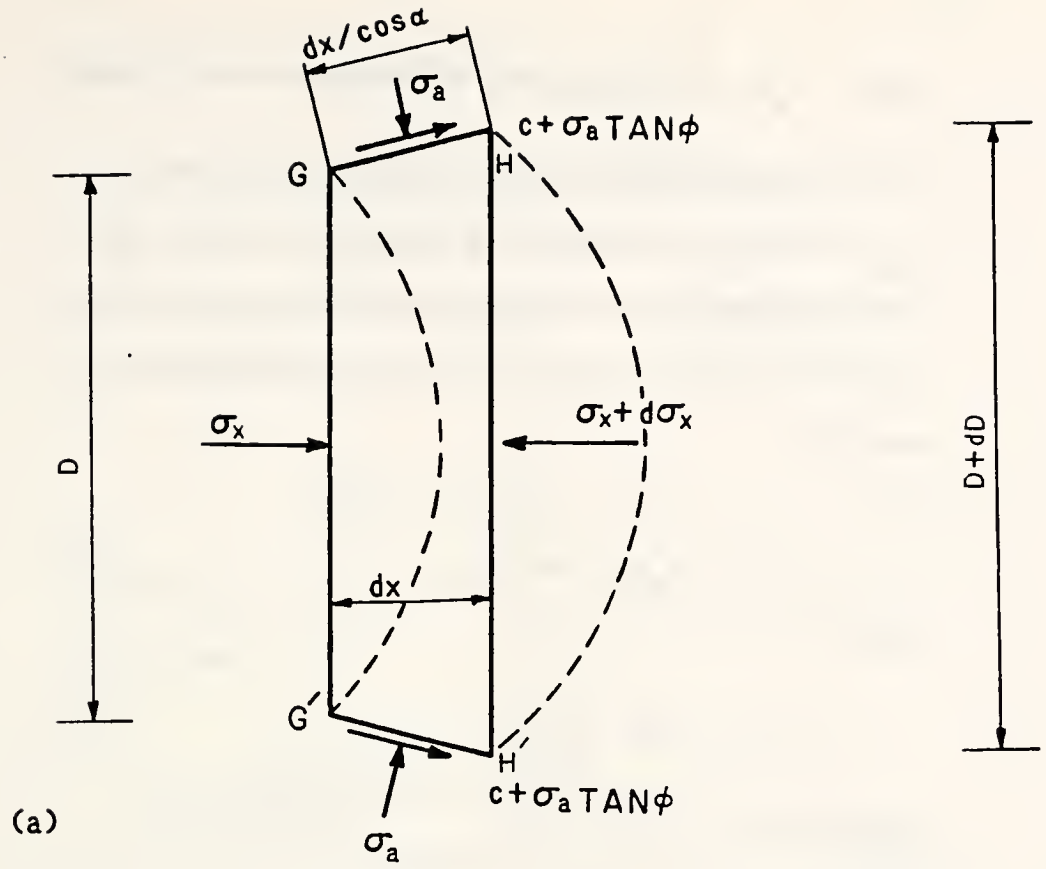

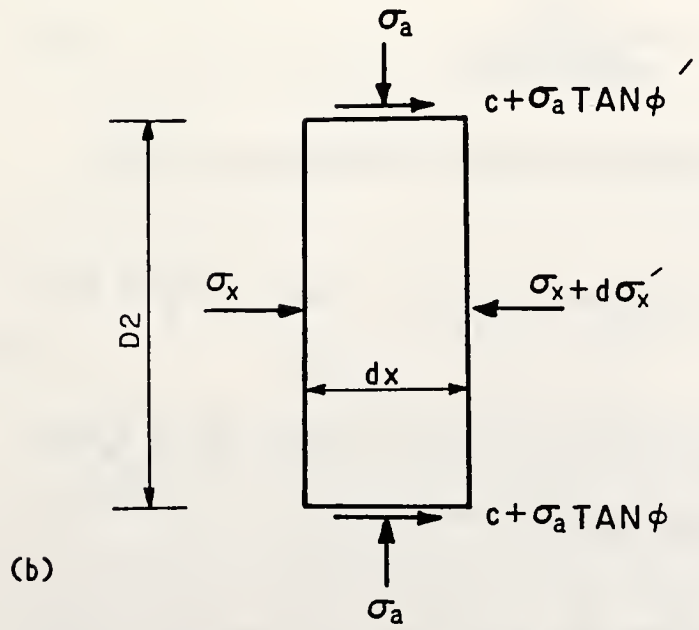

Figure 4 Stresses on Elements in Plastically Deforming Ground.

$$-Dd\sigma_x - \sigma_x dD + 2dx \{\sigma_a \tan(\frac{\pi}{4} + \frac{\phi}{2}) + \sigma_a \tan\phi + c\} = 0 \quad (3\text{-}2)$$

As it is assumed that σ_{aII} is approximately equal to σ_{aI}, then σ_{aII} corresponds to a principal stress σ_x from assumption 6. According to the Mohr-Coulomb yield criterion, failure occurs when the stresses satisfy the equation:

$$\sigma_a = \sigma_x N_\phi + 2c\sqrt{N_\phi} \quad (3\text{-}3)$$

where

$$N_\phi = \tan^2(\frac{\pi}{4} + \frac{\phi}{2}) \quad (3\text{-}4)$$

From geometry

$$dx = \frac{d(\frac{D}{2})}{\tan(\frac{\pi}{4} + \frac{\phi}{2})} \quad (3\text{-}5)$$

Substituting Equations (3-3) and (3-5) into (3-2):

$$Dd\sigma_x = dD \{N_\phi^{1/2}\tan\phi + N_\phi - 1)\sigma_x + c(2\tan\phi + 2N_\phi^{1/2} + N_\phi^{-1/2})\} \quad (3\text{-}6)$$

Integration of the above equation gives the state of stress in zone EBB'E':

$$\sigma_x = \frac{(C_1 D)^{(N_\phi^{1/2}\tan\phi + N_\phi - 1)} - c(2\tan\phi + 2N_\phi^{1/2} + N_\phi^{-1/2})}{N_\phi^{1/2}\tan\phi + N_\phi - 1} \quad (3\text{-}7)$$

where C_1 is a constant of integration.

Similarly, the equilibrium of the differential element shown in Figure 4b will give the state of stress in zone AEE'A' (Figure 1). Summing all forces in the x direction:

$$D_2 d\sigma_x = 2(\sigma_a \tan \phi + c)dx \tag{3-8}$$

Substituting Equation (3-3) into Equation (3-8) and integrating it:

$$\sigma_x = \frac{C_2 \exp\left(\frac{2N_\phi \tan\phi}{D_2} x\right) - c(2N_\phi^{1/2} \tan\phi + 1)}{N_\phi \tan\phi} \tag{3-9}$$

where C_2 is a constant of integration.

Finally, assumption 3 gives the normal stress on plane AA' (x = 0):

$$|\sigma_x|_{x=0} = \gamma \bar{z} N_\phi^{-1} - 2cN_\phi^{-1/2} \tag{3-10}$$

where $\bar{z}$ is the depth from ground surface and γ is the unit weight of the soil. Recognizing that the plane AA' is the x = 0 plane, Equation (3-10) can be considered as a boundary condition. The constant C_2 is obtained by introducing this boundary condition in Equation (3-9):

$$C_2 = \bar{\gamma z} \tan\phi + c \qquad (3\text{-}11)$$

The normal stress acting on plane EE′ is found by using Equation (3-9) and (3-11) at the distance x = AE.

From geometry,

$$AE = \{(D_1 - D_2)/2\} \tan(\pi/8 + \phi/4) \qquad (3\text{-}12)$$

then,

$$|\sigma_x|_{x=AE} = \frac{1}{N_\phi \tan\phi} \{(\bar{\gamma z}\tan\phi + c) \cdot \exp\left(\frac{D_1 - D_2}{D_2} \cdot N_\phi \tan\phi \tan\left(\frac{\pi}{8} + \frac{\phi}{4}\right)\right) - c\,(2N_\phi^{1/2}\tan\phi + 1)\} \qquad (3\text{-}13)$$

The constant C_1 is obtained by considering Equation (3-13) as a boundary condition and substituting it in Equation (3-7).

$$(C_1\ D_2)^{(N_\phi^{1/2}\tan\phi + N_\phi - 1)} = \frac{(N_\phi^{1/2}\tan\phi + N_\phi - 1)}{N_\phi \tan\phi} \{(\bar{\gamma z}\tan\phi + c)$$

$$\exp\left(\frac{D_1 - D_2}{D_2} N_\phi \tan\phi \tan\left(\frac{\pi}{8} + \frac{\phi}{4}\right)\right) - c(2N_\phi^{1/2}\tan\phi + 1)\}$$

$$+ c\,(2\tan\phi + 2N_\phi^{1/2} + N_\phi^{-1/2}) \qquad (3\text{-}14)$$

The lateral force per unit thickness of layer acting on plane BB′ in the x-direction is obtained by substitut-

ing the above value in Equation (3-7):

$$P_{BB'} = D_1(\sigma_x)_{D=D_1} = A\left[\frac{1}{N_\phi \tan\phi}\{(\gamma\bar{z}\tan\phi+c)\right.$$

$$\exp\left(\frac{D_1-D_2}{D_2} N_\phi \tan\phi \tan\left(\frac{\pi}{8}+\frac{\phi}{4}\right)\right) - c(2N_\phi^{1/2}\tan\phi + 1)\}$$

$$\left.+c\frac{2\tan\phi + 2N_\phi^{1/2} + N_\phi^{-1/2}}{N_\phi^{1/2}\tan\phi + N_\phi - 1}\right] - c\cdot D_1\frac{2\tan\phi + 2N_\phi^{1/2} + N_\phi^{-1/2}}{N_\phi^{1/2}\tan\phi + N_\phi - 1}$$

where

$$A = D_1\left(\frac{D_1}{D_2}\right)(N_\phi^{1/2}\tan\phi + N_\phi - 1)$$

(3-15)

The lateral force q acting on the pile per unit thickness of layer is the difference between the forces acting on planes BB′ and AA′ (Equations (3-10) and (3-15)):

$$q = P_{BB',-D_2}(\sigma_x)_{x=0} = A\,c\left[\frac{1}{N_\phi \tan\phi}\{\exp\left(\frac{D_1-D_2}{D_2} N_\phi \tan\phi\right.\right.$$

$$\left.\tan\left(\frac{\pi}{8}+\frac{\phi}{4}\right)\right) - 2N_\phi^{1/2}\tan\phi - 1\} + \left.\frac{2\tan\phi + 2N_\phi^{1/2} + N_\phi^{-1/2}}{N_\phi^{1/2}\tan\phi + N_\phi - 1}\right]$$

$$-c\{D_1\frac{2\tan\phi + 2N_\phi^{1/2} + N_\phi^{-1/2}}{N_\phi^{1/2}\tan\phi + N_\phi - 1} - 2D_2 N_\phi^{-1/2}\}$$

$$+\frac{\bar{\gamma}z}{N_\phi}\{A\ \exp(\frac{D_1-D_2}{D_2}N_\phi\tan\phi\ \tan(\frac{\pi}{8}+\frac{\phi}{4}))\ -\ D_2\} \qquad (3\text{-}16)$$

For a purely cohesionless soil, the cohesion c is zero and Equation (3-5) reduces to the following expression for the lateral force per unit thickness:

$$q = \frac{\bar{\gamma}z}{N_\phi}\{D_1(\frac{D_1}{D_2})^{N_\phi^{1/2}\tan\phi+N_\phi-1)}\exp(\frac{D_1-D_2}{D_2}N_\phi\tan\phi\ \tan(\frac{\pi}{8}+\frac{\phi}{4}))-D_2\} \qquad (3\text{-}17)$$

For a purely cohesive soil the angle of internal friction is zero and several of the above equations are modified, Equation (3-6) becomes:

$$\frac{dD}{D} = \frac{d\sigma_x}{3c} \qquad (3\text{-}18)$$

The state of stress in EBB′E′ is obtained by integrating this equation:

$$\sigma_x = 3c\ \log D + C_3 \qquad (3\text{-}19)$$

where C_3 is a constant of integration. After substituting Equation (3-3) into Equation (3-8) the following expression is obtained:

$$\frac{d\sigma_x}{c} = \frac{2}{D_2}\,dx \qquad (3\text{-}20)$$

Integration of the above equation gives the state of

stress in AEE'A':

$$\sigma_x = \frac{2c}{D_2} x + C_4 \qquad (3\text{-}21)$$

where C_4 is the constant of integration. From assumption 3 the state of stress in plane AA' is:

$$|\sigma_x|_{x=0} = \gamma\bar{z} - 2c \qquad (3\text{-}22)$$

If Equation (3-22) is considered as a boundary condition, substitution in the above expression gives the following for C_4:

$$C_4 = \gamma\bar{z} - 2c \qquad (3\text{-}23)$$

Then the normal stress acting on plane EE' is:

$$|\sigma_x|_{x=\{(D_1-D_2)/2\}\tan(\pi/8)} = c\left(\frac{D_1-D_2}{D_2}\tan\frac{\pi}{8}2\right)+\gamma\bar{z} \qquad (3\text{-}24)$$

Considering Equation (3-24) as a boundary condition, C_3 is obtained as:

$$C_3 = c\left(\frac{D_1-D_2}{D_2}\tan\frac{\pi}{8} - 3\log D_2 - 2\right) + \gamma\bar{z} \qquad (3\text{-}25)$$

Using Equations (3-25) and (3-19), the lateral force, $P_{BB'}$, on the plane BB' is:

$$P_{BB'} = D_1\{\sigma_x\}_{D=D_1} \qquad (3\text{-}26)$$

$$= D_1 \{c\ (3\log \frac{D_1}{D_2} + \frac{D_1-D_2}{D_2} \tan\frac{\pi}{8} - 2) + \gamma\bar{z}\}$$

Hence, for cohesive soils, the lateral force q per unit thickness of layer is:

$$q = P_{BB',-D_2}(\sigma_x)_{x=0} \qquad (3\text{-}27)$$

$$= c\ \{D_1(3\log \frac{D_1}{D_2} + \frac{D_1-D_2}{D_2} \tan\frac{\pi}{8}) - 2(D_1-D_2)\} + \gamma\bar{z}\ (D_1-D_2)$$

The total lateral force acting on a stabilizing pile due to the plastically deforming layer around the pile, F_t, is obtained by integrating Equations (3-16), (3-17) and (3-27), along the depth of the soil layer for c-ϕ, ϕ, and c materials, respectively.

Parametric Studies

The theory of plastic deformation involves numerous parameters that describe the geometry of the problem and the properties of the soil. As seen from the final expressions 3-16, 3-17 and 3-27, these parameters are the unit weight, γ, the depth, $\bar{z}$, the center to center distance between piles, D_1, the clear distance between piles, D_2, the angle of internal friction, ϕ, and the cohesion, c.

The lateral force per unit depth, q, is a linear function of parameters γ and $\bar{z}$. Hence, q increases

linearly as γ or $\bar{z}$ increases. The effects of the remaining parameters are more difficult to detect. The lateral force, F_t, is plotted versus the ratio D_2/D_1 for different values of c, ϕ, and pile diameter, b, in Figures 5, 6, and 7, respectively. In general, these results indicate that the lateral force decreases as the ratio D_2/D_1 increases. It is also apparent that the force increases with an increase in ϕ or c. This is to be expected, since it is harder for a stiffer soil to squeeze between the piles. Finally, the lateral force increases as the pile diameter, $D_1 - D_2$, increases (Figure 7).

Field and Laboratory Measurements

In order to test the validity of the theoretical approach for the estimation of the lateral forces on piles, Ito and Matsui (1975) compared observed field values to calculated ones. The observations were made in three different locations in Japan, at Katamachi, Higashitono and Kaniyama. Reinforced concrete piles about 1 ft in diameter were used in Katamachi and steel pipe piles of about the same diameter were used at the other two locations for the stabilization of landslides.

The field lateral forces were deduced from measured strains induced in the piles by the sliding soil

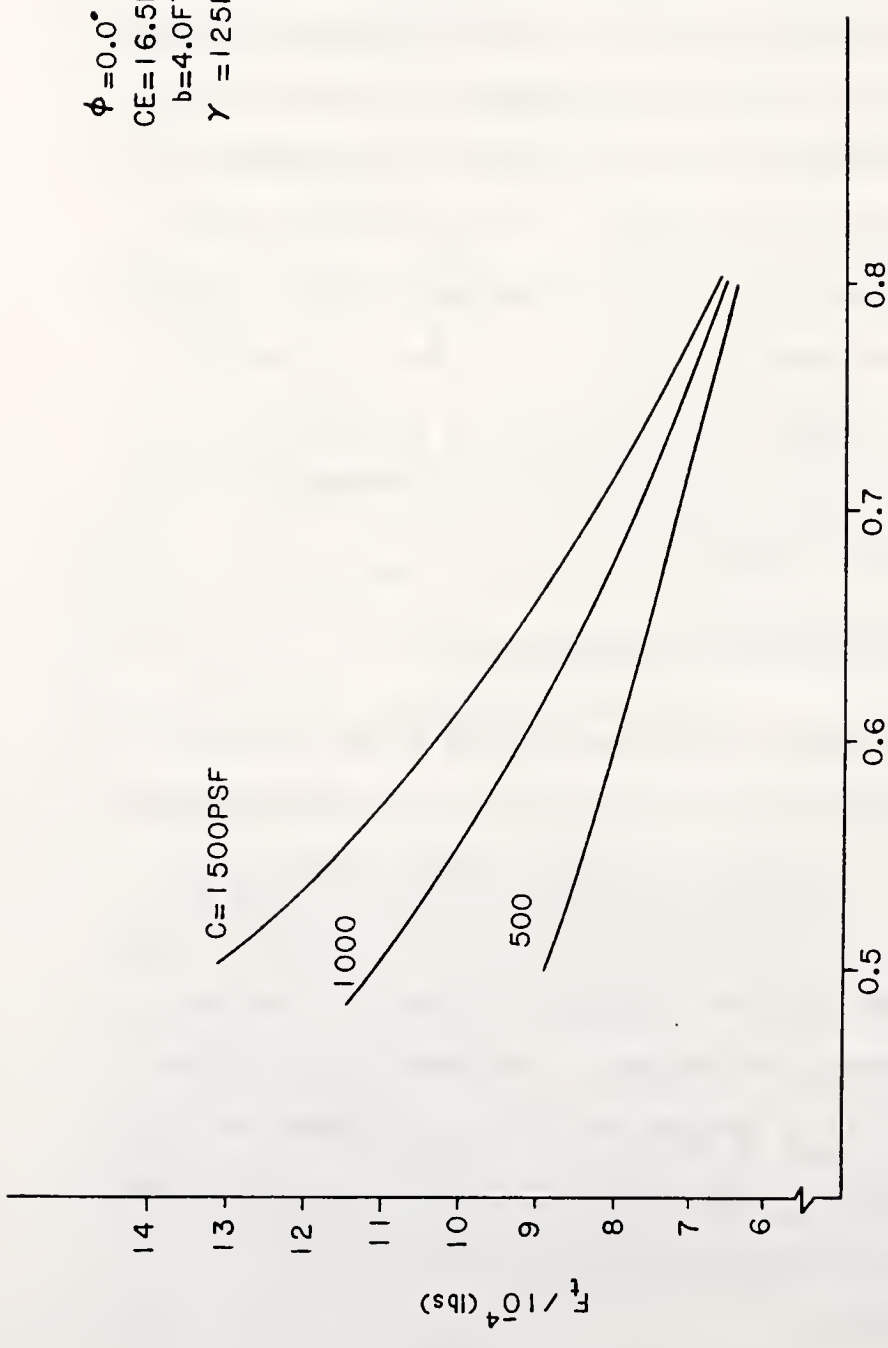

Figure 5 Force Acting on Piles versus Ratio D_2/D_1 for Different Cohesive Soils.

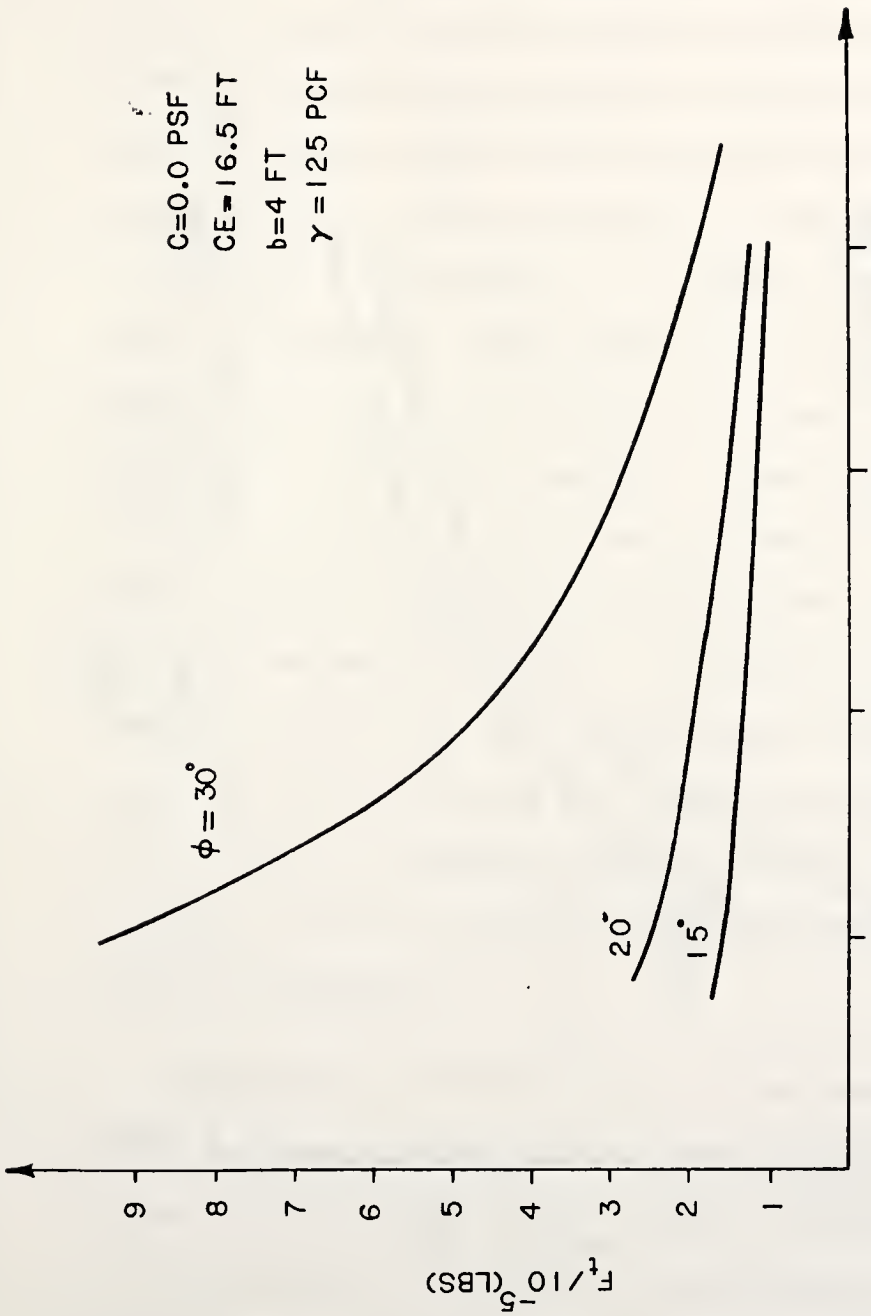

Figure 6 Force Acting on Piles versus Ratio D_2/D_1 for Different Cohesionless Soils.

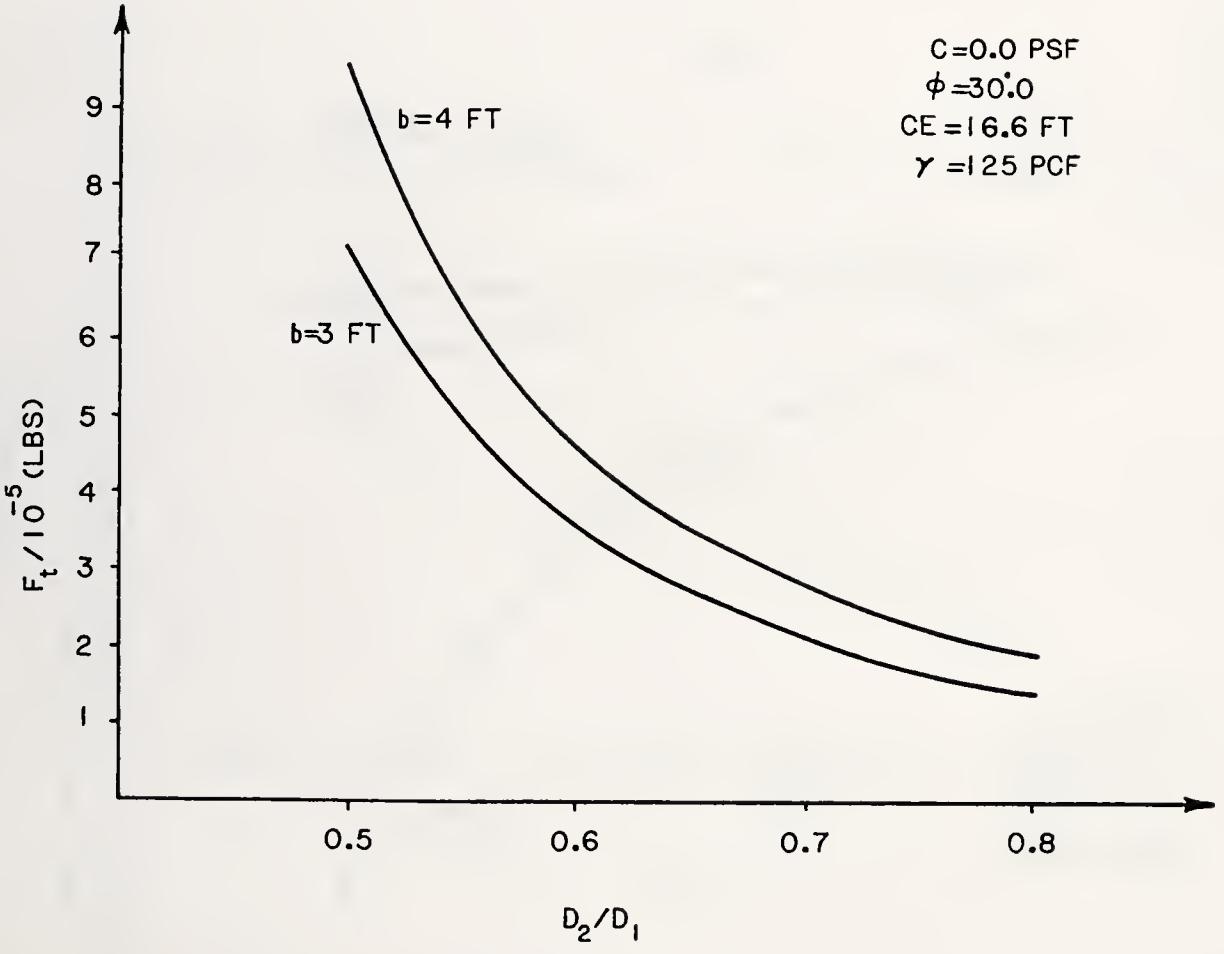

Figure 7 Force Acting on Piles versus Ratio D_2/D_1 for Different Pile Diameters.

masses. The theoretical forces were estimated using c and ϕ values obtained from shear and standard penetration tests. The experimental and theoretical results were compared and several conclusions were reached. Since the computed and measured forces were found to be within the same order of magnitude, it was concluded that the theory of plastic deformation can be used to predict the force acting on stabilizing piles. When the pile head was restricted, the distribution of the force was trapezoidal, which agrees with the theory. When the pile head was allowed to deflect, the distribution of the force was triangular. In most applications, the condition of restrained pile head will be used and the force on the pile as given by this method will give reasonable solutions. As will be seen in the remaining of this work, the bending moments and shear forces acting on a free head pile are much larger than those acting on a restrained head pile, assuming that the forces given by the theory of plastic deformation applies to both piles.

In addition to the field tests, Ito and Matsui (1982) performed a series of model tests on piles placed in sand or clay. The test apparatus consisted of a soil container with the model piles in a row and a lateral loading system. The soil was pushed through the piles slowly and its behavior was observed. A

series of marks were placed at the top of the soil layer to indicate the shape of the flow lines as the soil moved between the piles. It was observed that the disturbance of the flow lines appeared to occur mainly within the zone of plastic deformation that was originally assumed. This validates the assumption that the soil is in a plastic condition around the piles.

The relationship between the soil displacement and the lateral force on the pile was also investigated. It was found that the lateral force increases to a yield value, and then reaches an ultimate value with increasing soil displacement. In a logarithmic scale this relationship can be represented by a bilinear curve with an inflection point. The theoretical lateral forces given by Equations 3-16, 3-17, and 3-27 are very close to the experimental values at the inflection point (i.e., the yield value). The ultimate lateral force can be approximately estimated as 1.6 times the theoretical lateral yield force.

SAFETY FACTOR OF THE STABILIZED SLOPE

The stability of a slope can be investigated by a number of limit equilibrium methods, including the logarithmic spiral method, the friction circle method, and

the method of slices. Of these, the friction circle method was found to be the most convenient to take into account the force exerted on the slope by the piles in the limit equilibrium analysis. Parametric studies were performed to observe the change in the potential failure surface with the addition of the piles, and to obtain the relationships between the safety factor of the slope and the location and spacing of the piles.

The limit equilibrium calculations are based on an assumed shape of the rupture surface. The safety factor, FS, is defined as the ratio of the shear strength available to the shear strength required to maintain the slope in a state of limit equilibrium. Assuming the Mohr-Coulomb failure criterion, the factor of safety is given by:

$$FS = \frac{c_a + \sigma_n \tan \phi_a}{c_r + \sigma_n \tan \phi_r} \qquad (3\text{-}28)$$

where the subscripts denote available and required quantities, and σ_n is the normal force acting on the surface of rupture.

As an aid in determining FS, the factors of safety with respect to cohesion, F_c, and friction, F_ϕ, can be used:

$$F_c = \frac{c_a}{c_r} \quad \text{and} \quad F_\phi = \frac{\tan \phi_a}{\tan \phi_r} \qquad (3\text{-}29)$$

The "true" safety factor, FS, is obtained when F_c and F_ϕ are equal (Perloff and Baron, 1976):

$$FS = F_c = F_\phi \tag{3-30}$$

The Friction Circle Method

The Friction Circle Method (Taylor, 1937) considers the stability of the entire sliding mass as a whole and involves taking moments with respect to the center of a circular failure arc. By investigating all potential failure surfaces passing through the slope, the critical failure arc and safety factor are evaluated. This method gives reasonable values for the factor of safety when compared to other methods of slope stability analysis (Siegel, 1975). When all the normal stresses acting on the critical surface are assumed to be concentrated at one point, a lower bound value for the factor of safety is obtained. When the normal stresses are assumed to act at the two end points of the critical surface, an upper bound factor of safety is determined. In this analysis, the normal stresses are assumed to be concentrated at a single point on the failure surface. Therefore, the computed factor of safety is conservative.

The model used by Taylor (1937) for the analysis of homogeneous slopes is shown in Figure 8. The forces that act on the mass are the weight, W, the cohesion force required to maintain equilibrium, C_r, and the resultant of the normal and frictional forces, P.

The weight W acts vertically through the center of gravity of the mass and is determined by multiplying the unit weight, γ, of the soil by the area enclosed within the failure surface and the slope boundaries.

The resultant mobilized cohesion force C_r is equal to the product of the unit cohesion required for equilibrium, c_r, by the length of the chord $\overline{AB}$. If c_r is decomposed into its components parallel and perpendicular to the chord, the components perpendicular to the chord create equal and opposite moments around point O (Figure 8). Hence, only the components parallel to the chord contribute to the moment equilibrium equation. The line of action of C_r is parallel to the chord $\overline{AB}$ while its moment arm, a, is obtained by equating the following moments:

$$c_r.\overline{AB}.a = c_r.AB.R \qquad (3\text{-}31)$$

Therefore,

$$a = R.AB/\overline{AB} \qquad (3\text{-}32)$$

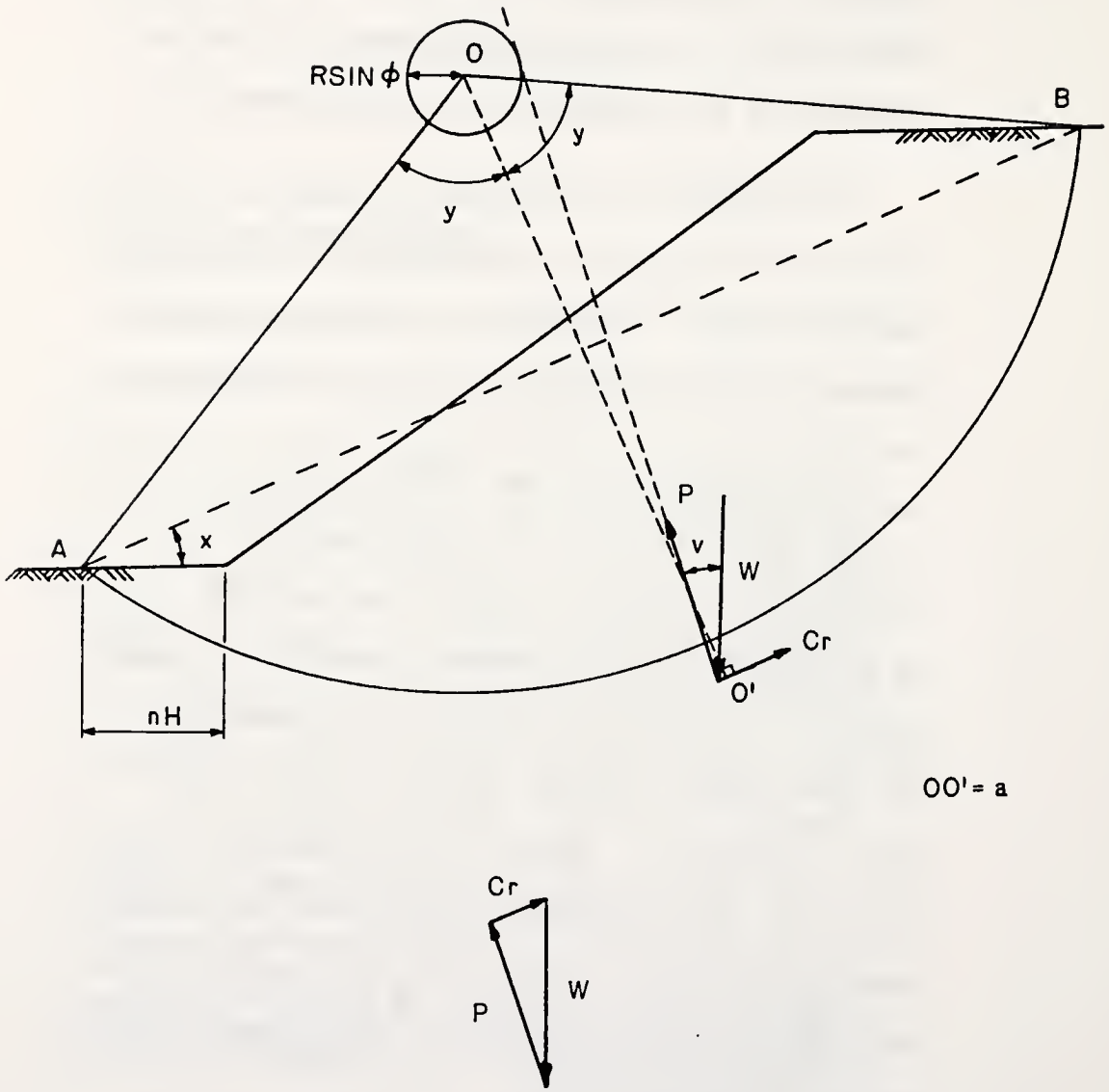

Figure 8 Forces on Unreinforced Slope.

The force P is the resultant of the normal and frictional forces concentrated at one point. It is almost tangent to a circle of radius $R\sin\phi$ as shown in Figure 8.

As a result of the above assumptions, a force polygon can be constructed (Figure 8). A detailed mathematical solution for the equilibrium equations of the slope is given by Taylor (1937). The following two expressions for the stability number were derived by Taylor for a toe failure and a failure below the toe, respectively:

$$\frac{c_a}{F_c \gamma H} = \frac{\frac{1}{2}\csc^2 x\,(y\csc^2 y - \cot y) + \cot x - \cot i}{2\cot x \cot v + 2} \qquad (3\text{-}33)$$

and

$$\frac{c_a}{F_c \gamma H} = \frac{\frac{1}{2}\csc^2 x\,(y\csc^2 y - \cot y) + \cot x - \cot i - 2r}{2\cot x \cot v + 2} \qquad (3\text{-}34)$$

where

x,y = angles describing the ϕ-circle (Figure 8)

i = slope angle

v = angle defining the force polygon of the slope (Figure 8)

H = height of the slope

η = ratio of the distance between the toe of the slope and point A (Figure 8) to the height of the slope.

The safety factor with respect to cohesion on any surface defined by angles x and y can be obtained using Equations 3-33 and 3-34. The true safety factor of any of these surfaces is obtained through successive iteration until F_c is equal to F_ϕ. The critical surface is the one which minimizes the factor of safety. This minimum value is the safety factor of the slope.

When a row of piles is inserted in the slope, the additional resistance provided by the piles changes both the safety factor and the critical surface. The new slope to be analyzed is shown in Figure 9. The forces applied to the slope are identical to the ones in Figure 8, with the exception of the force exerted on the slope by the piles, F_p. To obtain this force per unit width of the sliding mass, either Equation 3-16, 3-17 or 3-27 is integrated along the depth of the pile, and the result is divided by the center to center distance, D_1 (i.e., $F_p = \frac{F_t}{D_1}$).

The resistance force, F_p, can be incorporated in the force polygon (Figure 9) resulting in two new expressions for the stability number for a toe failure and a failure below the toe, respectively:

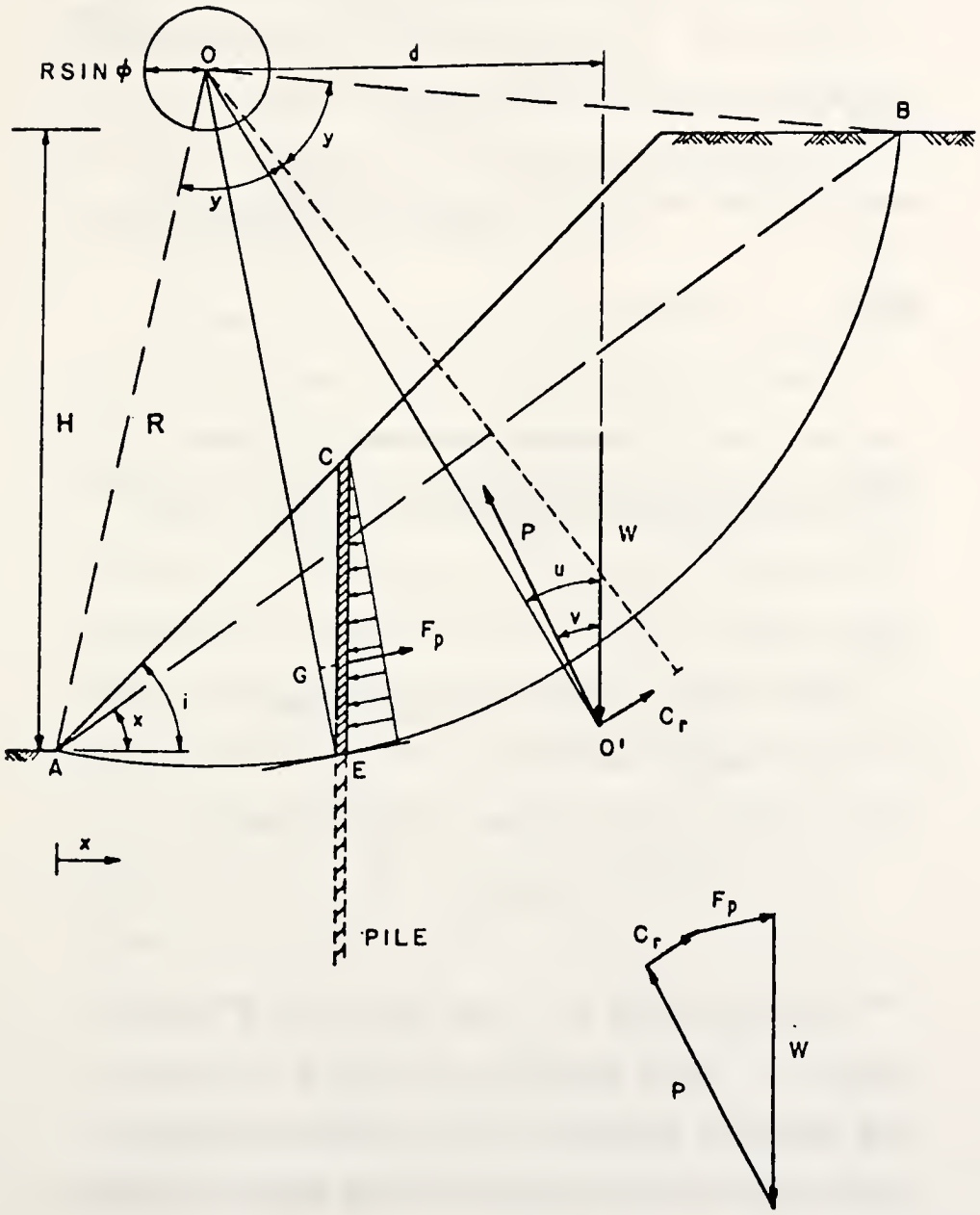

Figure 9 Forces on Slopes Reinforced with Piles.

$$\frac{c_a}{F_c \gamma H} = \frac{E - \frac{12F_p}{\gamma H^3}\left\{\frac{\cos(CEO)}{\sin v}\frac{H}{2}\,\mathrm{cscx}\,\mathrm{cscy}\,\sin\phi + OG\right\}}{6\,\csc^2 x\,\mathrm{cxcy}\,\sin\phi\left\{\frac{\cos x}{\sin v} + \csc(u-v)\cos(x-u)\right\}} \qquad (3\text{-}35)$$

where

$$E = 1 - 2(\cot^2 i + 3\cot i\,\cot x - 3\cot i\,\cot y + 3\cot x\,\cot y)$$

and

$$\frac{c_a}{F_c \gamma H} = \frac{\{E + 6\eta^2 - 6\eta\sin\phi\,\mathrm{cscx}\,\mathrm{cscy}\} - \frac{12F_p}{\gamma H^3}A}{6\csc^2 x\,\mathrm{cscy}\,\sin\phi\left\{\frac{\cos x}{\sin v} + \csc(u-v)\cos(x-u)\right\}} \qquad (3\text{-}36)$$

where

CEO = angle F_p forms with the horizontal

OG = moment arm of F_p

u = angle defining the force polygon of the slope (Figure 9)

The derivations for these equations are given in Appendix A. These equations can be used in exactly the same manner as Equations 3-33 and 3-34 to obtain the safety factor for the slope. The two additional parameters are the force F_p and the angle CEO, which defines the direction of F_p.

The line of action of F_p is assumed to pass through the centroid of the force diagram given by

Equations 3-16, 3-17 and 3-27. This assumption is reasonable since each individual pile is preventing movement essentially by cantilever action. The direction of F_p is assumed to be parallel to the line tangent to the failure surface at the point of intersection of that surface with the piles.

The magnitude of F_p is a function of the length of the pile from the ground surface to the failure surface, shown by distance CE in Figure 9. For each set of angles, x and y, selected to investigate a particular surface in the slope, the distance CE changes and, consequently, the magnitude of the force changes. To take this into account, the length of the pile above the failure surface was expressed as a function of both the ϕ-circle parameters, angles x and y, and the location of the pile. For each set of values, x and y, chosen to determine a failure surface, a new pile length, and thus a new F_p, is calculated. This force is then used in Equations 3-35 or 3-36 to determine a new stability number. The calculations necessary to determine the length CE are discussed in Appendix B.

Parametric Studies

A computer program was developed to perform the two-dimensional slope stability analysis presented in the previous section. The listing and user's manual

for this program are given in Appendix C. It can be used to calculate the factor of safety of a slope made of a homogenous material and reinforced by a single row of piles. The soil properties are defined by the unit weight, γ, cohesion, c, and friction angle, ϕ. The program was used to perform parametric studies to investigate the effect of the location, spacing, and size of the piles on the stability of the slope.

When piles are inserted in the slope, the location of the critical surface changes since an additional force, F_p, is introduced in the limit equilibrium equations. This is illustrated in Figure 10 for a slope of height 45 ft and angle 30 degrees with material properties c, ϕ, and γ equal to 500 psf, 10 degrees and 125 pcf, respectively. The original factor of safety of the slope (without the pile reinforcement) was 1.08, obtained for the critical surface OAB. After insertion of a row of piles with diameter ratio D_2/D_1 of 0.6, placed 45 feet upslope, the factor of safety increased to 1.82 and the critical surface changed to O'AB'. Insertion of piles 70 feet upslope resulted in a factor of safety of 1.64 and the critical surface O''AB''.

Without the piles, any surface below or above the critical one gives a higher safety factor. With the addition of the piles, every possible surface in the slope is reexamined. To obtain a factor of safety for

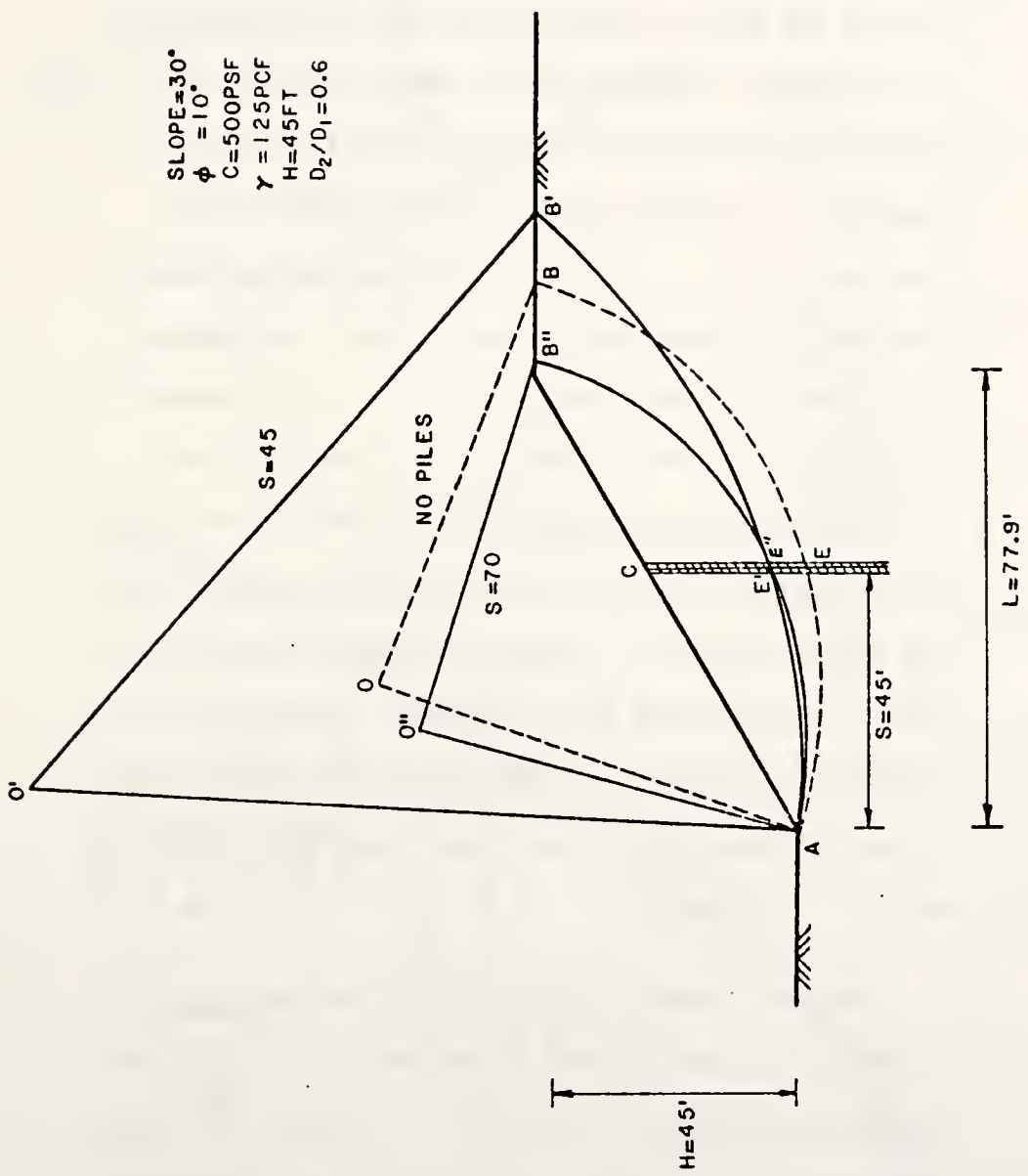

Figure 10 Critical Surfaces of a Shallow Slope as a Function of Pile Row Location.

each surface, the weight of the failure wedge, the soil resistance, and the reaction from the piles, F_p, are balanced. F_p is a function of the pile length from the face of the slope to the surface under investigation. As an example, when the surface AEB, which was the critical surface before the piles were inserted, is examined, the distance CE is used to calculate the reaction force F_p. As the surface becomes shallower, this distance decreases and the force F_p decreases. As F_p decreases, both the effect of F_p on the safety factor and the rate of change of the safety factor decrease. When F_p is large, it has a predominant effect on the safety factor whereas the other resisting forces are negligible. As F_p becomes smaller, the effect of these forces becomes more important. Consequently, the intersection of the resulting critical surface with the piles is located above the original surface (points E′ and E′′ in Figure 10).

Figure 11 shows how the location of the piles, indicated by the distance S from the toe of the slope, influences the factor of safety of the same slope for a given ratio D_2/D_1. For each value of S the safety factor was computed for both the original critical surface (solid curve in Figure 11) and the new critical surface which was found after the addition of the piles (dashed line in Figure 11).

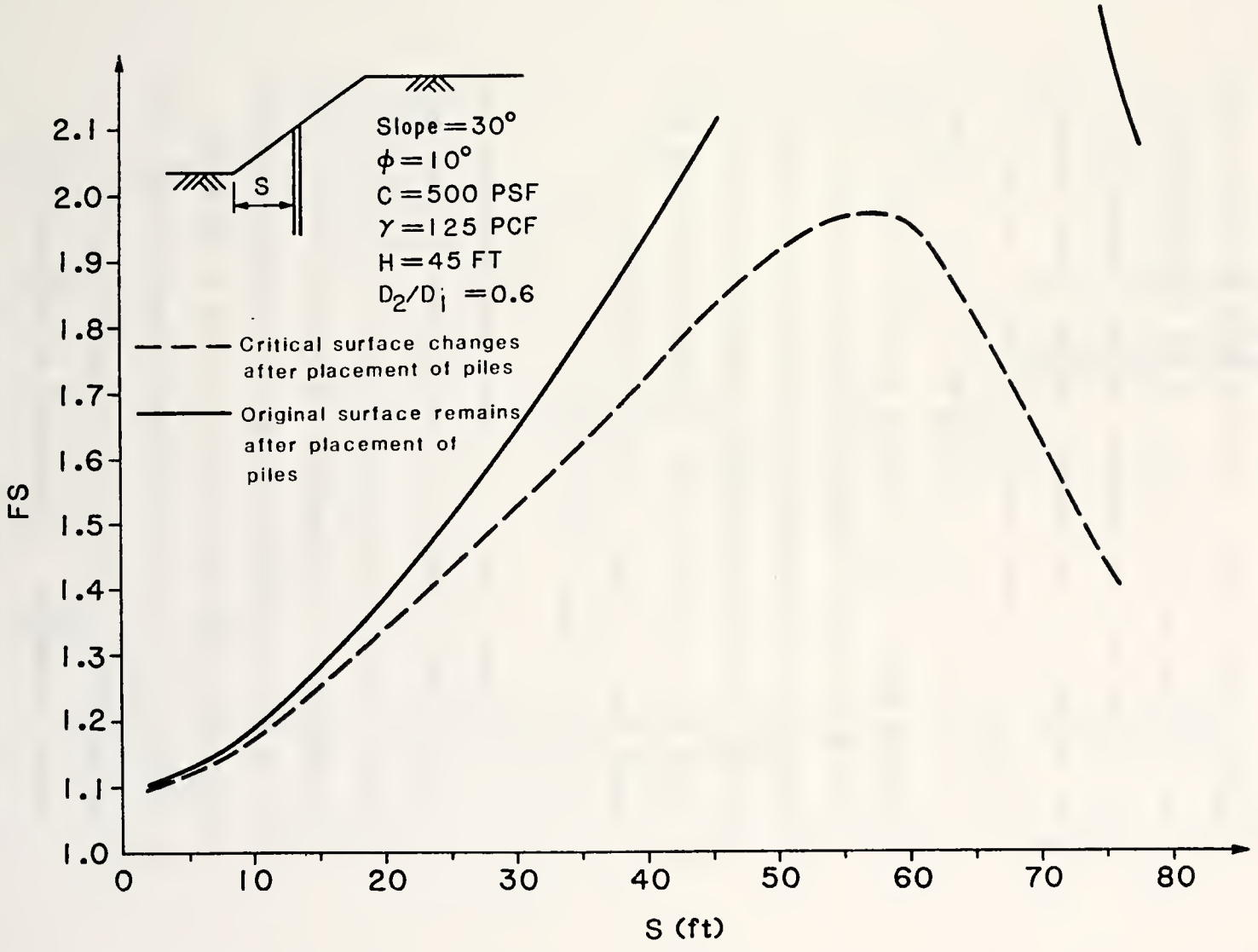

Figure 11 Effect of Pile Location on the Factor of Safety of a Shallow Slope.

These results indicate that the safety factor computed on the original surface becomes very large for S between 45 and 75 feet. For this range of values of S, the force exerted by the piles on the original surface is so large that the components of soil strength are not required for equilibrium. For the actual critical surface, the reaction force F_p is smaller and the actual factor of safety is less than computed for the original surface. The force F_p is plotted against distance S for both the original and the new surface in Figure 12. As an example, for S=45 feet, the force exerted on the slope (original surface) is equal to 49,000 lb/ft, and the factor of safety 2.10, while the actual factor of safety (critical surface) is only 1.82, with a force of 30,000 lb/ft.

The safety factor of a steep slope reinforced with piles reaches a maximum when the piles are placed very close to the top of the slope (Figure 13). The critical surfaces of a steep slope remain deep and the factor of safety keeps increasing as S increases until the piles are placed very close to the top of the slope (Figure 14). Then, the surfaces become shallower, the distance CE′ is very small, and the safety factor starts decreasing. A comparison of the behavior of steep and shallow slopes is given in Figure 15. The normalized safety factor, FS/FS_{max}, where FS_{max} is the

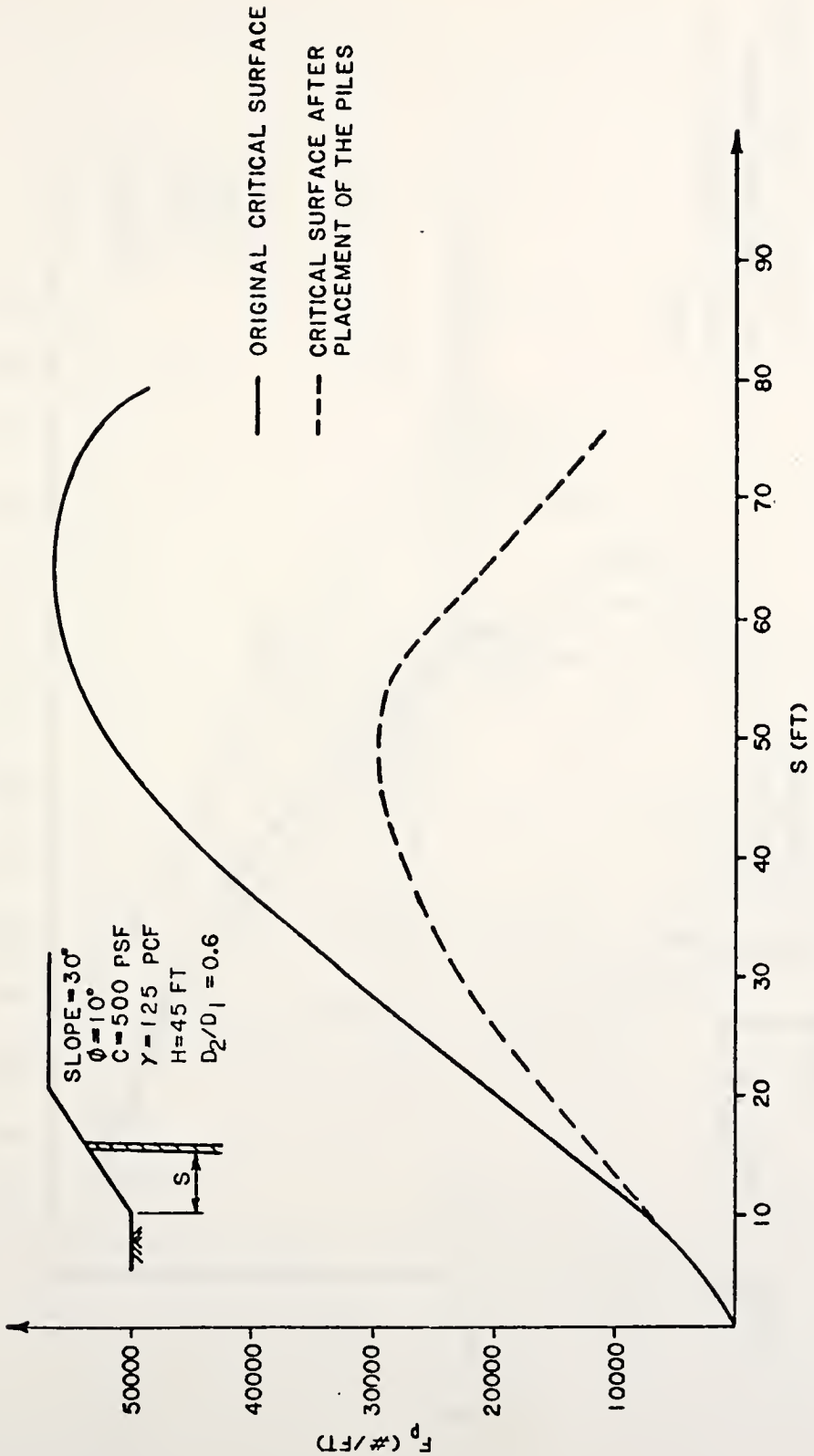

Figure 12 Effect of Pile Location on the Reaction Force Provided by the Piles.

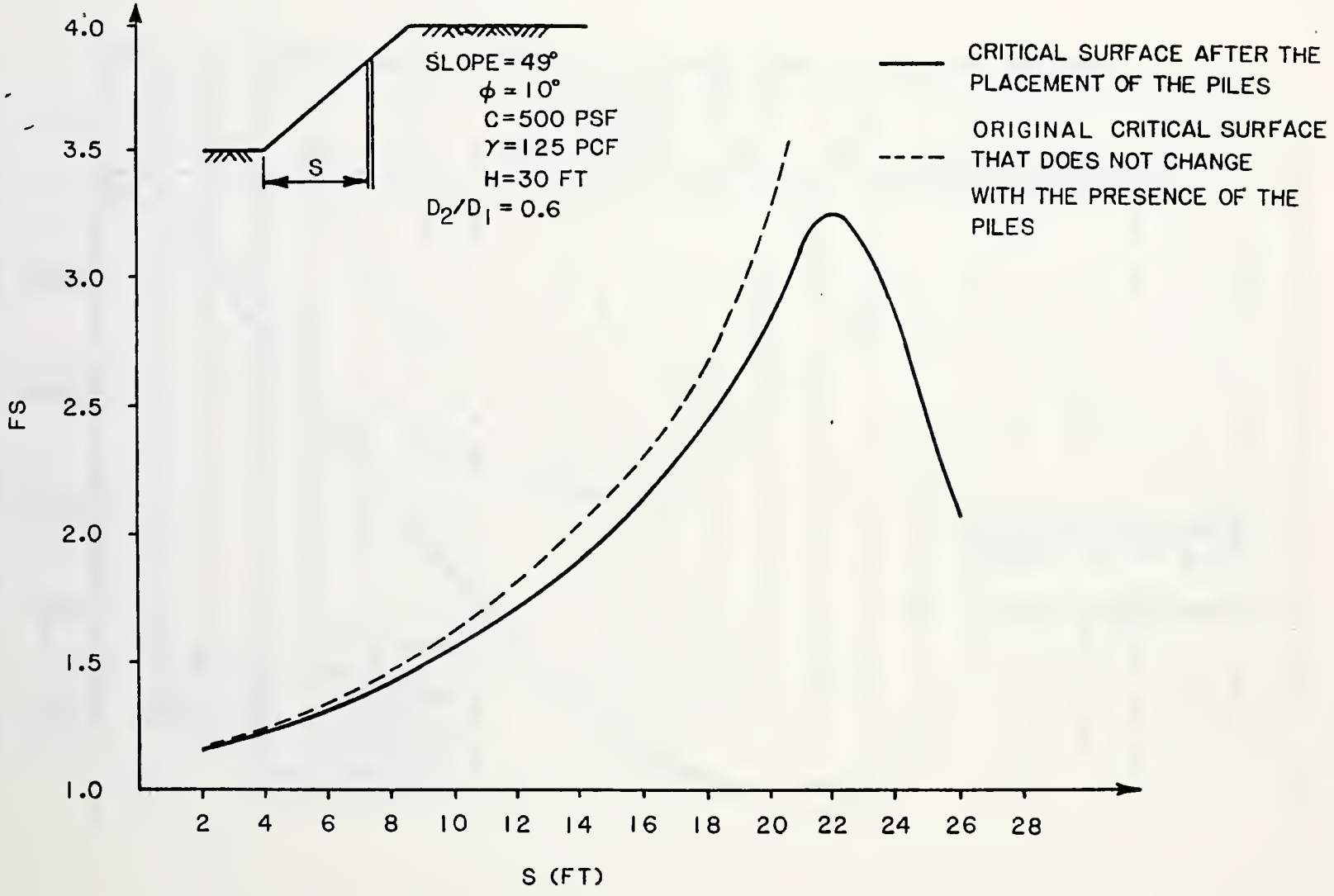

Figure 13 Effect of Pile Location on the Factor of Safety of a Steep Slope.

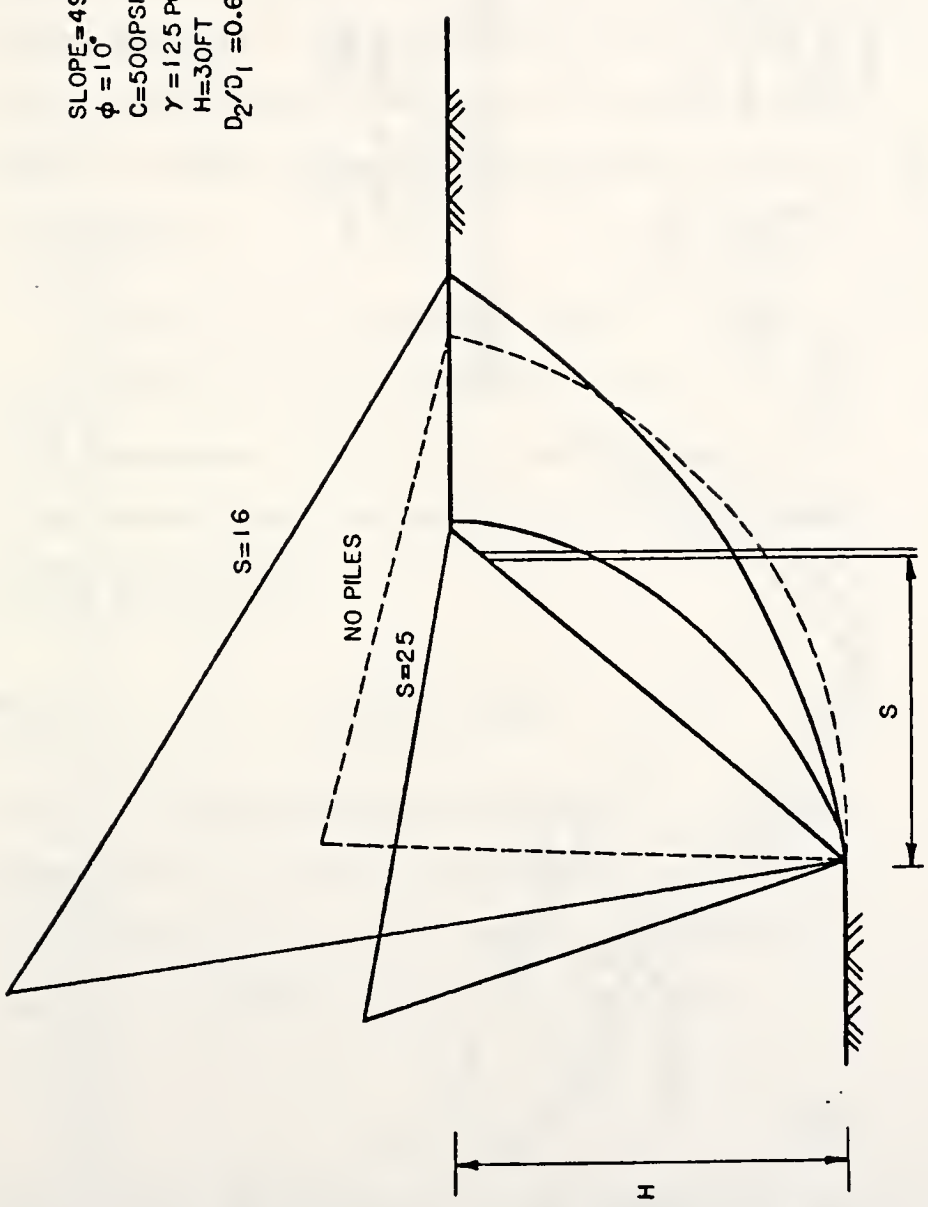

Figure 14 Critical Surfaces of a Steep Slope as a Function of Pile Row Location.

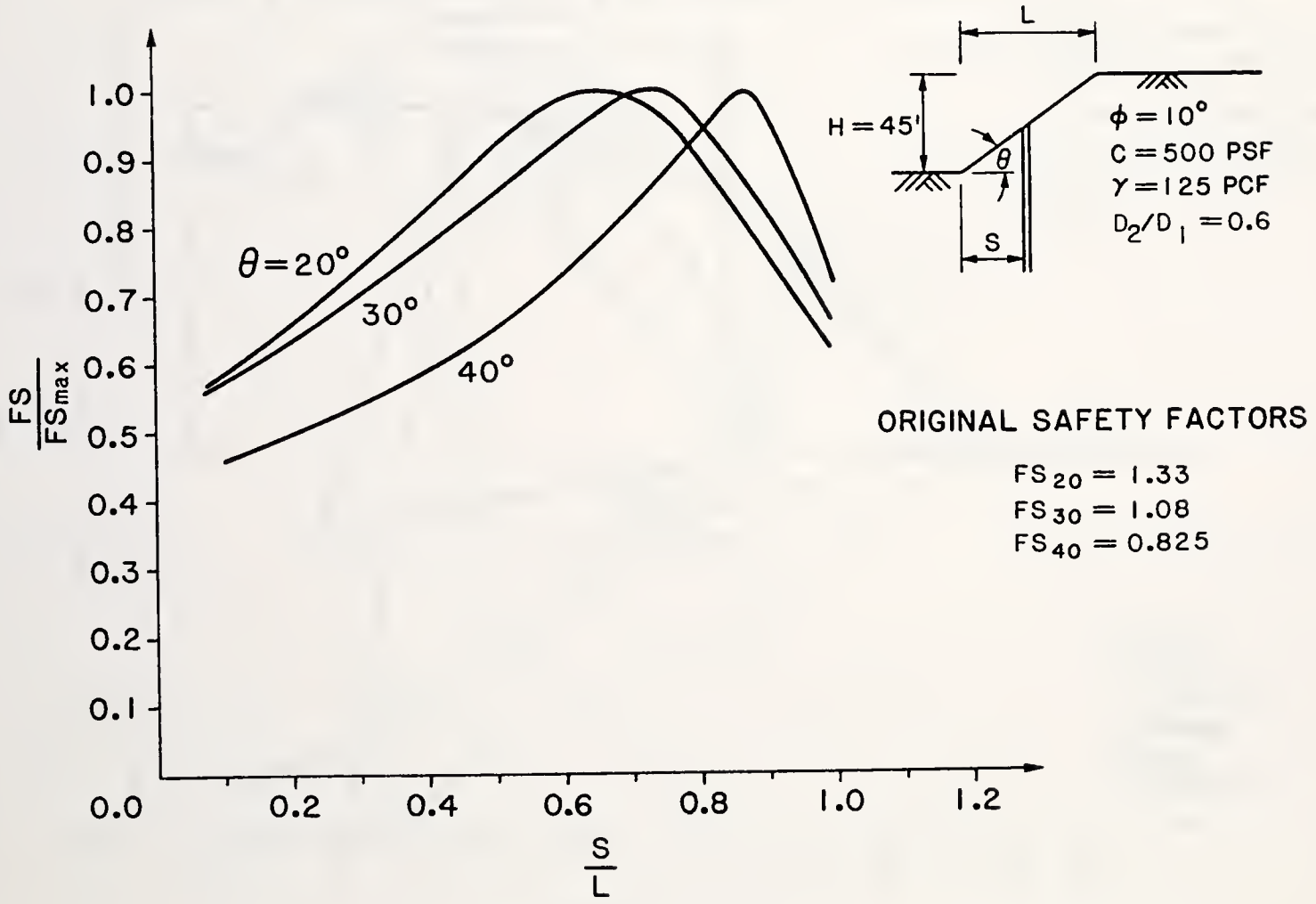

Figure 15 Normalized Curves of the Safety Factor versus Distance S for Different Slopes of the Same Height.

maximum possible safety factor for a constant ratio D_2/D_1, is plotted versus the normalized distance, S/L, where L is the horizontal distance from the toe to the top to the slope. The figure shows that the piles need to be placed closer to the top of a steep slope than that of a shallow slope for a maximum safety factor to be achieved.

According to the assumptions made by Ito and Matsui (1975), the force acting on the slope is equal to F_p regardless of the state of equilibrium of the slope. Based on that assumption, the stability number can be expressed as:

$$c_a/F_c\gamma H = f(F_p) \qquad (3\text{-}37)$$

However, an overestimation of the force F_p can lead to unconservative results in the design of the slope. A more practical approach for design is to introduce the notion of a mobilized lateral force, F_m, where:

$$F_m = F_p/a \qquad (3\text{-}38)$$

with a being greater than 1.0. The mobilized force is used to analyze the slope, but the total force per unit length will be used to design the pile. This results in a conservative design for both the piles and the slope.

It is proposed herein to scale the force F_p by the factor of safety with respect to cohesion of the reinforced slope (i.e. $a = F_c$). The resulting stability number is:

$$c_a/F_c\gamma H = f(F_p/F_c) \qquad (3\text{-}39)$$

This equation can be solved by iteration, until F_c is equal to F_ϕ (for the critical surface, $F_c = F_\phi = FS$). In these iterations, the force F_p is divided by the safety factor, FS (i.e., $F_m = F_p/FS$). Physically, this implies that F_m will be equal to F_p for a slope at the point of incipient failure, but will decrease as the original degree of stability of the slope increases. The critical surface falls between the critical surface obtained without the piles, and the one obtained with the piles providing a fully mobilized force. The curve relating the factor of safety to the distance S (Figure 16) has a shape similar to the previous curves. However, the rate of increase of FS is less than for a fully mobilized force, and the peak value is not as sensitive to S as before. For the example in Figure 10, piles located anywhere between 45 and 65 feet from the toe of the slope provide a factor of safety of about 1.55.

The previous results were obtained for a constant ratio D_2/D_1. The effect of this ratio on the factor of

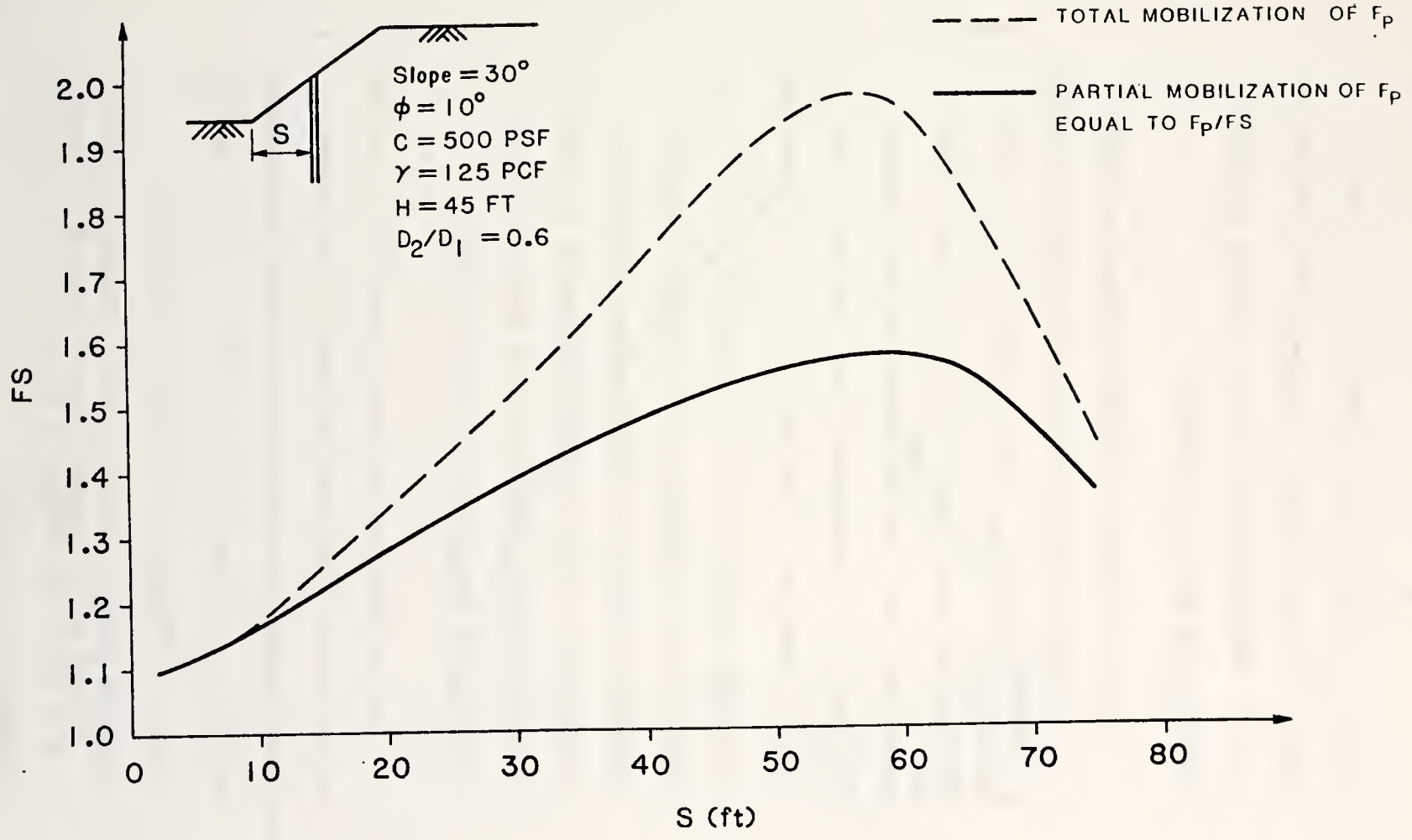

Figure 16 Effect of the Degree of Mobilization of F_p on the Factor of Safety.

safety is illustrated in Figure 17 for a slope of height 30 ft, slope angle 49 degrees, and a distance S of 7 ft. As expected the factor of safety decreases significantly as D_2/D_1 increases.

Figure 18 shows the relation between the safety factor and the distance S for a steep slope for ratios D_2/D_1 of 0.538 (dashed line), and 0.6 (solid line). The force per unit length of the pile given by Equations (3-16) and (3-27) decreases with an increase of the ratio D_2/D_1, regardless of the position of the pile upslope. However, to find the force F_p, the force per unit length diagram has to be integrated over the distance CE which increases as S increases. Hence, the difference between the curves becomes larger as S increases due to the nonlinear increase of F_p with S. After the maximum safety factor is reached, the two curves become asymptotic for the same reason.

The variation of the safety factor with S for different values of the friction angle, ϕ, and cohesion, c, was investigated for a slope of height 18 ft, angle 30 degrees and a ratio D_2/D_1 of 0.716. The shapes of the curves (Figures 19 and 20) are the same as described before. Since F_p is an increasing function of ϕ, c and S, its influence on the safety factor also increases with c and ϕ.

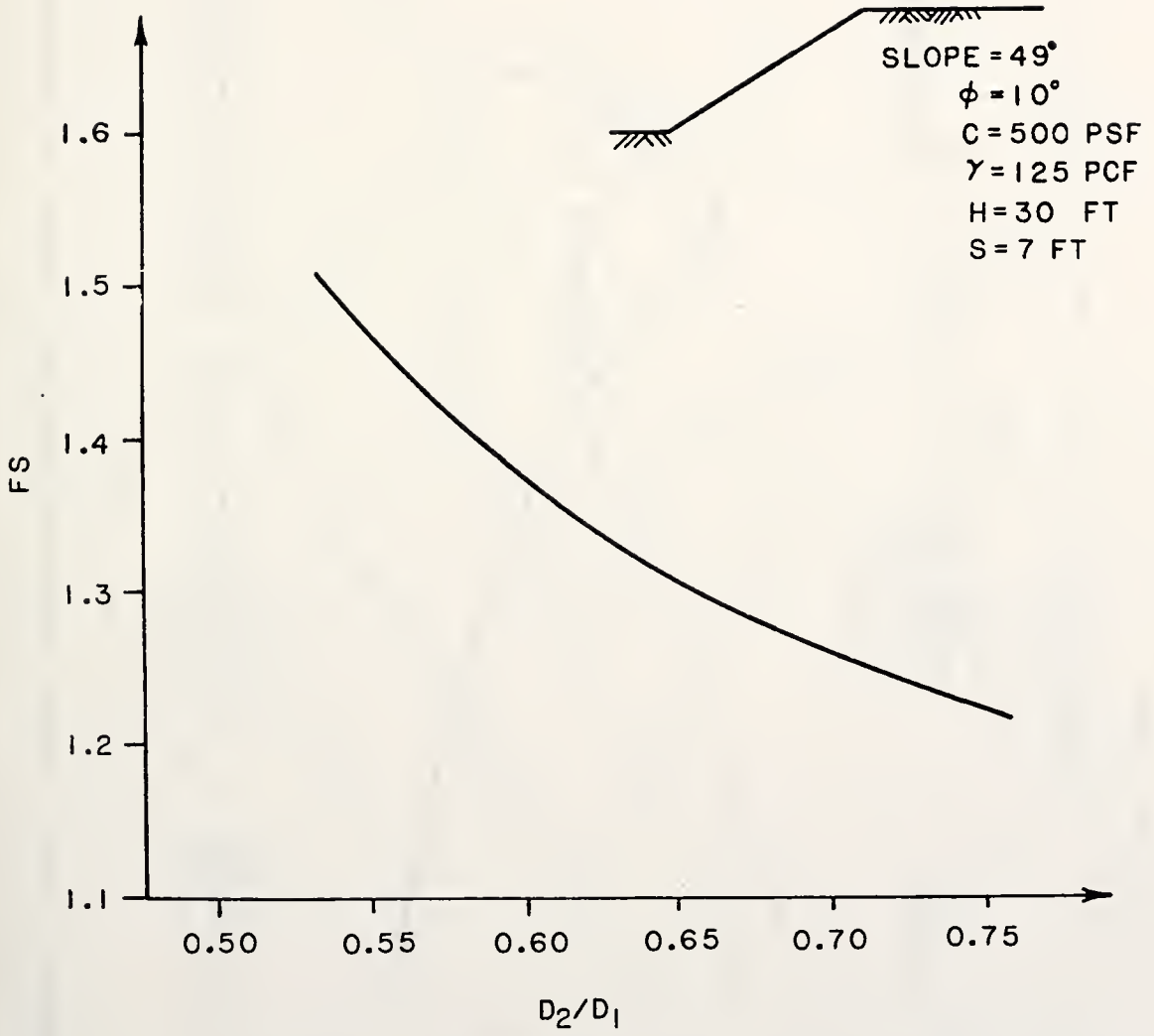

Figure 17 Safety Factor versus Ratio D_2/D_1.

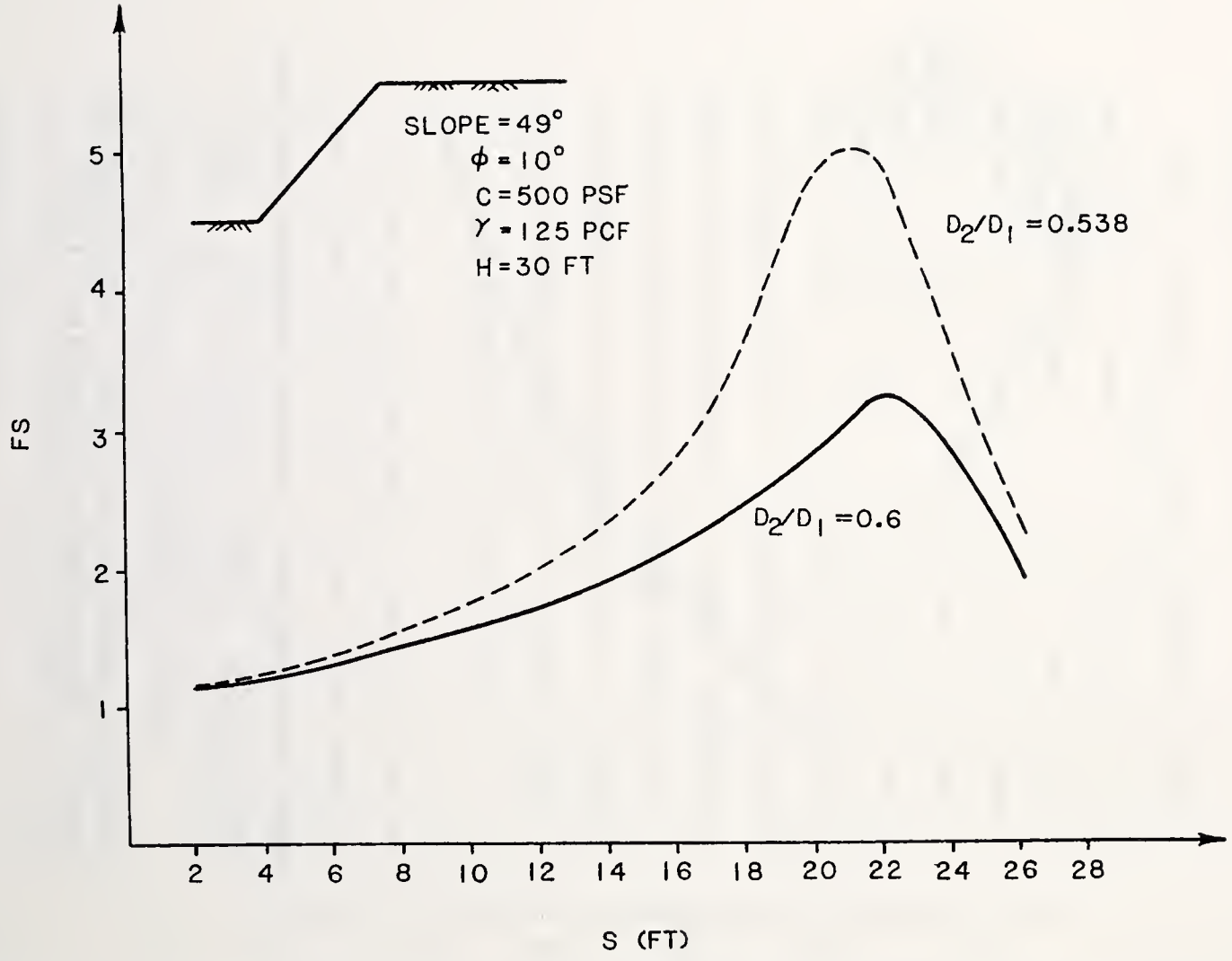

Figure 18 Safety Factor versus Location of the Piles Upslope for Different Ratios of D_2/D_1.

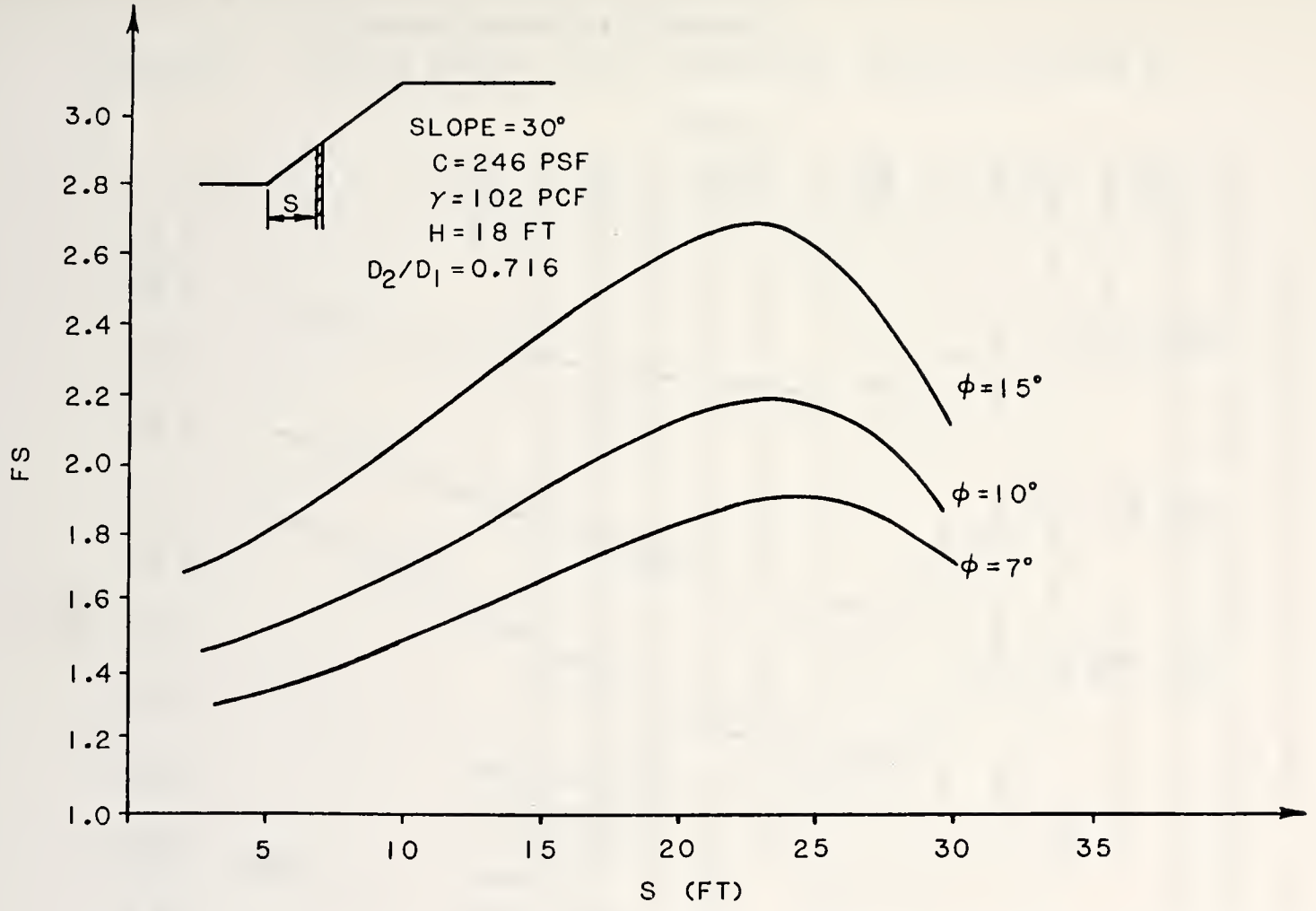

Figure 19 Factor of Safety versus Position of the Piles Upslope for Different Values of Friction Angle.

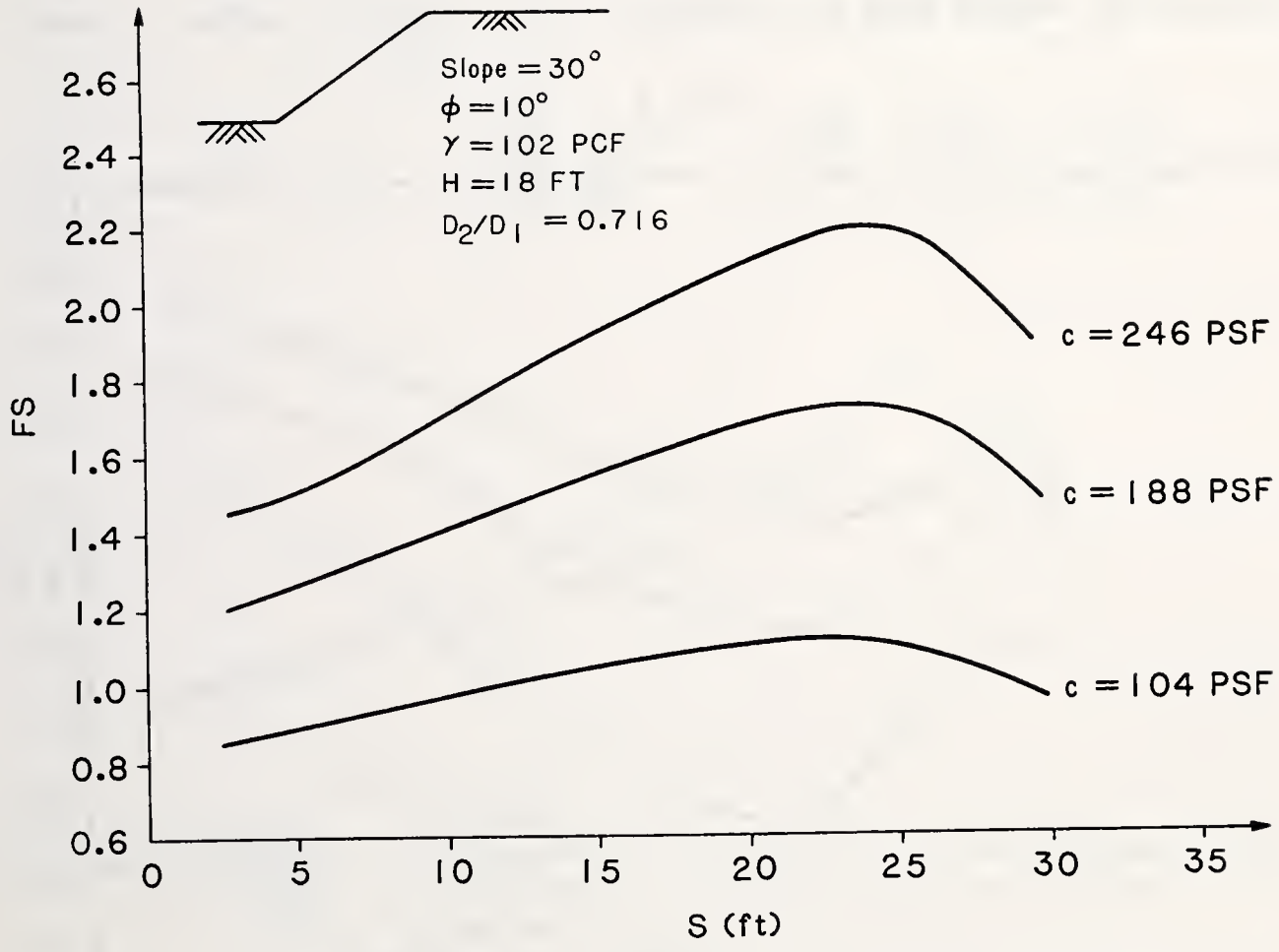

Figure 20 Safety Factor versus Position of the Piles Upslope for Different Values of Cohesion.

SUMMARY

A theoretical approach to the calculation of the lateral forces induced on piles placed in moving soils has been discussed. Field tests indicate the the proposed equations can be used to predict the forces on piles used in the stabilization of slopes. Laboratory tests also validate the major assumptions behind the theoretical derivation. The Friction Circle Method was adapted to incorporate the resistance provided by the row of piles into the slope stability analysis. Computer programs were developed to compute both the lateral force and the factor of safety of the slope. Parametric studies were performed to investigate the effects of the geometric and material parameters on the failure surfaces and factors of safety of typical slopes.

CHAPTER IV. LATERALLY LOADED PILES

In designing the piles to resist lateral loads, the deflection, bending moment and shear force profiles along the piles are required. In this chapter, these values are obtained by solving the differential equation (beam equation) governing the pile displacements. A closed form solution of this equation is used to analyze the pile section which extends above the critical surface. The force intensity on that section is calculated using the principle of plastic deformation derived in Chapter 3 (Equations 3-16, 3-17, and 3-27). A finite difference method is proposed to analyze the pile section which is embedded below the critical surface. The forces acting on this section are calculated using the subgrade reaction model. Several techniques to obtain the modulus of subgrade reaction for the soil or rock below the critical surface are discussed, and recommendations are made for their use in the pile analysis calculations.

THE CONCEPT OF SUBGRADE REACTION

The subgrade reaction model, which was originally proposed by Winkler in 1867, characterizes the soil as a series of unconnected linearly elastic springs (Hetenyi, 1946). The beam (or pile) reaction at a point is simply related to the deflection at that point. One disadvantage of this soil model is the lack of continuity. It is obvious that the displacements at a point are influenced by stresses and forces at other points within the soil. However, the subgrade reaction approach provides a relatively simple and efficient analysis and enables factors such as variation of soil stiffness with depth and layering of the soil profile to be taken into account. It is used here to determine the displacements, bending moments and shear forces in a pile stabilizing a slope.

GOVERNING EQUATIONS

A beam (or pile) supported along its entire length by an elastic medium, and subjected to a system of concentrated forces and distributed loads, deflects and creates continuously distributed reaction forces in the supporting medium. It is assumed that the intensity p

of these forces is proportional to the deflection y of the beam (Figure 21a):

$$p = Ky \tag{4-1}$$

For a pile of width b, the elastic constant K is related to the modulus of subgrade reaction K_S by:

$$K = b\,K_S \tag{4-2}$$

The differential equation governing the beam displacements, y, is obtained by satisfying the equilibrium of an element of length dz (Figure 21b):

$$EI\,\frac{d^4y}{dz^4} = -Ky + q \tag{4-3}$$

where: E = Modulus of elasticity of the pile

I = Moment of inertia of the pile

q = Intensity of the distributed load

The geometry of the pile used to stabilize a slope is shown in Figure 22. The following notation is adopted in this figure and in the sequel:

$\bar{z}$ = depth from the ground surface

z = depth from the sliding surface

q_1 = force/unit length acting on the pile at the ground surface (z = -CE)

q_2 = force/unit length acting on the pile at

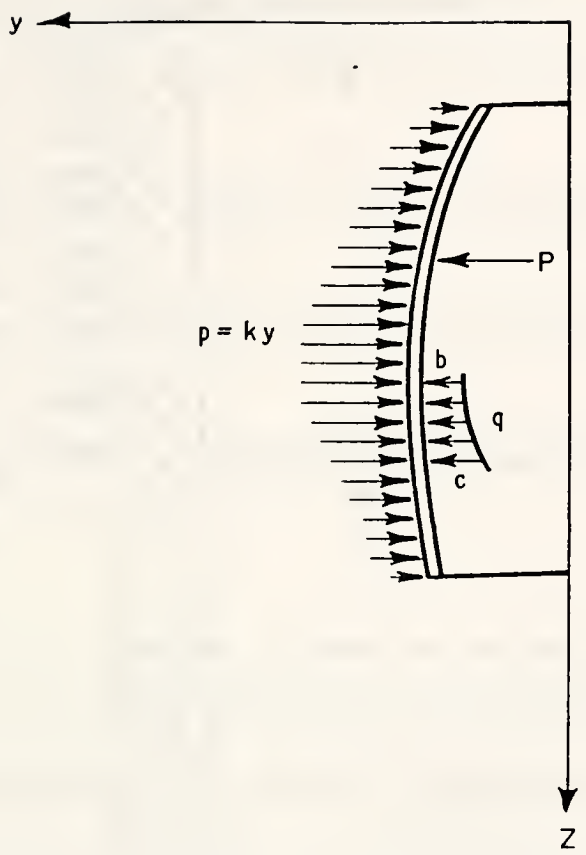

Figure 2 1 (a) Beam on Elastic Foundation
(After Hetenyi, 1946).

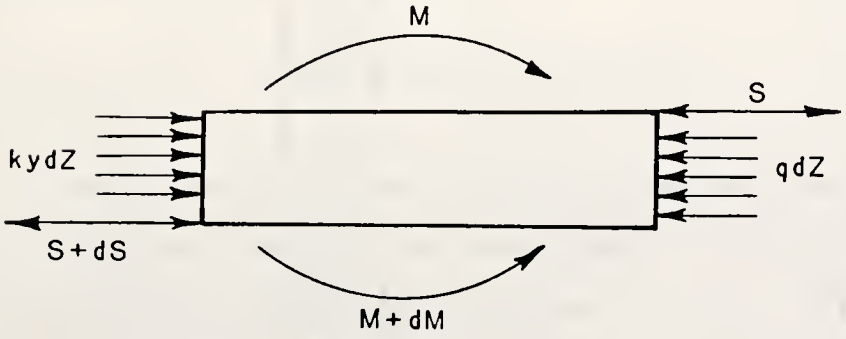

Figure 2 1 (b) Cross Section of a Beam on Elastic Foundation
(After Hetenyi, 1946).

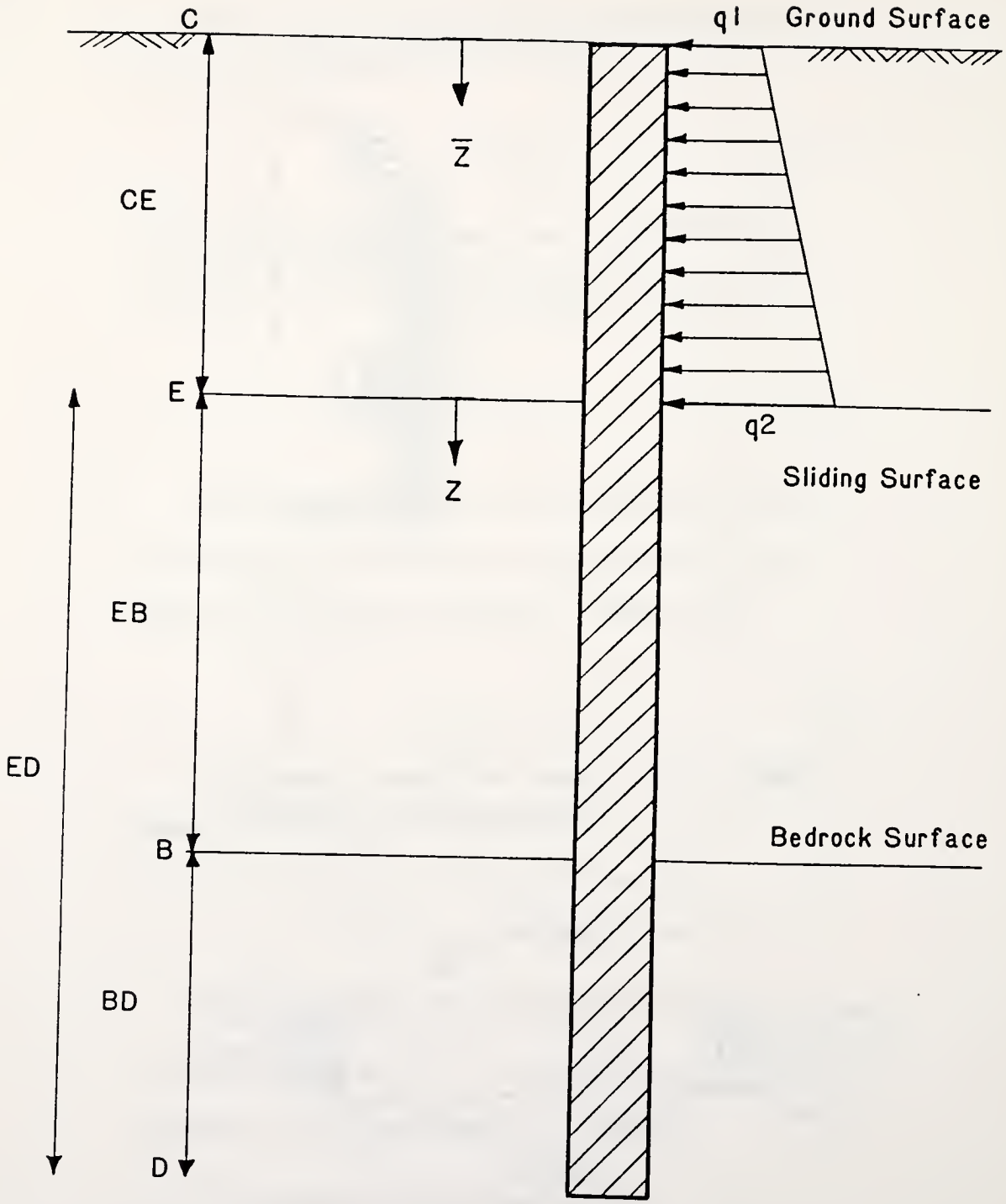

Figure 22 Stabilizing Piles Embedded in Bedrock.

the failure surface (z = 0)

CE = length of pile from ground surface to failure surface

ED = length of pile from failure surface to the pile tip

EB = length of pile from failure surface to bedrock surface

BD = length of pile from bedrock surface to the pile tip

It is convenient to decompose the pile equation into two equations governing the pile deflection above and below the failure surface, respectively:

$$EI \frac{d^4 y_1}{dz^4} = q(z) \qquad (-CE \leq z \leq 0) \qquad (4\text{-}4a)$$

$$EI \frac{d^4 y_2}{dz^4} = -K\, y_2 \qquad (z \geq 0) \qquad (4\text{-}4b)$$

where y_1 and y_2 are the pile deflections above and below the sliding surface respectively, and q(z) is the applied lateral pressure given by:

$$q(z) = q_2 + \frac{q_2 - q_1}{CE} z \qquad (4\text{-}5)$$

where q_1 and q_2 are obtained according to the methodology developed in the previous chapter.

SOLUTION TECHNIQUES

Equation (4-4a) is a simple beam equation and a closed form solution can be readily obtained by direct integration. A finite difference scheme was chosen to solve Equation (4-4b), because closed form solutions to this equation are difficult to develop when the elastic constant is varying with depth.

Closed Form Solution of Equation (4-4a)

The solution to Equation (4-4a) is obtained by direct integration:

$$y_1 = a_0 + a_1 z + a_2 z^2 + a_3 z^3 + \frac{f_1}{24\ EI} z^4 + \frac{f_2\ z^5}{120\ EI} \quad (4\text{-}6a)$$

where

$$f_1 = q_2$$

$$f_2 = \frac{q_2 - q_1}{CE}$$

and a_0, a_1, a_2, and a_3 are constants of integration. The slope, bending moment, and shear force can be obtained by:

$$\text{Slope} = \frac{dy_1}{dz}$$

$$\text{Moment} = -EI \frac{d^2 y_1}{dz^2} \quad (4\text{-}6b)$$

$$\text{Shear} = -EI \frac{d^3 y_1}{dz^3}$$

where

$$\frac{dy_1}{dz} = a_1 + 2a_2 z + 3a_3 z^2 + \frac{f_1}{6\ EI} z^3 + \frac{f_2}{24\ EI} z^4 \qquad (4\text{-}6c)$$

$$\frac{d^2 y_1}{dz^2} = 2a_2 + 6a_3 z + \frac{f_1}{2\ EI} z^2 + \frac{f_2}{6\ EI} z^3$$

and

$$\frac{d^3 y_1}{dz^3} = 6a_3 + \frac{f_1}{EI} z + \frac{f_2}{2\ EI} z^2$$

Sign conventions are given in Figure 21b.

Finite Difference Solution of Equation (4-4b)

A finite difference scheme is used to solve Equation (4-4b). The embedded length below the failure surface is discretized in MT equally spaced intervals of length λ (Figure 23). The interval length is:

$$\lambda = \frac{ED}{MT} \qquad (4\text{-}7)$$

and the location of any node m is defined by:

$$z = m\lambda \qquad (4\text{-}8)$$

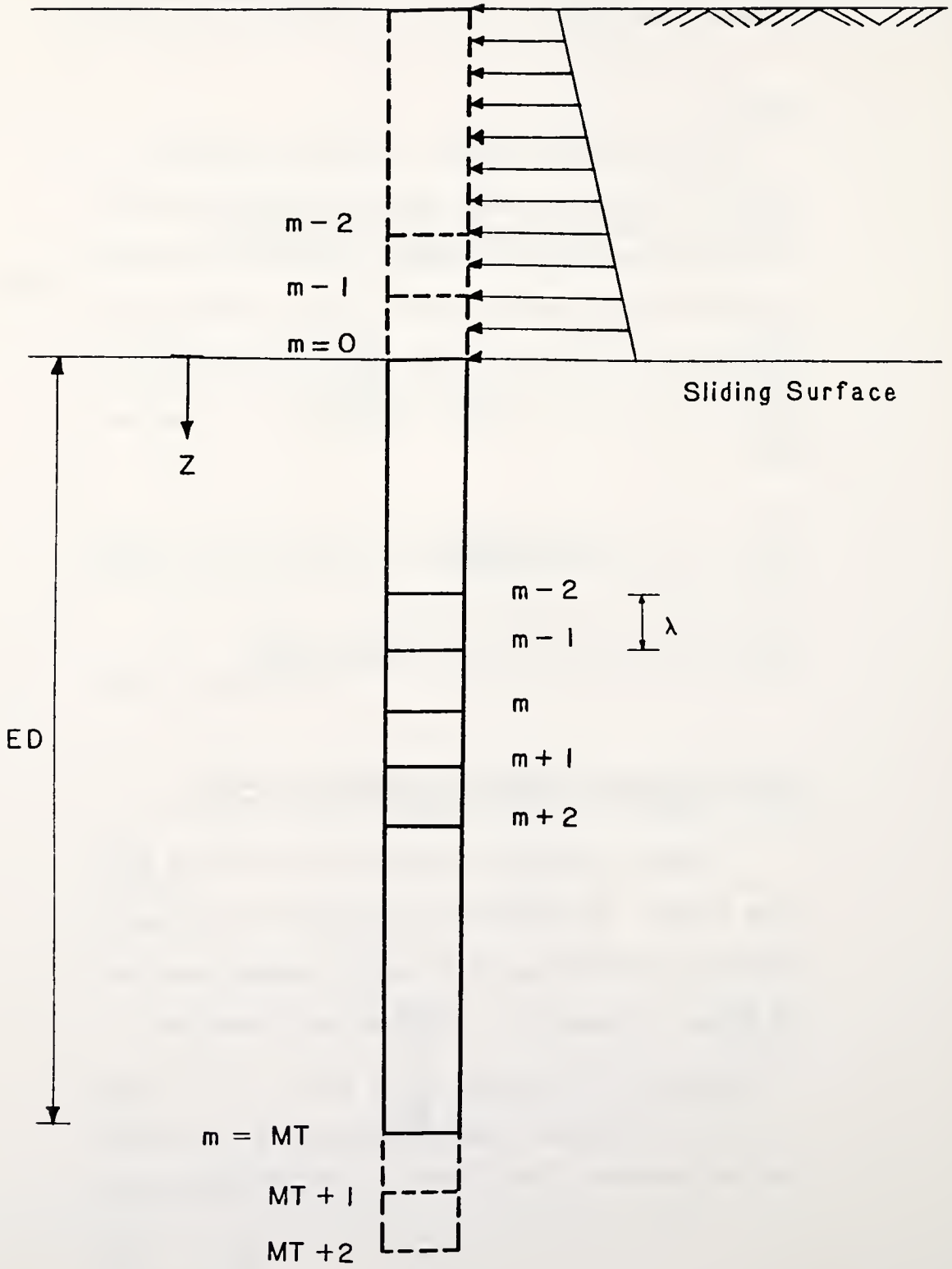

Figure 23 Finite Difference Solution for a Pile.

The discretized form of Equation (4-4b) is:

$$EI \left(\frac{d^4y}{dz^4}\right)_m = b(K_S)_m \, y_m \qquad (4\text{-}9)$$

where EI is the pile stiffness, b is the pile diameter, $(K_S)_m$ is the modulus of subgrade reaction of the soil at node m, y_m is the deflection at point m, and $\left(\frac{d^4y}{dz^4}\right)$ is the fourth derivative of the displacement at node m.

In general, the modulus of subgrade reaction varies with depth, and the value $(K_S)_m$ in Equation (4-9) is different for each node m. This can be taken into account either by inputting a value for the modulus at each node or by introducing an empirical variation with depth. Palmer and Thomson (1948) proposed the following expression for the variation of K_S with depth:

$$K_S = K_{SL} \left(\frac{z}{ED}\right)^n \qquad (4\text{-}10a)$$

where K_{SL} is the value of K_S at the pile tip (z = ED) and n is an empirical constant equal to or greater than zero. According to Poulos and Davis (1980), this equation is widely used to predict pile behavior using the subgrade reaction approach. It is proposed herein to modify this expression to account for soil resistance at the point z = 0 (i.e., at the failure surface).

Also, two different equations will be used to represent the material above and below the soil rock interface, respectively:

$$K_S = K_{S0} + (K_{SL} - K_{S0}) \left(\frac{z}{EB}\right)^{n_1} \qquad z < EB \qquad (4\text{-}10b)$$

$$K_R = K_{R0} + (K_{RL} - K_{R0}) \left(\frac{z - EB}{BD}\right)^{n_2} \qquad z > EB \qquad (4\text{-}10c)$$

where $K_{S0} = K_S$ at $z = 0$

$K_{SL} = K_S$ at $z = EB$

K_R = coefficient of subgrade reaction of the material below $z = EB$

$K_{R0} = K_R$ at $z = EB$

$K_{RL} = K_R$ at $z = ED$

n_1 and n_2 are empirical indices greater than or equal to zero. Typical values for K_S, K_R, n_1 and n_2 will be presented in later sections.

These expressions for the soil constant can be introduced in the finite difference equations to provide a set of simultaneous equations with the nodal displacements as unknowns. Finite difference approximations for the first, second, third and fourth derivatives of the displacement below the critical surface are:

$$\left(\frac{dy_2}{dz}\right)_m = \frac{y_{m+1} - y_{m-1}}{2\lambda}$$

$$\left(\frac{d^2y_2}{dz}\right)_m = \frac{y_{m+1} - 2y_m + y_{m-1}}{\lambda^2} \qquad (4\text{-}11)$$

$$\left(\frac{d^3y_2}{dz^3}\right)_m = \frac{y_{m+2} - 2y_{m+1} + 2y_{m-1} - y_{m-2}}{2\lambda^3}$$

and

$$\left(\frac{d^4y_2}{dz^4}\right)_m = \frac{y_{m-2} - 4y_{m-1} + 6y_m - 4y_{m+1} + y_{m+2}}{\lambda^4}$$

Substituting equations (4-11), (4-10b) and (4-10c) in the finite difference equation (4-9), the following expressions are obtained for each node m

for $z \leq EB$

$$y_{m-2} - 4y_{m-1} + 6y_m - 4y_{m+1} + y_{m+2} = a\ b\left[K_{SO} + (K_{SL} - K_{SO})\left(\frac{z}{EB}\right)^{n_1}\right] y_m \qquad (4\text{-}12a)$$

and for $z > EB$

$$y_{m-2} - 4y_{m-1} + 6y_m - 4y_{m+1} + y_{m+2} = a\ b\left[K_{RO} + (K_{RL} - K_{RO})\left(\frac{z-EB}{BD}\right)^{n_2}\right] y_m \qquad (4\text{-}12b)$$

where

$$a = \frac{\lambda^4}{EI} \qquad (4\text{-}12c)$$

The number of equations that the finite difference scheme generates is equal to the number of nodes, MT + 1. Four additional imaginary points (Figure 23) are needed for the complete solution of equation (4-9), which brings the number of unknowns to MT + 5. In addition to the MT + 5 unknown displacements, four constants of integration, a_0, a_1, a_2, and a_3 are unknowns. This brings the total number of unknowns to MT + 9. The total number of equations includes the MT + 1 finite difference equations, two boundary conditions at the pile top, two boundary conditions at the pile end and four continuity equations (at the failure surface), which brings the total number of equations to MT + 9, equal to the number of unknowns. The boundary conditions and continuity equations are discussed in the following section.

Boundary Conditions

To ensure continuity of the pile at the sliding surface, the following continuity relations are necessary:

$$[y]_{z=0} = [y_1]_{z=0} = [y_2]_{z=0}$$

$$[\theta]_{z=0} = [\frac{dy_1}{dz}]_{z=0} = [\frac{dy_2}{dz}]_{z=0}$$

$$[M]_{z=0} = [\frac{d^2y_1}{dz^2}]_{z=0} = [\frac{d^2y_2}{dz^2}]_{z=0} \qquad (4\text{-}13)$$

$$[V]_{z=0} = [\frac{d^3 y_1}{dz^3}]_{z=0} = [\frac{d^3 y_2}{dz^3}]_{z=0}$$

where θ is the slope of the beam, M is the moment, and V is the shear at $z = 0$.

Using the above equations, the constants of integration a_0, a_1, a_2, and a_3 are expressed as:

$$a_0 = y_0$$

$$a_1 = \frac{y_1 - y_1}{2\lambda}$$

$$2a_2 = \frac{y_1 - 2y_0 + y_{-1}}{\lambda^2} \qquad (4\text{-}14)$$

$$6a_3 = \frac{y_2 - 2y_1 + 2y_{-1} - y_{-2}}{2\lambda^3}$$

In addition to the continuity equations, boundary conditions at the top and bottom of the pile have to be satisfied. If the pile is driven in hard rock a fixed end condition can be assumed; In this case, the deflection and rotation at the end of the pile ($z = ED$) are prevented ($y = 0$, $\theta = 0$), resulting in:

$$y_{MT} = 0$$

$$\text{and,} \qquad y_{MT+1} - y_{MT} - 1 = 0 \qquad (4\text{-}15a)$$

If the pile is driven in soft rock the moment and shear at the end of the pile can be assumed to be zero. In this case, the two boundary conditions become:

$$y_{MT+2} - y_{MT-2} - 2y_{MT+1} + 2y_{MT-1} = 0$$

$$y_{MT+1} - 2y_{MT} + y_{MT-1} = 0 \qquad (4\text{-}15b)$$

At the top of the pile (z = -CE), the boundary conditions depend on the type of restraint. One of the following four conditions should model closely the restraint of the pile in the field.

Condition 1 - Free Head

The moment and the shearing force at the pile head (z = -CE) are zero:

$$[M]_{z=-CE} = -EI \left[\frac{d^2y_1}{dz^2}\right]_{z=-CE} = 0$$

and, (4-16)

$$[V]_{z=-CE} = -EI \left[\frac{d^3y_1}{dz^3}\right]_{z=-CE} = 0$$

Substituting equation (4-6c) into the above equations gives:

$$2a_2 - 6a_3CE + \frac{f_1}{2EI} CE^2 - \frac{f_2}{6EI} CE^3 = 0$$

and, (4-17)

$$6a_3 - \frac{f_1}{EI} CE + \frac{f_2}{2EI} CE^2 = 0$$

The following relations are obtained for the moment and shear by substituting equation (4-14) in equation (4-17):

$$(CE)y_{-2} + (2\lambda - 2CE)y_{-1} - (4\lambda)y_0 + (2\lambda + 2CE)y_1 - (CE)y_2$$

$$= 2\lambda^3 \left[\frac{f_2}{6EI} CE^3 - \frac{f_1}{2EI} CE^2\right] \quad (4\text{-}18a)$$

and

$$-y_{-2} + (2)y_{-1} - (2)y_1 + y_2 = 2\lambda^3\left[\frac{f_1}{EI} CE - \frac{f_2}{2EI} CE^2\right] \quad (4\text{-}18b)$$

Condition 2 - Unrotated Head

The slope and the shearing force at the pile head ($z = -CE$) are zero.

$$[\theta]_{z=-CE} = \left[\frac{dy_1}{dz}\right]_{z=-CE} = 0 \quad (4\text{-}19a)$$

$$[V]_{z=-CE} = -EI \left[\frac{d^3y_1}{dz^3}\right]_{z=-CE} = 0 \quad (4\text{-}19b)$$

The final expression for the shear is the same as

the one for the free head condition (Equation 4-18b). The expression for the slope is obtained by substituting equation (4-6c) into equation (4-19a):

$$a_1 - 2a_2\,CE + 3a_3\,CE^2 - \frac{f_1}{6EI}\,CE^3 + \frac{f_2}{24\,EI}\,CE^4 = 0 \quad (4\text{-}20a)$$

Introducing the values of a_1, a_2, and a_3 given in equation (4-14), the following relation is obtained:

$$(-CE^2)y_{-2}+(2CE^2-4\,\lambda CE-2\,\lambda^2)y_{-1}+(8\,\lambda CE)y_0+(2\,\lambda^2-4\,\lambda CE-2CE^2)y_1$$

$$+\,(CE^2)y_2 = 4\lambda^3\,[\frac{f_1}{6EI}\,CE^3 - \frac{f_2}{2\,\lambda EI}\,CE^4] \quad (4\text{-}20b)$$

Condition 3 - Hinged Head

In the hinged head condition, the deflection and the moment at the pile head (z = -CE) are zero:

$$[y]_{z=-CE} = [y_1]_{z=-CE} = 0 \quad (4\text{-}21a)$$

$$[M]_{z=-CE} = -EI\,[\frac{d^2y_1}{dz}]_{z=-CE} = 0 \quad (4\text{-}21b)$$

The final expression for the moment is the same as the one for free head condition of equation (4-18a). The expression for the deflection is obtained by substituting equation (4-6c) into equation (4-21a):

$$a_0 - a_1 CE + a_2 CE^2 - a_3 CE^3 + \frac{f_1}{24\ EI} CE^4 - \frac{f_2}{120\ EI} CE^3 = 0 \qquad (4\text{-}22a)$$

Introducing a_0, a_1, a_2, and a_3 given in Equation (4-14), the following relation is obtained:

$$(CE^3)y_{-2} + (6\lambda^2 CE + 6\lambda CE^2 - 2CE^3)y_{-1} + (12\lambda^3 - 12\lambda CE^2)y_0$$

$$+(6\lambda CE^2 - 6\lambda^2 CE + 2CE^3)y_1 - (CE^3)y_2 = 12\lambda^3$$

$$[-\frac{f_1}{24EI} CE^4 + \frac{f_2}{120\ EI} CE^5] \qquad (4\text{-}22b)$$

Condition 4 - Fixed Head

The deflection and the slope at the pile head (z = -CE) are zero:

$$[y]_{z=-CE} = [y_1]_{z=-CE} = 0 \qquad (4\text{-}23a)$$

$$[\theta]_{z=-CE} = [\frac{dy_1}{dz}]_{z=-CE} = 0 \qquad (4\text{-}23b)$$

The final expression for the deflection is the same as the one for the hinged head condition given by equation (4-22b), and the expression for the slope is the same as the one for the unrotated head condition given by equation (4-20b).

COEFFICIENTS OF SUBGRADE REACTION

Coefficients of Subgrade Reaction for Soils

The theory of subgrade reaction is used to model the pile-soil interaction below the failure surface. Estimates of the coefficient of subgrade reaction, K_S, are necessary to evaluate the pile displacements, moments and shear forces. In this section, published criteria and data on K_S are reviewed and recommendations are made for their use in design applications.

Two fundamental assumptions are made in this theory: (1) The coefficient of subgrade reaction, K_S, at every point is independent of the contact pressure, and (2) it has the same value at every point along the contact face. Both of these assumptions are approximations of the true conditions. Loading tests performed on actual subgrades show that the settlement does not increase linearly with increasing pressure. The assumption of linearity is usually not valid for pressures larger than about half the ultimate bearing capacity of the soil. This limit should always be taken into consideration in problems involving coefficients of subgrade reaction. The second assumption is also an approximation. The subgrade reaction does not have the same value everywhere on the surface of contact.

Depending on the elastic properties of the subgrade, the pressure at the rim is either greater or smaller than at the center. However, the errors resulting from this assumption can be neglected in practical problems (Terzaghi, 1955).

The coefficient of subgrade reaction is generally determined by one of the following three methods: (1) full scale lateral-loading tests; (2) in situ tests such as plate loading tests, pressuremeter and flat dilatometer tests; and, (3) empirical correlations with other soil properties.

There are several techniques to perform lateral loading tests on piles. One method is to instrument the pile so that the soil pressures and the pile deflections are measured directly (Matlock and Ripperberger, 1958; Bishop and Mason, 1954). This method provides a direct evaluation of K_s, but it is time consuming and relatively expensive. A more convenient procedure is to measure the ground line deflection and rotation and back-calculate K_s assuming an approximate distribution with depth (Reese and Cox, 1969; Welch, 1972). A method that has been used successfully in the past is the placement of strain gages at points along the pile. The strain readings are converted to moment values by the use of calibration curves. Then, deflections are computed from the beam equation.

The use of plate loading tests has been discussed by Terzaghi (1955). The main problem with this approach is the extrapolation of the results. Terzaghi assumed that the coefficient of horizontal reaction for a vertical pile surrounded by sand is a function of the depth below the surface, $\bar{z}$, the width of the pile, b, the effective unit weight of the sand, γ', and the relative density of the sand. At a depth $\bar{z}$ below the surface, the modulus of elasticity of sand, E_s, is given by:

$$E_s = \gamma' \bar{z} A \qquad (4\text{-}24)$$

where A is a dimensionless coefficient depending only on the relative density of the sand (Table 1). Terzaghi proposed the following relationship between K_S and E_s:

$$K_S = \frac{E_s}{1.35b} \qquad (4\text{-}25a)$$

Substitution of equation (4-25a) into equation (4-24) gives:

$$K_S = \frac{A\gamma'}{1.35} \frac{\bar{z}}{b} \qquad (4\text{-}25b)$$

For a pile embedded in stiff clay, Terzaghi recommended a constant value of K_S with depth:

Table 1

Values of dimensionless coefficient A, to calculate k_s (tons/ft^3) for a pile embedded in moist or submerged sand (Terzaghi, 1955).

Relative density of sand	Loose	Medium	Dense
Range of values of A	100-300	300-1000	1000-2000
Recommended values of A	200	600	1500

$$K_S = \frac{1}{1.5\ b}\ \overline{K_{S1}} \qquad (4\text{-}26)$$

where $\overline{K_{S1}}$ is the coefficient of vertical subgrade reaction of a plate of width equal to one foot. In this equation b is in feet, and the value of K_S is obtained in tons/ft^3. Recommended values of $\overline{K_{S1}}$ are given in Table 2.

Additional suggestions for the calculation of K_S include the equations proposed by Chen (1978), which are based on the pressuremeter modulus, E_d. In cohesionless soil:

$$K_S = 3.3\ \frac{E_d}{b} \qquad (4\text{-}27a)$$

and in cohesive soil:

$$K_S = 1.6\ \frac{E_d}{b} \qquad (4\text{-}27b)$$

where E_d is the pressuremeter modulus in tons/ft^2 and K_S is given in tons/ft^3.

Another relation that uses the pressuremeter modulus was derived by Yoshida and Yoshinaka (1972):

$$K_S = \frac{2.31}{b}\ E_d\ (b)^{1/4} \qquad (4\text{-}28)$$

Empirical correlations between K_S and the Young's Modulus, E_s, have been suggested by several authors. Vesic (1961) extended the work of Biot (1937) for a

Table 2

Values of $\overline{k_{S1}}$ in tons/ft^3 for a square plate (1x1 ft) resting on precompressed clay (Terzaghi, 1955).

Consistency of Clay	Stiff	Very Stiff	Hard
Values of q_u (tons/ft^2)	1-2	2-4	>4
Range for $\overline{k_{S1}}$ (square plates)	50-100	100-200	>200
Recomended values (square plates)	75	150	300

beam placed on an infinite elastic foundation and subject to a concentrated load. His results indicated that the coefficient of subgrade reaction for a long beam can be expressed as:

$$K_S = \frac{0.65}{b} \left[E_s \frac{b^4}{EI}\right]^{1/12} \frac{E_s}{1 - \mu_s^2} \qquad (4\text{-}29a)$$

where μ_s is the Poisson ratio and E_s is the Young's modulus of the subgrade. Broms (1964) and Francis (1964) suggested that this equation can be applied to piles, and they used it to estimate the modulus K_S for the lateral resistance of piles. Francis, however, considered that the medium extends on both sides of the pile, and concluded that the above expression should be doubled:

$$K_S = \frac{1.30}{b} \left[E_s \frac{b^4}{EI}\right]^{1/12} \frac{E_s}{1 - \mu_s^2} \qquad (4\text{-}29b)$$

Equation (4-29b) can be used for either sand or clay subgrades. For long piles in soft clay, Gibson, in an unpublished report, suggested that a soil stiffness E_s be assessed for two different conditions, instantaneous and long term loading. Following this suggestion, E_s may be calculated as either: (1) a secant modulus measured at 50% of the ultimate undrained triaxial compression test for instantaneous

loading (μ_s should be taken as 0.5 for this condition); or (2) as $\frac{3(1 - 2\mu)}{m_v}$ for the long term condition (μ_s = 0.40), where m_v is the modulus of volume decrease obtained from oedometer or drained triaxial tests. For piles in sand, any of the equations given in Table 3 can be used to calculate the Young's modulus. These equations have been used to predict vertical static compression and can be used in the case of lateral loading under the assumption that the soil is isotropic and homogeneous. Correlations between E_s and the cone resistance, q_c, need some additional experimental verification and should be used with caution (Jamiolkowski and Garassino, 1977).

In general, it is expected that the coefficient of subgrade reaction will increase with depth in sand and will either increase or remain constant with depth in clay. Terzaghi (1955) recommends values of nl = 1 (to be used in Equation 4-10) in sand and nl = 0 in clay. Davisson and Prakash (1967) suggested that nl = 0.15 is a more realistic value for clay under undrained conditions. Broms (1974) stated that the coefficient of subgrade reaction for cohesive soils is approximately proportional to the unconfined compressive strength. As the unconfined compressive strength of normally consolidated clay increases linearly with depth, the coefficient of subgrade reaction should increase in a similar manner.

Table 3

Young's modulus for vertical static compression of sand from standard penetration number and static cone resistance (Das, 1983)

Reference	Relationship	Soil types	Basis	Remarks
Schultze and Meizer (1965)	$E_s = \nu\sigma_o^{0.522}$ kg/cm^2 $\nu = 246.2 \log N - 263.4\ \sigma_o + 375.6 \pm 57.6$ $0 < \sigma_o < 1.2$ kg/cm^2 σ_o = effective overburden pressure	Dry sand	Penetration tests in field and in test shaft. Compressibility based on e, e_{max}, and e_{min} (Schultze and Moussa (1961)	Correlation Coefficient = 0.730 for 77 tests
Webb (1969)	$E_s = 5(N + 15)$ ton/ft^2 $E_s = 10/3(N + 5)$ ton/ft^2	Sand Clayey sand	Screw plate tests	Below water table
Farrent (1963)	$E_s = 7.5(1 - \nu^2)N$ ton/ft^2 ν = Poisson's ratio	Sand	Terzaghi and Peck loading settlement curves	
Begemann (1974)	$E_s = 40 + C(N - 6)$ kg/cm^2 $N > 15$ $E_s = C(N + 6)$ kg/cm^2 $N < 15$ C = 3 (silt with sand) to 12 (gravel with sand)	Silt with sand to gravel with sand		Used in Greece
Trofimenkov (1974)	$E_s = (350$ to $500) \log N$ kg/cm^2	Sand		U.S.S.R. practice

N = standard penetration number

Table 3 - continued

Reference	Relationship*	Soil types	Basis	Remarks
Schultze and Meizer (1965)	$E_s = \nu\sigma_o^{0.522}$ kg/cm^2 $\nu = 246.2\log N - 263.4\ \sigma_o + 375.6 \pm 57.6$ $0 < \sigma < 1.2$ kg/cm^2 σ_o = effective overburden pressure	Dry sand	Penetration tests in field and in test shaft. Compressibility based on e, e_{max}, and e_{min} (Schultze and Moussa, (1961)	Correlation coefficient = 0.730 for 77 tests
Webb (1969)	$E_s = 5(N + 15)$ ton/ft^2 $E_s = 10/3(N + 5)$ ton/ft^2	Sand Clayey sand	Screw plate tests	Below water table
Farrent (1963)	$E_s = 7.5(1 - \ ^2)N$ ton/ft^2 = Poisson's ratio	Sand	Terzaghi and Peck loading settlement curves	
Begemann (1974)	$E_s = 40 + C(N - 6)$kg/cm^2 $N > 15$ $E_s = C(N + 6)$ kg/cm^2 $N < 15$ C = 3(silt with sand) to 12 (gravel with sand)	Silt with sand to gravel with sand		Used in Greece
Trofimenkov (1974)	$E_s = (350$ to $500)\log N$ kg/cm^2	Sand	U.S.S.R. practice	

Table 3 - continued

Reference	Relationship	Soil types	Remarks
Buisman (1940)	$E_s = 1.5\ q_c$	Sands	Overpredicts settlements by a factor of about 2
Trofimenkov (1964)	$E_s = 2.5\ q_c$ $E_s = 100 + 5\ q_c$	Sand	Lower limit Average
De Beer (1967)	$E_s = 1.5\ q_c$	Sand	Overpredicts settlements by a factor of 2
Schultze and Melzer (1965)	$E_s = \frac{1}{m_v}\ \nu\sigma_o^{0.522}$ $\nu = 301.1 \log q_c - 382.3\ \sigma_o + 60.3 \pm 50.3$ σ_o = effective overburden pressure	Dry sand	Based on field and lab penetration tests - compressibility based on e, e_{max}, and e_{min} Correlation coefficient = 0.778 for 90 tests valid for σ_o = 0 to 0.8 kg/cm^2
Bachelier and Parez (1965)	$E_s = \alpha q_c$ α = 0.8 to 0.9 α = 1.3 to 1.9 α = 3.8 to 5.7 α = 7.7	Pure sand Silty sand Clayey sand Soft clay	
Thomas (1968)	$E_s = \alpha q_c$ α = 3 to 12	3 sands	Based on penetration and compression tests in large chamber Lower values of α at higher values of q_c; attributed to grain crushing

Table 3 - continued

Reference	Relationship	Soil types	Remarks
Webb (1969)	$E_S = \frac{5}{2}(q_c + 30)$ ton/ft^2 $E_S = \frac{5}{3}(q_c + 15)$ lb/ft^2	Sand below water table Clayey sand below water table	Based on screw plate tests: correlated well with settlement of oil tanks
Vesic (1970(	$E_S = 2(1 + D_R^2)q_c$ D_r = relative density	Sand	Based on pile load tests and assumptions concerning state of stress
Schmertmann (1970(	$E_S = 2q_c$	Sand	Based on screw plate tests
Bogdanovic (1973)	$E_S = \alpha q_c$ $q_c = 40$ kg/cm^2 $\alpha = 1.5$ $20 < q_c < 40$ $\alpha = 1.5$ to 1.8 $10 < q_c < 20$ $\alpha = 1.8$ to 2.5 $5 < q_c < 10$ $\alpha = 2.5$ to 3.0	Sand, sandy gravels Silty saturated sands Clayey silts with silty sand and silty saturated sands with silt	Based on analysis of soil settlements over a period of 10 years
Schmertmann (1974)	$E_S = 2.5q_c$ $E_S = 3.5q_c$	NC sands NC sands	L/B = 1 to 2, axisymmetric L/B $\geq$ 10, plane strain
De Beer (1974)	$E_S = 1.6q_c - 8$ $E_S = 1.5q_c, q_c > 30$ kg/cm^2 $E_S = 3q_c, q_c < 30$ kg/cm^2 $E_S > 1.5q_c$ or $E_S = 2q_c$ $E_S = 1.9q_c$	Sand Sand Sand Sand	Bulgarian practice Greek practice Italian practice

Table 3 - continued

Reference	Relationship	Soil types	Remarks
	$E_S = \frac{5}{2}(q_c + 3200)$ kN/m^2	Fine to medium sand	South African practice
	$E_S = \frac{5}{3}(q_c + 1600)$ kN/m^2	Clayey sands, PI<15%	
	$E_S = \alpha q_c$, $1.5<\alpha<2$	Sands	U.K. practice
Trofimenkov (1974)	$E_S = 3q_c$	Sands	U.S.S.R. practice
	$E_S = 7q_c$	Clays	

The values of the coefficient of subgrade reaction can be obtained by: (1) the use of empirical formulas (equations 4-25b and 4-26); (2) the use of in situ parameters (equations 4-27a to 4-28); and, (3) the use of empirical correlations (Equation 4-29b). These equations can be used in the pile analysis computations. As an example, assuming that the material below the critical surface is cohesionless, either equation (4-25b), (4-27a) or (4-29b) can be used to determine the coefficient of subgrade reaction. When equation (4-25b) is used, the constants K_{S0} and K_{SL} needed in equation (4-12a) can be obtained by equating $\bar{z}$ to CE and CB, respectively (Figure 22). The value of nl for this case is equal to 1. When Equation (4-27a) is used, a value of $(K_S)_m$ can be introduced at each node m (m = 0 to m = MT, as shown in Figure 23). When Equation (4-29b) is used, the values of K_{S0}, K_{SL}, and nl depend on the equation chosen to calculate E_s (Table 3).

Three methods to calculate the modulus of subgrade reaction in soils have been reviewed. The use of any of these methods can provide satisfactory results since the computed pile deflections, bending moments, and other quantities will not be very sensitive to small changes in soil modulus values (Matlock and Reese,

1960). However, the use of pressuremeter data is preferable since it eliminates the approximations required to interpret plate load test data and empirical correlations. In addition, the pressuremeter provides modulus values in the horizontal direction which are desirable in the case of horizontally loaded piles.

Coefficients of Subgrade Reaction for Rocks

A soft rock can be treated as a soil in the sense that it can be given a value K_R equivalent to K_S in soil. Geologists overlook this value and prefer to use load-deformation curves to predict the deformation modulus or in-situ Young's Modulus, E_R, of the rock. Therefore, it is necessary to either perform field tests or use correlations between K_R and reported values of the Young's modulus.

In situ methods of directly obtaining p-y curves for rock are: (1) jacking tests (using thin flatjacks); (2) dilatometer tests; and, (3) pressuremeter tests. The jacking test is similar in principle to the plate load test. The deformation resulting from the application of a load of known intensity to a given rock area is measured and the deformation modulus is calculated by using the theory of elasticity. Performing jacking tests for a small scale job is not practical (Wallace, et al., 1970). Data from such tests are

sometimes available for rocks frequently encountered in a given region. Dilatometer tests have several advantages over the jacking tests: (1) the dilatometer can be inserted in boreholes of conventional diameter for site investigation; (2) the tests can be performed at great depths; and, (3) large radial pressures can be applied (Rocha, 1970). Pressuremeter tests have also been used successfully in the past for the calculation of the modulus of soft rocks (Dixon, 1970).

A load-deformation curve such as the one shown in Figure 24 can be obtained from any of these three tests. The modulus of this curve is a subgrade reaction modulus. A conservative value of the modulus is obtained by taking the slope of the curve from the origin to the point of total deformation and maximum load. Unfortunately, these values are rarely reported in the literature, but are merely used for the calculation of the deformation modulus E_R.

When field tests cannot be performed, K_R can be back-calculated using the values reported in the literature for the deformation modulus, E_R. For example, if the rock is considered elastic, the following relation exists for a modulus obtained with a jacking test:

$$y = p\ b\ \left(\frac{1 - \mu^2}{E_R}\right) \qquad (4\text{-}30)$$

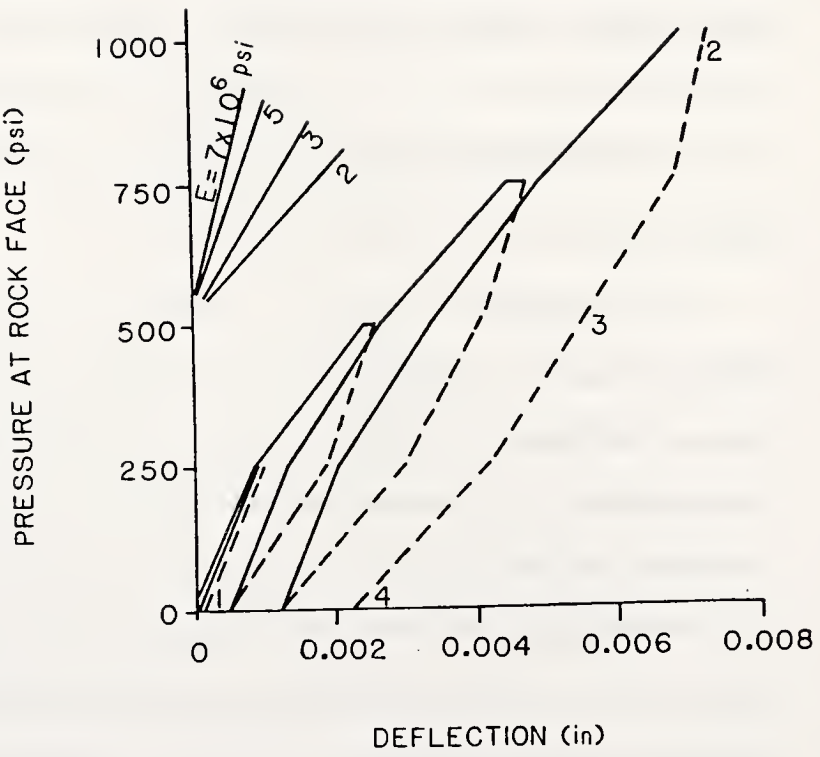

Figure 24 Load deformation Curve from Plate Jack Test (After Coon and Merritt, 1970).

where b is the diameter or side of the loading plate and p is the pressure applied to the plate. For a 1x1 ft square plate, Equation (4-30) can be written as:

$$\frac{P}{y} = \frac{E_R}{(1 - \mu^2)} \qquad (4\text{-}31)$$

If the in situ modulus, E_R, is not available, it can be obtained by using the laboratory Young's modulus, E_{t50}, and the Rock Quality Designation, RQD. E_{t50} is considered to be the characteristic modulus of the intact rock, and is the slope of the stress-strain curve at 50 percent of the unconfined strength. Typical values of E_{t50} are given in Table 4. It has been found that there is a correlation between RQD and the ratio of the moduli $\frac{E_R}{E_{t50}}$ (Figure 25 and Table 5). These empirical relationships are based upon data from twelve construction projects (Coon and Merritt, 1970).

SUMMARY

A method to analyze piles embedded through a failure surface into either bedrock or a stiff soil layer has been developed. The portion of the pile above the failure surface has been analyzed using a closed form solution. The portion below the failure surface has been analyzed using a finite difference

Table 4
Modulus of elasticity of rocks.

Rock	Modulus of Elasticity $\times 10^6$ PSi	Poisson's Ratio μ
Granite	2.77-8.3	.15-.24
Gneiss	2.7-8.3	.11
Quartzite	5.7-8.3	
Schist	.6-2.8	.08-.20
Sandstone	.69-11.1	.17
Shale	1.4-4.9	
Mudstone	2.8-6.9	
Coal	1.4-2.8	
Limestone	1.4-11	.16-.23

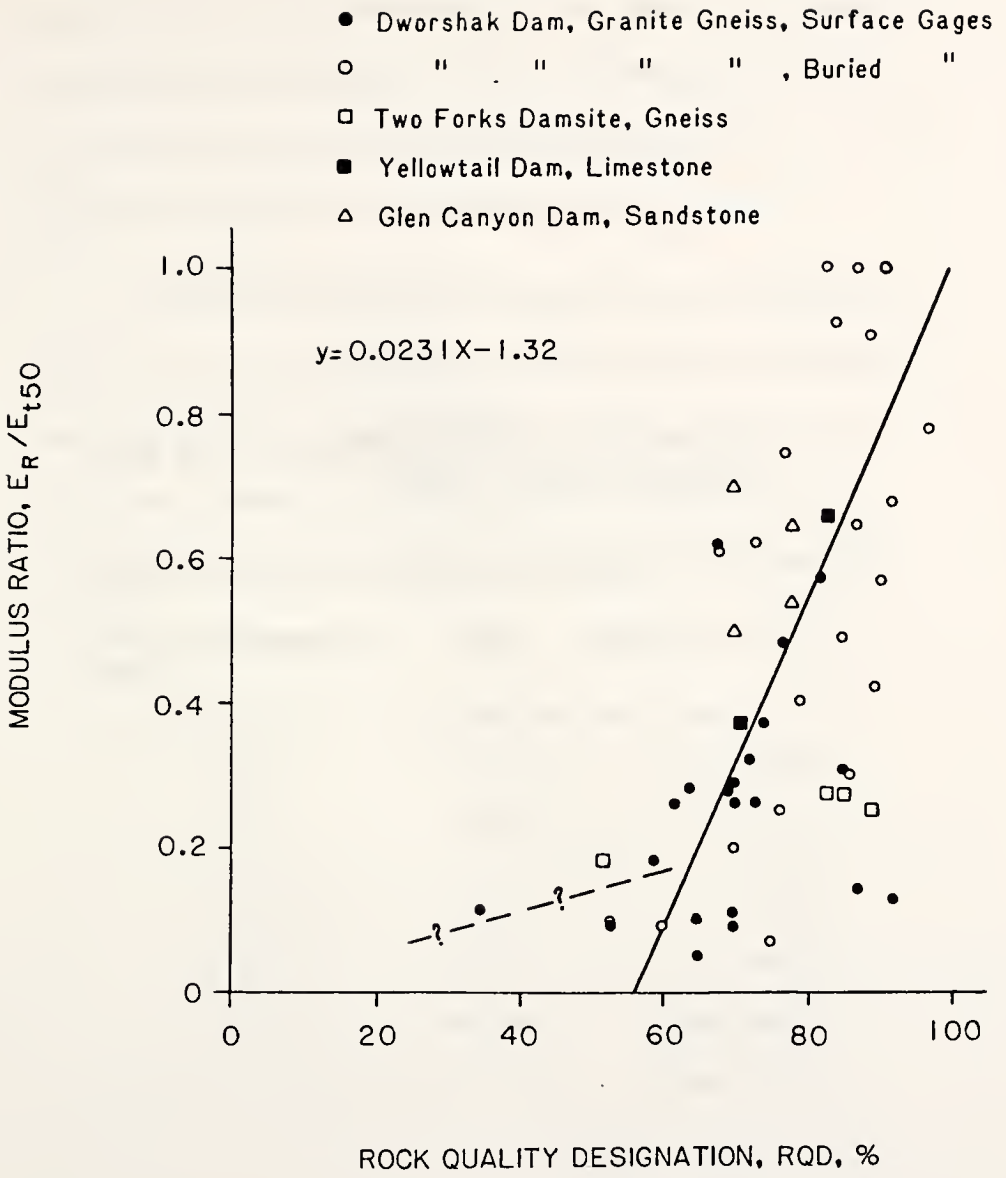

Figure 25 Comparison of RQD and the Modulus Ratio E_R/E_{t50} (After Coon and Merritt, 1970).

Table 5
Correlation between deformability and RQD
(Coon and Merritt, 1970).

Classification	RQD	Deformability $\frac{E_R}{E_{t50}}$
Very Poor	0-25	>0.2
Poor	25-50	>0.2
Fair	50-75	0.2-0.5
Good	75-90	0.5-0.8
Excellent	90-100	0.8-1.0

solution and the assumptions of the theory of a beam on an elastic foundation. Finally, recommendations for the values of the subgrade reaction, K_S and K_R, as well as their variations with depth, have been made.

A computer program which uses these concepts has been developed to calculate the displacement, bending moment and shear force along the length of the pile. The user's manual, a listing of the program, and an example of the input and output are given in Appendix D.

CHAPTER V. SLOPE STABILIZATION AND PILE DESIGN

Effective stabilization of a slope with piles requires not only that the stability of the slope be assured, but also that the piles be adequately dimensioned. In this section, the parameters that affect the stability of the slope and the design of the piles are analyzed. A step-by-step procedure is proposed to select these parameters and achieve an efficient stabilization scheme. A typical application is given for the stabilization of the shallow slope shown in Figure 26. The factor of safety of the slope and the displacement, moment, and shear profiles along the piles are calculated by using the methodologies developed in Chapters 3 and 4, respectively. Finally, a structural design example is given to illustrate how various factors can be modified to arrive at an optimum pile design.

The slope in Figure 26 has a height of 45 ft, a slope angle of 30 degrees, and is made of a homogeneous material. The friction angle of the soil, ϕ, is 10

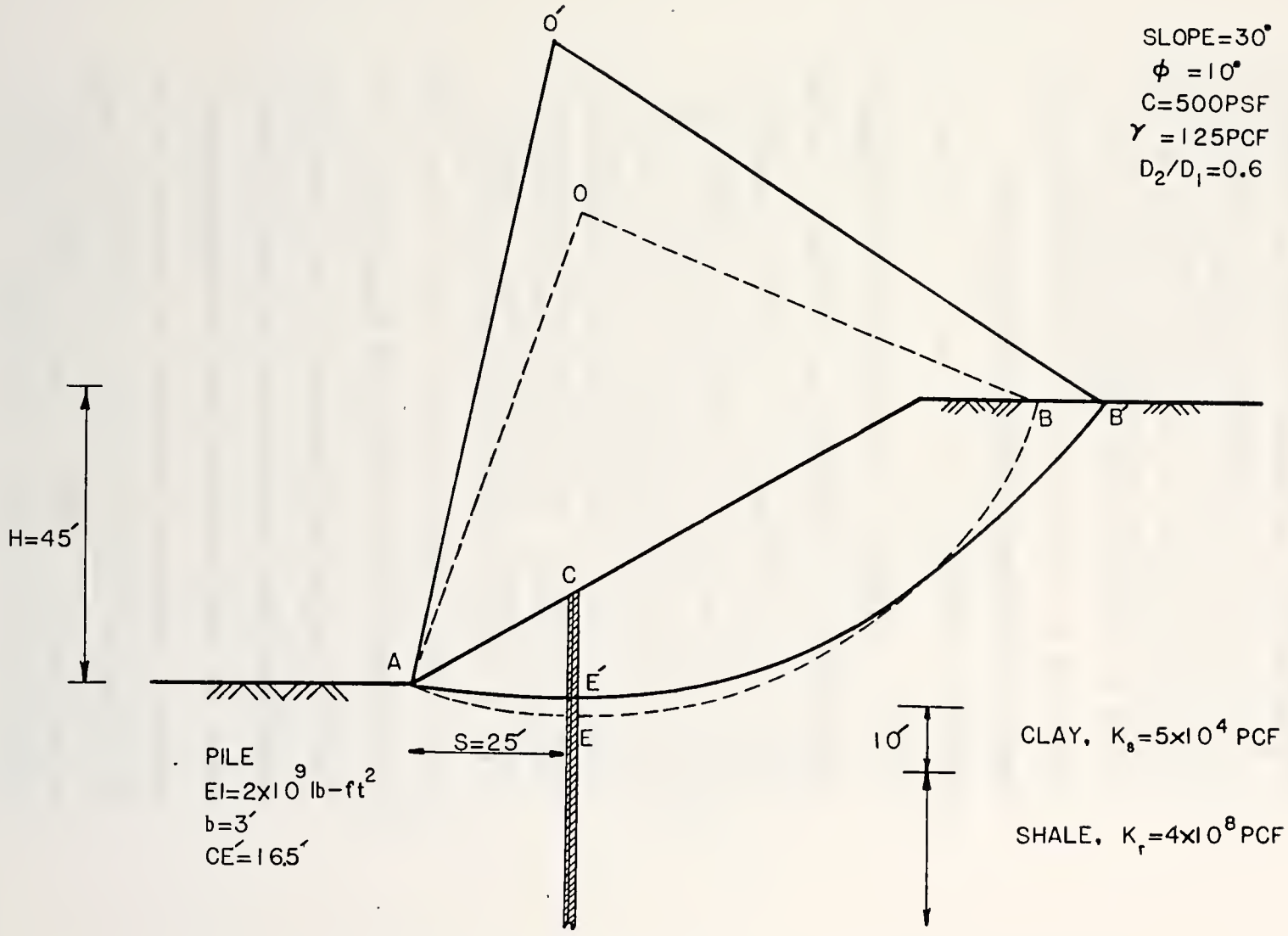

Figure 26 Slope Configuration of the Example Problem.

degrees, the cohesion, c, is 500 psf, and the unit weight, γ, is 125 pcf. The critical surface, indicated by a dashed line, corresponds to a minimum safety factor of 1.08. The distance from the ground surface to the critical surface, CE, is 19 ft. A factor of safety of 1.08 is insufficient and the slope will be reinforced with a row of piles. The following steps are proposed to achieve an efficient design of the slope/pile system.

1) A parameter, a, which represents the degree of mobilization of the force F_p, must be chosen. As indicated in Chapter 3, the slope stability program gives the user two choices: (1) total mobilization of F_p; and (2) partial mobilization of F_p, in which case a force $F_m = F_p/a$ is used to represent the reaction provided by the piles. It is proposed herein that the ratio, a, between the total force and the mobilized force be taken equal to the safety factor of the slope, FS. Physically, this implies that F_m is equal to the total force, F_p, when the slope is in a state of limit equilibrium, but it decreases as the degree of stability of the slope increases. This recommendation will provide a conservative assessment of the stability of the reinforced slope. To achieve a conservative design of the piles, the notion of a mobilized force is not introduced in the analysis of the piles.

2) The horizontal distance, S, between the pile row and the toe of the slope may be dictated by site conditions or arbitrarily chosen (at the first step of the design). In this example, S is taken as 25 ft. With the piles placed at that location, the distance from the ground surface to the new critical surface, CE′, is equal to 16.5 ft.

3) The slope stability program, which is listed in Appendix C, is used to find the factor of safety of the reinforced slope, as a function of the pile diameter, b, the center-to-center distance between the piles, D_1, and the location of the pile row upslope, indicated by the horizontal distance S measured from the toe. The effect of both the pile spacing and diameter on the factor of safety of the slope can be conveniently expressed by a plot of the factor of safety versus the ratio D_1/b for a given value of S (Figure 27).

4) A desirable factor of safety for the slope is selected. For this example, it is assumed that the required factor of safety is 1.30, which is a value commonly used in the stability of slopes.

5) A ratio D_1/b can be selected from Figure 27. In this example, the ratio should be less than 2.8 to satisfy the requirement of a minimum factor of safety

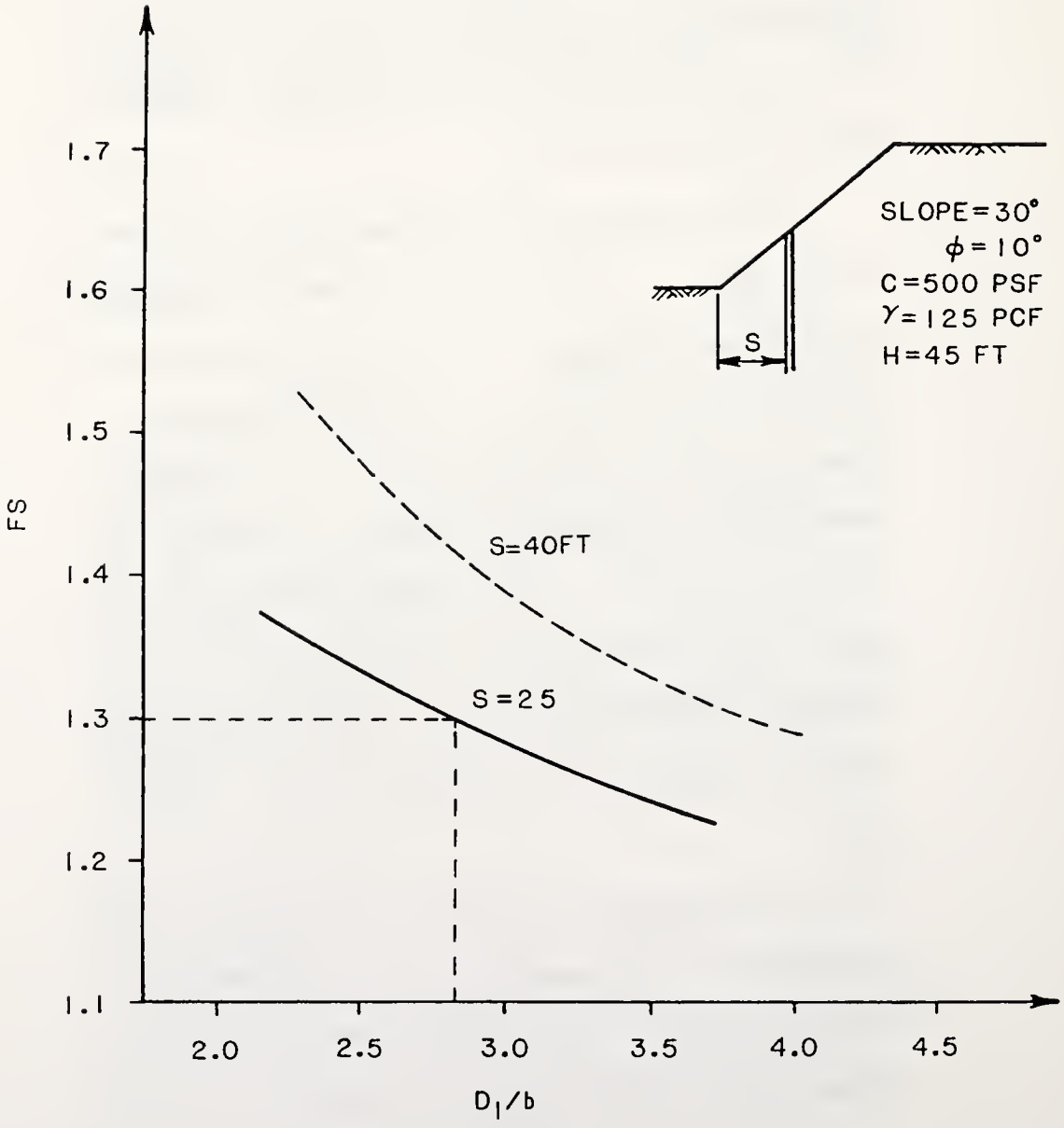

Figure 27 Safety Factor versus Ratio D_1/b.

of 1.30 for the slope. A conservative value of 2.5 is chosen here. Note that large ratios D_1/b should be avoided because the assumption of a plastic state around the piles is not fulfilled for excessive spacing between the piles.

6) In the initial design stage, a pile diameter is arbitrarily chosen. In the present example, the piles are assumed to be 2 ft in diameter with a center-to-center distance of 5 ft (to satisfy a D_1/b ratio of 2.5). Assuming that a reinforced concrete pile is used, the pile stiffness can be expressed as the product of the Young's Modulus of concrete and the gross moment of inertia of the cross section. For a concrete with a compressive strength of 4000 psi, the pile stiffness is 4×10^8 lb-ft^2.

7) The pile stability program listed in Appendix D is used to find the displacement, bending moment, and shear force along the length of the pile. The pile is analyzed as a beam embedded in an elastic foundation. The magnitude of the force per unit length acting on the pile section above the critical surface is obtained from Equations 3-16, 3-17 or 3-27. The force per unit length acting on the pile section below the critical surface is a function of both the pile stiffness and the nature of the foundation. In this example, the foundation consists of a clay layer, which extends 10

ft below the critical surface and is underlain by bedrock. The coefficient of subgrade reaction of the clay is assumed to be 5×10^4 pcf (Equation 4-26 and Table 2). The bedrock is a soft shale with a coefficient of subgrade reaction of 4×10^8 pcf (Equation 4-31 and Table 4).

The displacement, bending moment, and shear profiles corresponding to the selected parameters are given in Figures 28, 29 and 30 for the four possible boundary conditions at the pile top discussed in Chapter 4 (BC = 1,2,3,4): (1) free head; (2) unrotated head; (3) hinged head; and (4) fixed head. Figure 29 reveals that the hinged head condition results in the smallest bending moment in the pile, followed in order by conditions (4), (2), and (1). Based on this, a restrained pile head (hinged or fixed) is recommended. In addition, experimental results (Ito and Matsui, 1975) indicate that the lateral load acting on piles due to plastically deforming ground can be best estimated by the theory of plastic deformation under the condition of a restrained pile top. Therefore, the free head condition should be avoided in order to both limit the moment and shear on the pile and closely estimate the force acting on the piles. A restrained head condition can be obtained by connecting the pile heads with a beam which is fixed by tension anchors. The

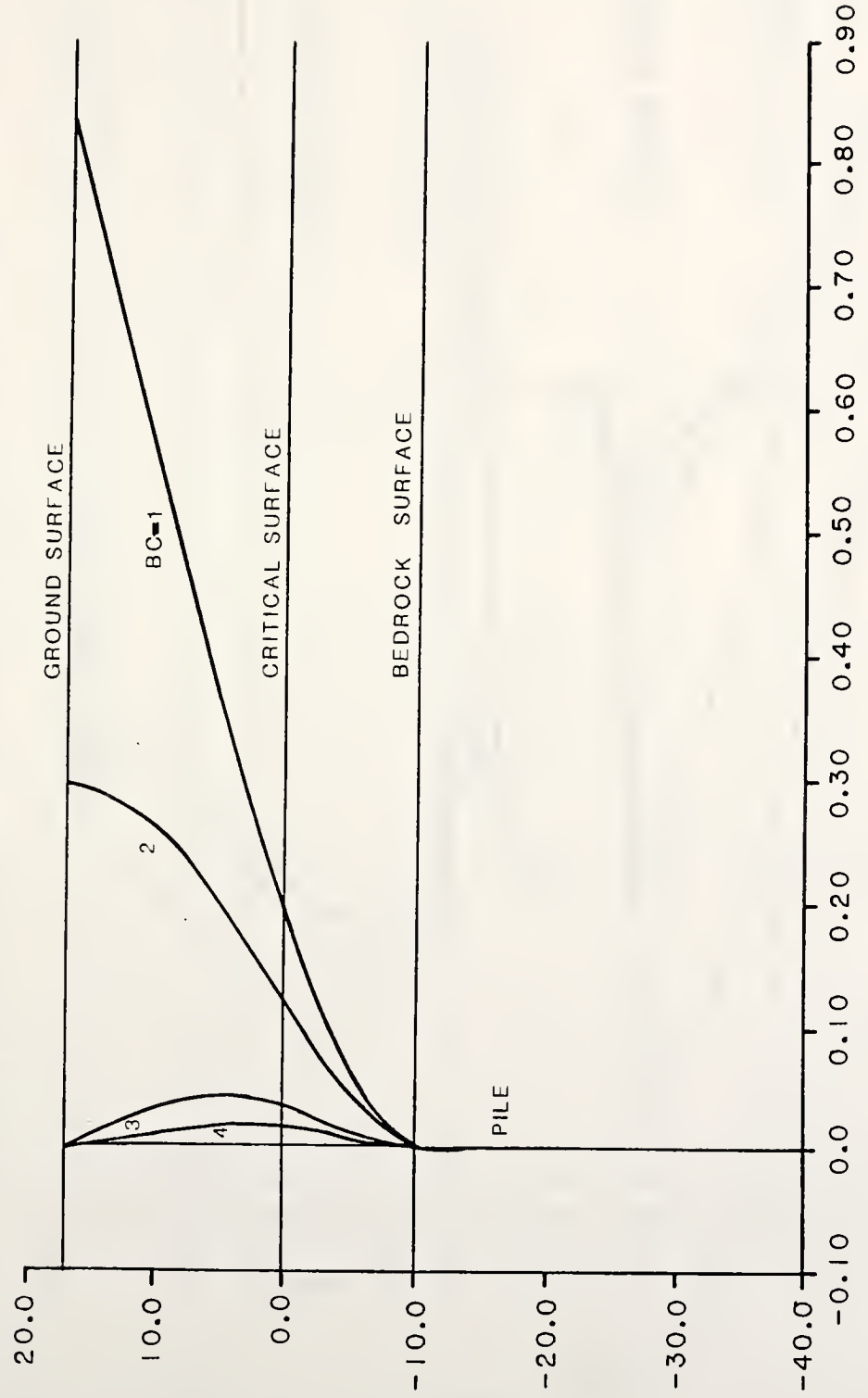

Figure 28 Displacement Along the Pile for Four Boundary Conditions.

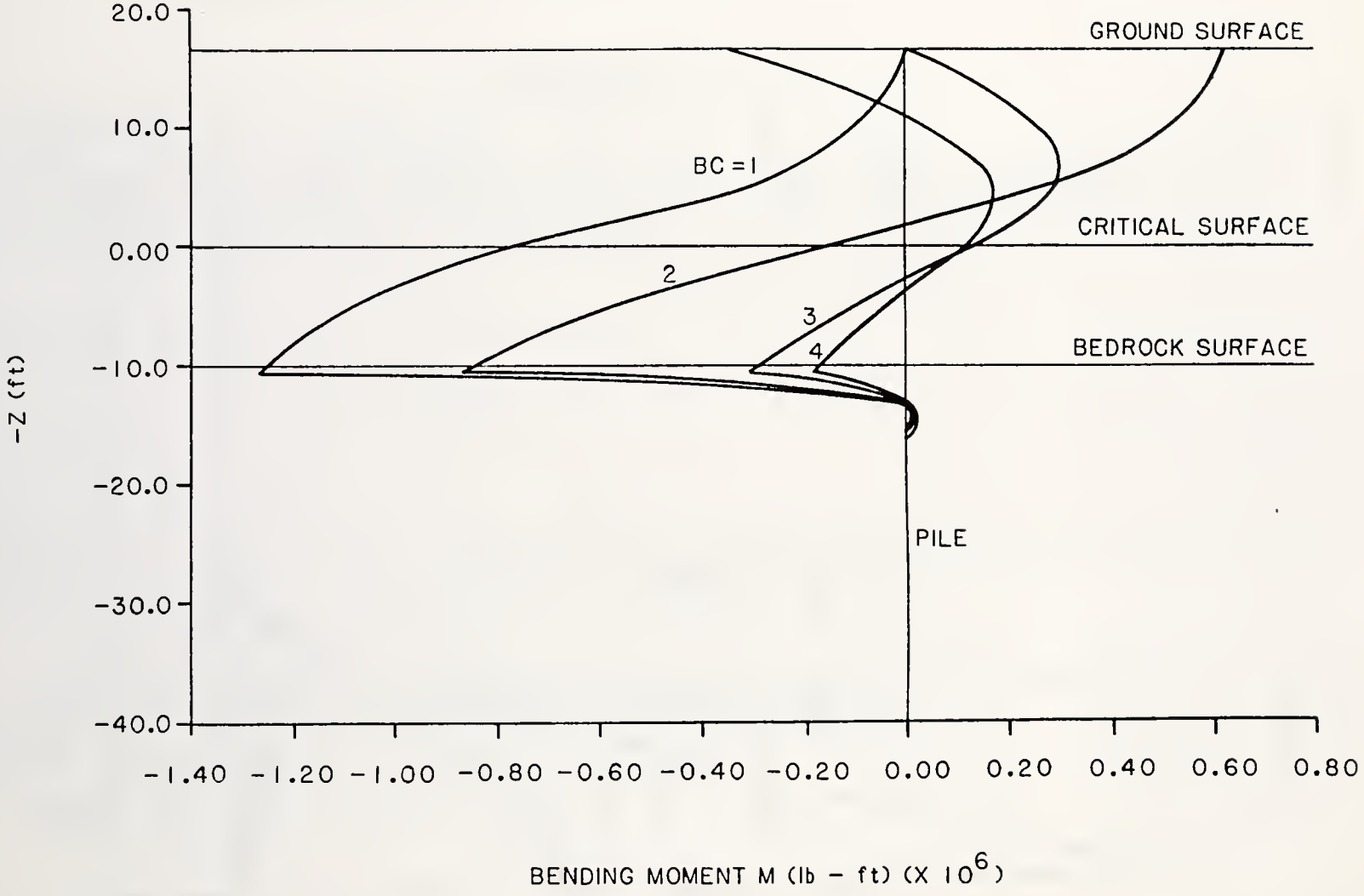

Figure 29 Bending Moment Along the Pile —Four Boundary Conditions.

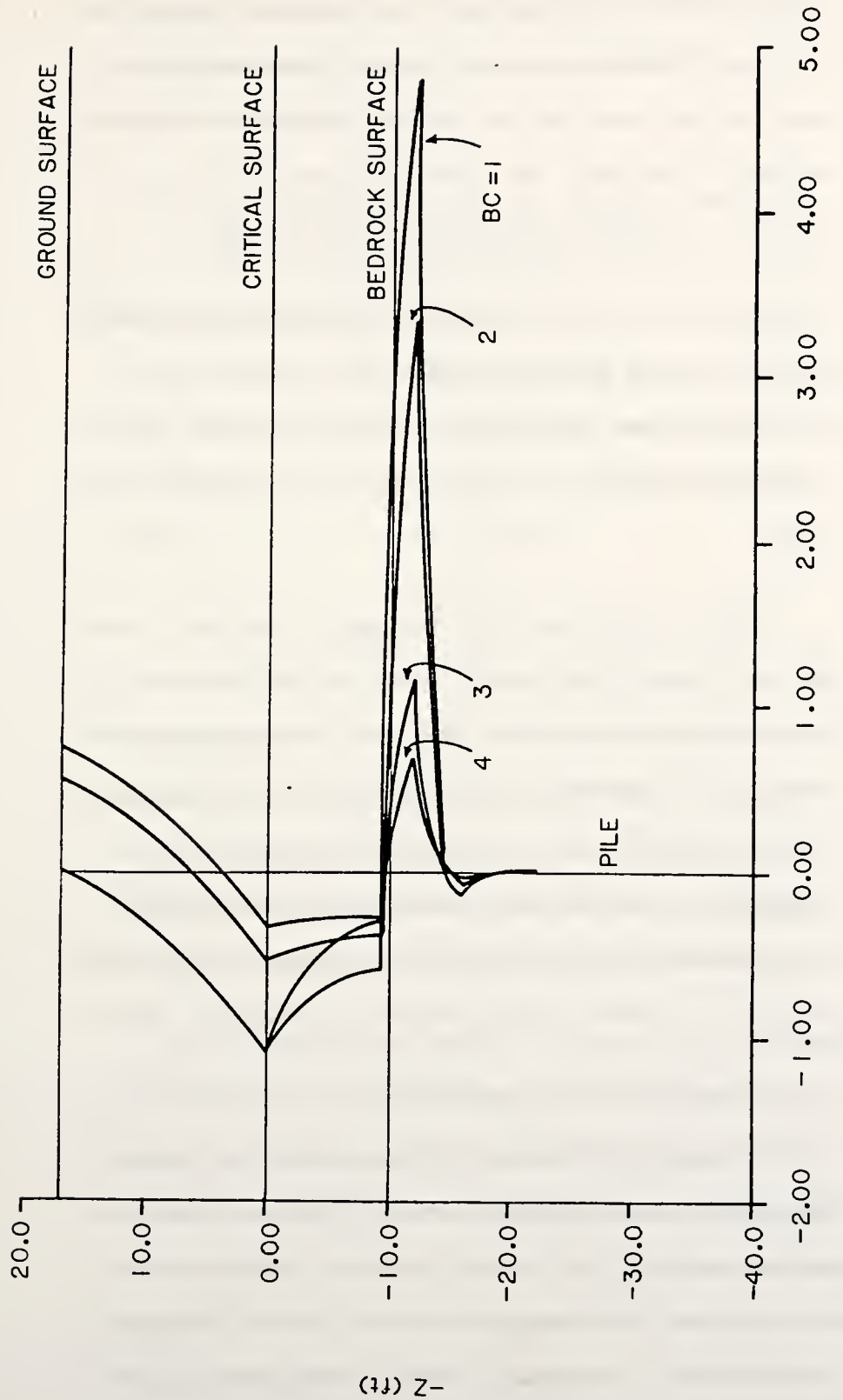

Figure 30 Shear Force Along the Pile – Four Boundary Conditions.

unrotated head condition can be obtained by simply connecting the pile heads with a beam. The constraint used for the pile analysis should approximate the conditions in the field as closely as possible. In this example, the fixed head condition is assumed.

8) The structural analysis of the pile can now be performed. The maximum displacement, moment, and shear, acting on the pile are the three factors that should be considered to assure that the design is adequate.

First, the maximum displacement is checked. Shannon and Wilson (1964) used a limiting displacement of 2 in. to design the piles in the Seattle Freeway stabilization, and this value is assumed here as the maximum tolerable deflection. Choosing an appropriate pile diameter will satisfy this restriction. The maximum displacement for the fixed head condition in Figure 28 is 0.24 in., which is well within the tolerable limit.

Second, the steel reinforcement required for the pile to resist the maximum bending moment is designed. The bending moment diagram shown in Figure 29 has a maximum value of 317 ft-kips (boundary condition 4). In accordance with the ACI code, the moment should be increased by a factor of 1.7 to a design value of 539 ft-kips. The CRSI handbook (1978) is consulted to

obtain the appropriate steel design. In this example, the maximum moment can be resisted using 12 No. 10 rebars of grade 60 steel.

Third, the maximum shear is checked. When the pile is embedded in rock, high shear forces will occur. The shear provided by the concrete, V_c, is considered to be the product of an average shear stress (usually $2\sqrt{f'_c}$, where f'_c is the strength of the concrete) by the effective cross sectional area of the member (McCormac, 1978). In this example,

$$V_c = 2\sqrt{4000} \times 452 = 5.7 \times 10^4 \text{ lbs}$$

The maximum shear that the member must withstand is 1.7 times the maximum applied shear obtained from Figure 30, and is found to be $1.7 \times (7.3 \times 10^4 \text{ lbs}) = 1.2 \times 10^5$ lbs. Since this exceeds the strength provided by the concrete alone, stirrups must be provided.

As an alternative design, a pile of 3 ft in diameter could be used. In this case, the center-to-center spacing is increased to 7.5 ft, and the resulting stiffness is 2×10^9 lb-ft^2. The maximum displacement on the pile is 0.1 inch (Figure 31). The maximum bending moment is 550 ft-kips (Figure 32). The pile can be designed with 12 No. 10 bars to resist a factored moment of 935 ft-kips. The shear strength provided by

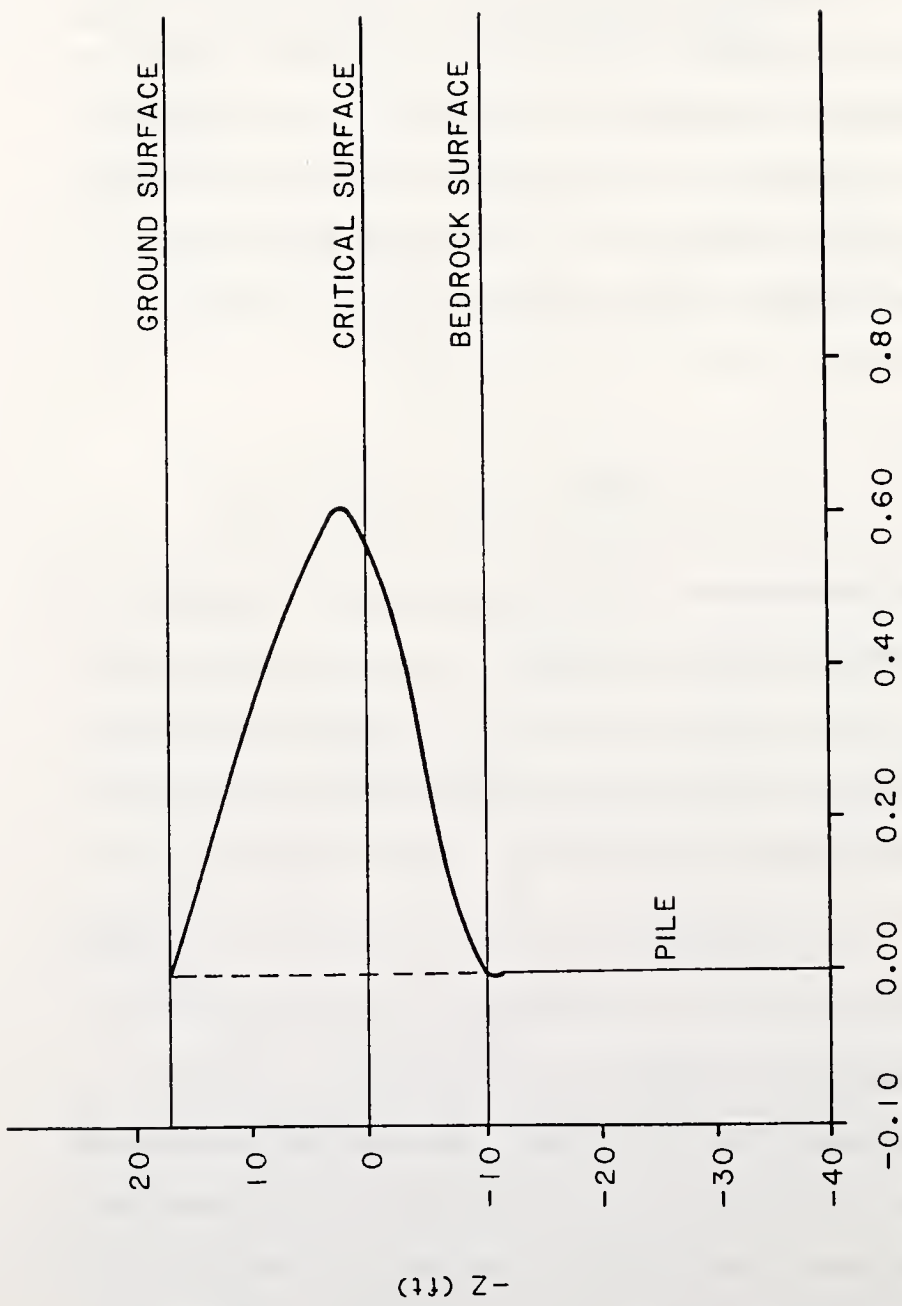

Figure 31 Displacement Along the Fixed Head Pile.

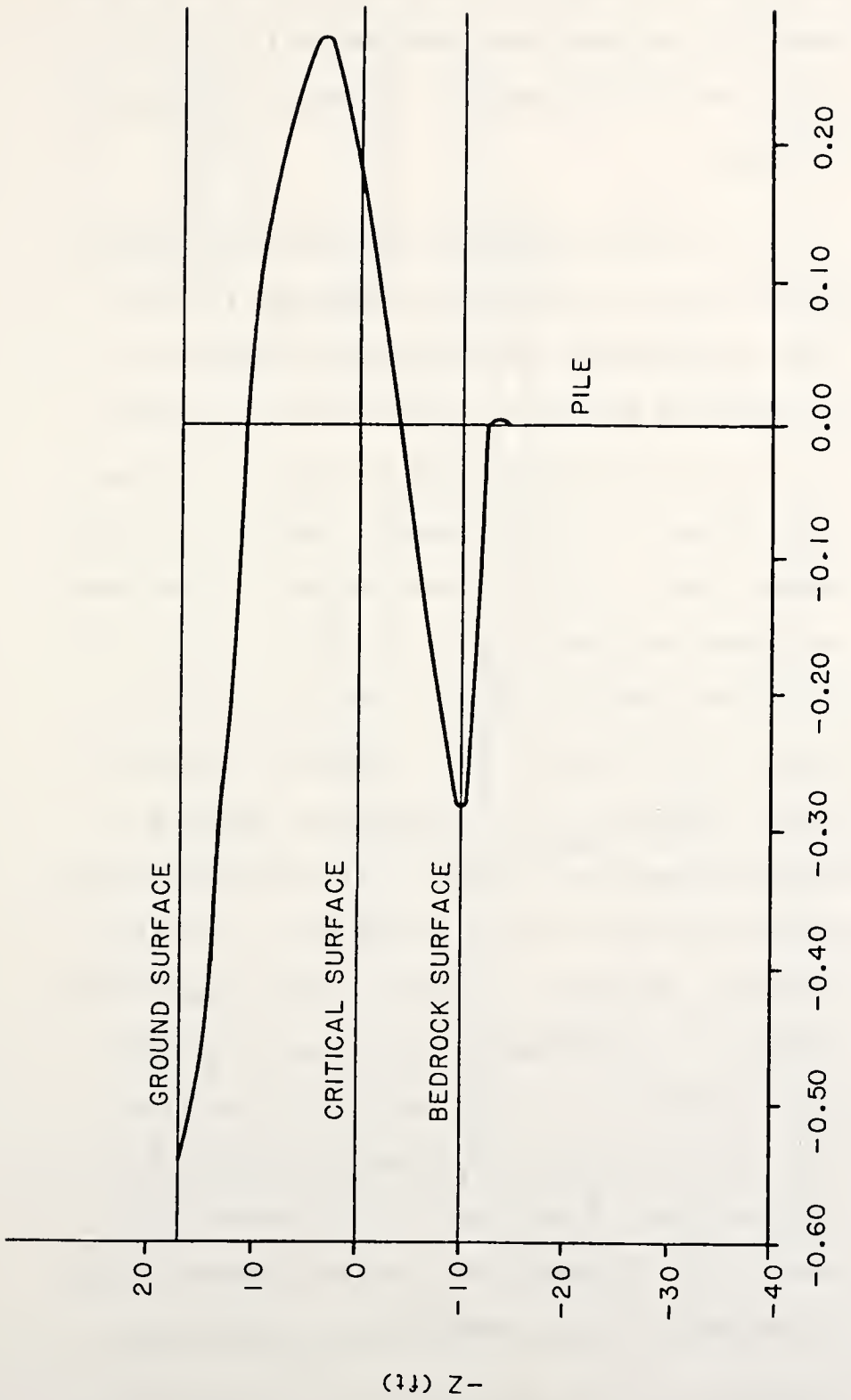

Figure 32 Bending Moment Along the Fixed Head Pile.

the concrete is 1.29×10^5 lbs and the factored maximum shear that the member must withstand is $1.7 \times (1.1 \times 10^5) = 1.87 \times 10^5$ (Figure 33). Stirrups would again be provided.

9) An optimum design can be obtained by minimizing the cost of materials and construction for different configurations of the slope/pile system. The two parameters that can be varied are the pile diameter, b, and the distance of the pile row from the toe of the slope, S. For this example, increasing the pile diameter from 2 ft to 3 ft increases the required spacing between the piles from 5 ft to 7.5 ft. Hence, for a landslide about 1000 ft wide*, 200 piles of 2 ft in diameter or 134 piles of 3 ft in diameter will assure a factor of safety of 1.30 for the slope. Changing the distance between the pile row and the toe of the slope has also an effect on the number of piles. To illustrate this, the factor of safety is plotted against the ratio D_1/b for a distance S = 40 ft upslope (broken line in Figure 27). In this case, to achieve a safety factor of 1.30, the ratio D_1/b must be equal to 3.5. Therefore, only 143 piles of 2 ft in diameter or 100 piles of 3 ft in diameter are required. However, placing the piles 15 feet further upslope increases both

* A slide of such magnitude, but with different slope configuration and material, occurred during construction of I-471 in Ohio.

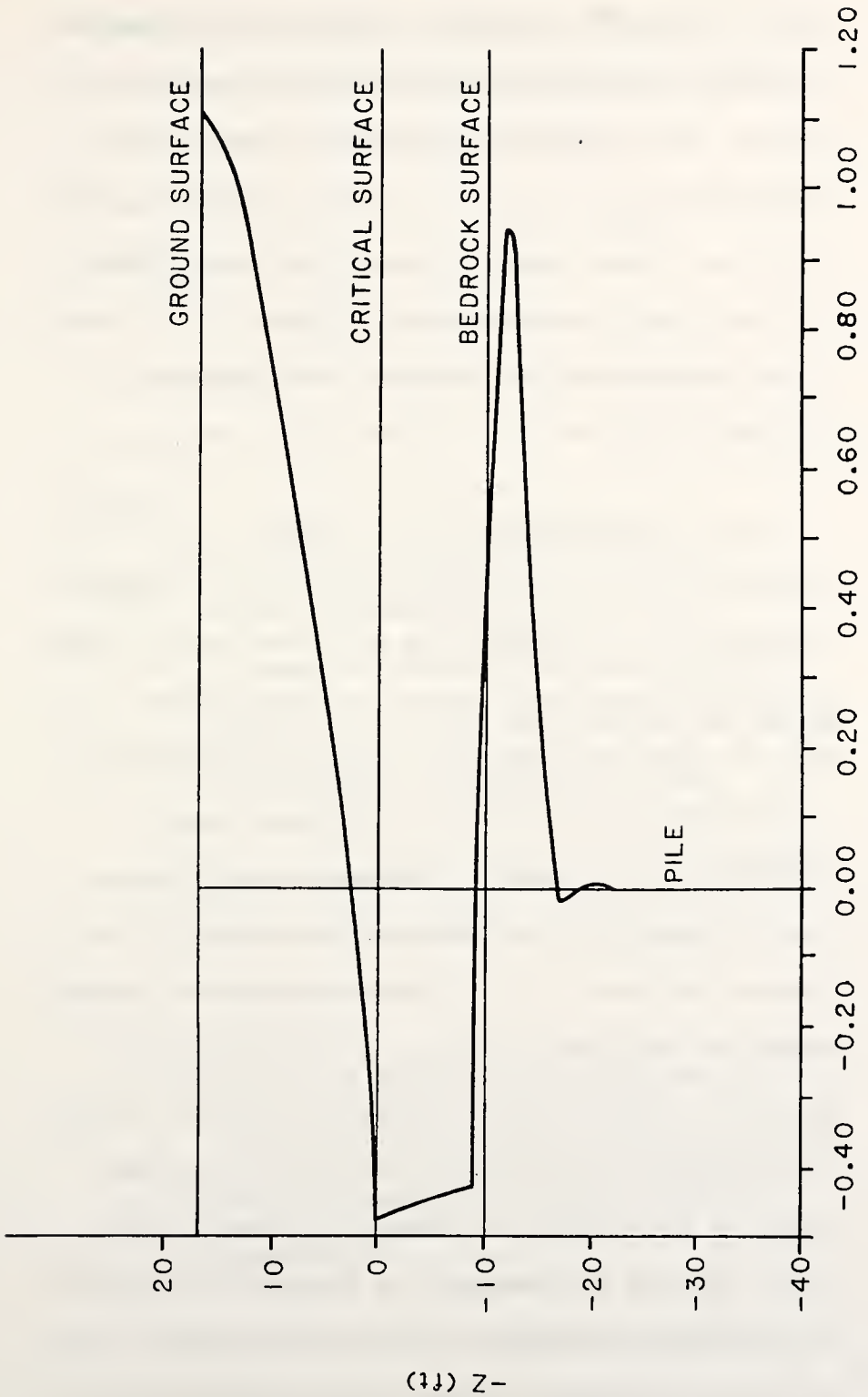

Figure 33 Shear Force Along the Fixed Head Pile.

the pile length required to penetrate the critical surface and the loads that act on the pile, and consequently, the required reinforcement. Hence, this alternative could prove to be less economical than the first one. Other considerations in the selection of the final design would include the degree of difficulty in the installation of the pile row at each location and labor costs.

10) After dimensioning the diameter of the pile, the length of the pile is determined. It is suggested that the pile be embedded to a sufficient depth so that the bending moment and shear force approach zero. To find the appropriate depth, a pile of infinite length is analyzed and the point at which these values approach zero is located. Embedding the pile deeper than this point will not increase its stability. Considering the case of a 3 ft diameter pile, the bending moment and shear force are zero at a distance 18 ft below the critical surface (Figure 32 and 33). Therefore, the pile will penetrate about 26.5 ft of soil (CE′ + 10 ft) and will be embedded 8 ft in the soft rock. Although the embedment is relatively important for this particular case, it has to be recognized that the required embedment length decreases considerably as the stiffness of the foundation material increases. The piles must always penetrate the critical surface of

the unreinforced slope. Otherwise, the slope would fail on its original failure surface and the piles would not contribute to its stability.

SUMMARY

A step-by-step procedure has been proposed to analyze the stabilization of a slope with a row of piles:

1) A parameter a is used to determine the degree of mobilization of F_p. It is proposed herein to scale the force acting on the piles according to the degree of stability of the slope (a = FS).

2) The horizontal distance, S, which indicates the location of the piles upslope is selected.

3) A graph of the factor of safety of the slope versus the ratio D_1/b is constructed using the slope stability program listed in Appendix C.

4) A minimum factor of safety is specified.

5) The ratio D_1/b which satisfies the required factor of safety is selected.

6) The pile diameter b is arbitrarily chosen, while the distance D_1 is determined by the ratio D_1/b.

7) A boundary condition for the pile head is chosen. This condition will have to be fulfilled during construction.

8) The displacement, bending moment, and shear force along the pile are calculated using the pile stability program listed in Appendix D. Then, the pile is designed structurally.

9) If desired, an optimum solution can be obtained by changing the pile diameter and/or the pile row location (i.e., the distance S)

10) The depth of embedment of the pile is determined.

This systematic approach, used in conjunction with the programs listed in Appendix C and D, provides the means for an efficient selection of the appropriate pile dimensions and reinforcement required for stabilization of a slope.

CHAPTER VI. SUMMARY AND CONCLUSIONS

This study is part of a project undertaken at Purdue University to develop a methodology for the design and analysis of slopes stabilized with piles. Different aspects of this problem have been considered, the most important of which are: (1) the calculation of the force exerted on the piles by the slope; (2) the effect of a row of piles on the stability of the slope; and (3) simultaneous slope stability analysis and pile design (dimensioning) to meet minimum safety requirements for both the slope and the piles. The following steps have been taken:

- Available techniques for calculating the pressure acting on passive piles have been reviewed. The "plastic state" method (Ito and Matsui, 1975) was selected and implemented in a computer program. This provides an estimate of the pressure acting on the pile regardless of the state of equilibrium of the slope.

-A computer program has been developed to calculate the safety factor of a slope reinforced with a single row of piles. The ϕ-circle slope stability method has been extended to take into account the force exerted by the piles on the slope. It is recommended that the force exerted by the piles be assumed equal to the maximum value, calculated using the plastic state assumption, divided by the factor of safety of the slope.

-Parametric studies have been performed to obtain relationships between the safety factor and parameters such as pile diameter, center-to-center distance, and location of the pile row.

-A computer program has been developed to compute the displacement, bending moment, and shear force at each point along the pile. The pile is analyzed in two sections. Since the pressure acting on the section above the critical surface is known, this section is solved using a closed-form solution. The section below the critical surface is analyzed using the finite difference method. It is assumed

that the pressure acting at any point along the pile is a function of the deflection and modulus of subgrade reaction at that point. Experimental methods which can be used to determine the modulus of subgrade reaction have been discussed. Published empirical values have been reviewed.

-A step-by-step procedure has been proposed for the design of both the slope and the piles. When a desired safety factor for the slope and a location of the pile row are chosen, the pile diameter, center-to-center distance, and the reinforcement can be determined so that both the stability of the slope and the integrity of the piles are insured. A typical example, including the structural design of the piles, has been given.

The most important conclusions of this study are as follows:

-After installation of the piles, the potential failure surface is expected to become shallower.

-As the distance S, which indicates the pile location upslope, increases, the factor of safety changes with a rate which is a function of the ratio D_2/D_1 (clear distance/center-to-center distance between the piles). As this ratio decreases, the rate of change in the safety factor increases.

-The factor of safety increases more rapidly in strong soils than in weak ones. For conventional values of the factor of safety, the piles can be placed closer to the toe for a strong soil than for a weak soil.

-The factor of safety of the slope decreases as the ratio of the center-to-center spacing to the diameter of the piles, D_1/b, increases.

-For a given ratio D_1/b, there is a range of values of S which will satisfy a required factor of safety. Generally, the piles must be located closer to the top of the steeper slopes than of the shallower ones.

-The pile top should be restrained (fixed or hinged end) to minimize the bending moments and shear forces applied to the piles.

-A satisfactory design of the slope/pile system can be achieved to satisfy the stability of the slope and to insure the structural integrity of the piles.

REFERENCES

Andrews, G.H. and Klassell, J.A. (1964), "Cylinder Pile Retaining Wall,", Highway Research Record No. 56, pp.83,97.

Baguelin, F., Frank, R., and Guegaz, Y. (1976), "Calcul Sur Ordinateur des Pieux Sollicites Horizontalement ou Subissant des Poussees Parasites" - Bulletin de liaison des laboratoires des Ponts et Chaussees, No. 84, Juillet-Aout, p. 113-120.

Baker, R.F.and Marshall, H.C. (1958), "Control and Correction in Landslides and Engineering Practice", Ed. by E.B. Eckel, Highway Research Board Special Report 29, pp.150-158.

Baker, R. F. and Yonder, E. J. (1958), "Stability Analysis and Density Control Works in Landslides and Engineering Practice", E.B. Eckel, Ed., Highway Research Board Special Report 29, pp. 189-216.

Begemann-Deleeuw, E. H. (1972), "Horizontal Earth Pressure on Foundation Piles as a Result of Nearby Soil Fills", Proceedings of the 5th European Conference on Soil Mechanics and Foundation Engineering, Vol. I, pp. 309, Madrid.

Biot, M. A. (1937) "Bending of an Infinite Beam on an Elastic Foundation", Journal of Applied Mechanics, American Society of Mechanical Engineers, Vol. 59, p. 42.

Bishop, J. A. and Mason, A. G. (1954), "Piles Subjected to Lateral Thrust, Part I", Supplement to Symposium on Lateral Load Tests on Piles., American Society of Testing and Materials, SPT No. 154-A.

Brinch Hansen, J. (1961), "The Ultimate Resistance of Rigid Piles Against Transversal Forces", Copenhagen - The Danish Geotechnical Institute, Bulletin No. 12.

Bowles, J. E. (1968), Foundation Analysis and Design, McGraw-Hill, New York.

Broms, B. B. (1964), "Lateral Resistance of Piles in Cohesive Soils", Journal of Soil Mechanics and Foundation Division, American Society of Civil Engineers, Vol. 90, SM2, pp. 27-63.

Broms, B.B. and Bennermark, H. (1967), "Shear Strength of Soft Clay," Discussion, Proceedings, Geotechnical Conference, Oslo, Vol.2, pp. 118-120.

Broms, B.B. (1969), "Stability of Natural Slopes and Embankment Foundations," Discussion, Proceedings, 7th International Conference of Soil Mechanics and Foundation Engineering, Mexico, Vol 3, pp.385-394.

Broms, B. B. (1974) "Lateral Resistance of Piles in Cohesive Soils", Journal of Soil Mechanics and Foundation Division, American Society of Civil Engineers, SM2, March, pp. 27-63.

Canizo, L. and Merino, M. (1977) "Elastic Solutions to the Bending of Piles due to Nearby Surcharges", Paper presented at Specialty Session No. 10, 9th International Conference of Soil Mechanics and Foundation Engineering, Tokyo.

Chen, W. W. (1978) Discussion: "Laterally Loaded Piles: Program Documentation", Journal of Soil Mechanics and Foundation Division, American Society of Civil Engineers, GT1, January, pp. 161-162.

Coon, R. F. and Merritt, A. H. (1970) "Predicting In Situ Modulus of Deformation Using Rock Quality Indexes", Determination of the In Situ Modulus of Deformation of Rock, American Society of Testing and Materials, STP 477, pp. 154-173.

Coyle, H. M., Bierschwale, M. W (1983) "Design of Rigid Shafts in Clay for Lateral Load", Journal of Soil Mechanics and Foundation Division, American Society of Civil Engineers, Vol. 109, No. 9, September, pp. 1147-1164.

Crandall, S. H. (1956) "Engineering Analysis", McGraw-Hill Book Company, Inc., New York.

D'Appolonia, E., Alperstein, R. and D'Appolonia, D.J. (1977), "Behavior of a Colluvial Slope", Journal of Soil Mechanics and Foundation Division, American Society of Civil Engineers, Vol. 93, SM 4, pp. 447-473.

Das, B. M. (1983), "Advanced Soil Mechanics", McGraw Hill, New York.

Dash U. and Jovino, P.L. (1980), "Root Piles at Monnesen Pen", Transportation Research Record 749.

Davisson, M. T. (1970), "Lateral Load Capacity of Piles", Highway Research Record, No. 333, pp. 104-112.

Davisson, M. T. and Gill, H. L., (1963), "Laterally Loaded Piles in a Layered Soil System", Journal of Soil Mechanics and Foundation Division, American Society of Civil Engineers, Vol. 89, SM3, pp. 63-94.

Davisson, M. T. and Prakash, S. (1963) "A Review of Soil-Pile Behavior", Highway Research Record, No. 39:25-48.

DeBeer, E. E. (1977), "The Effects of Horizontal Loads on Piles, Due to Surcharge of Seismic Effects", Proceedings, Special Session 10, 9th International Conference, Soil Mechanics and Foundation Engineering, Tokyo.

DeBeer, E. E. and Wallays, M. (1970), "Stabilization of a slope in Schist by Means of Bored Piles Reinforced with Steel Beams", Proceedings 2nd International Congress Rock Mechanics, Belgrade, Vol. 3, pp. 361-369.

DeBeer, E. E. and Wallays, M., (1972), "Forces Induced in Piles by Unsymmetrical Surcharges on the Soil Around the Piles", Proceedings, 5th European Conference Soil Mechanics and Foundation Engineering, Madrid Vol. 1, pp. 325-332.

Desai, C. S. and Christian, J. T. (1977) "Numerical Methods in Geotechnical Engineering", McGraw-Hill Book Company, New York.

Dixon, S. J. (1970) "Pressuremeter Testing of Soft Bedrock", Determination of the In Situ Modulus of Deformation of Rock, American Society of Testing and Materials, STP 477, pp. 126-136.

Francis, A. J. (1964) "Analysis of Pile Groups with Flexural Resistance", Journal of Soil Mechanics and Foundation Division, American Society of Civil Engineers, SM3, May, pp. 1-32.

Fukuoka, M. (1977), "The Effect of Horizontal Loads on Piles Due to Landslides", Proceedings, Special Session 10, 9th International Conference, Soil Mechanics and Foundation Engineering, Tokyo.

Goughour and DiMaggio, (1978), "Soil Reinforcement Methods on Highway Projects", Symposium on Earth Reinforcement, American Society of Civil Engineers Annual Convention, Pittsburg, Pennsylvania, April, pp. 371-399.

Hetenyi, M. (1946) "Beams on Elastic Foundation", University of Michigan, Press.

Hovland, H.J. and Willoughby, D.F. (1982), "The Analysis of Wall Supports to Stabilize Slopes", Application of Walls to Landslide Control Problems, Ed. by R.B. Reeves, American Society of Civil Engineers, National Convention, Las Vegas, Nevada, April 29, pp. 19-29.

Hutchinson, J.H. (1977), "Assessment of the Effectiveness of Corrective Measures in Relation to Geological Conditions and Types of Slope Movement", Bulletin of the International Association of Engineering Geology, No.16, pp. 131-155.

Ito, T. and Matsui, T. (1975) "Methods to Estimate Lateral Force Acting on Stabilizing Piles", Soils and Foundations, Vol. 15, No. 4, December, pp. 43-59.

Ito, T. and Matsui, T. (1978), "Discussion: Methods to Estimate Lateral Force Acting on Stabilizing Piles", Soils and Foundations, Vol. 18, No. 2, June, pp. 41-44.

Ito, T., Matsui, T. and Hong, W. P. (1979), "Design Method for the Stability Analysis of the Slope with Landing Pier", Soils and Foundations, Vol. 19, No. 4, December, pp. 43-57.

Ito, T., Matsui, T. and Hong, W.P. (1981), "Design Method for Stabilizing Piles Against Landslide--One Row of Piles", Soils and Foundations, Vol. 21, No. 1, March, pp. 21-37.

Ito, T., Matsui, T. and Hong, W. P. (1982), "Extended Design Method for Multi-row Stabilizing Piles against Landslide", Soils and Foundations, Vol. 22, No. 1, March, pp. 1-13

Jamiolkowski, M. and Garassino, A. (1977), "Soil Modulus of Laterally Loaded Piles", Proceedings, Special Session 10, 9th International Conference, Soil Mechanics and Foundation Engineering, Tokyo.

Jamiolkowski, M. and Garassino, A. (1977), "The Effect of Horizontal Loads on Piles, due to Surcharge or Seismic Effects", Proceedings of the Specialty Session 10, July 14, 9th International Conference of Soil Mechanics and Foundation Engineering, Tokyo, pp. 43-58.

Kishida, H. and Nadai, S. (1977), "Large Deflection of a Single Pile under Horizontal Load", Proceedings, Special Session 10, 9th International Conference, Soil Mechanics and Foundation Engineering, Tokyo.

Matlock, H. and Ripperberger, E. A. (1954) "Measurement of Soil Pressure on a Laterally Loaded Pile", Procedure, American Society of Testing and Materials, Vol. 58, pp. 1245-1259.

Matlock, H. and Reese, L. C., (1960), "Generalized Solutions for Laterally Loaded Piles", Journal of Soil Mechanics and Foundation Division, American Society of Civil Engineers, Vol. 86, SM5, pp. 63-91.

Matsui, T., Hong, W. P. and Ito, T. (1982), "Earth Pressures on Piles in a Row due to Lateral Soil Movements", Soils and Foundations, Vol. 22, No. 2, June, pp. 71-81.

Merriam, R. (1960), "Portuguese Bend Landslide, Palos Verdes Hills, California", Journal of Geology, Vol. 68, pp. 140-153.

Mindlin, R. D. (1936) "Force at a Point in the Interior at a Semi-Infinite Solid", Physics, Vol. 7, May.

Morgenstern, N.R. (1982), "The Analysis of Wall Supports to Stabilize Slopes", Application of Walls to Landslide Control Problems, Ed. by R.B. Reeves, American Society of Civil Engineers National Convention, Las Vegas, Nevada.

Nethero, M.F. (1982), "Slide Control by Drilled Pier Walls", Application of Walls to Landslide Control Problems, Ed. by R.B. Reeves, American Society of Civil Engineers National Convention, Las Vegas, Nevada.

Nicoletti, J.P. and Keith, J.M. (1969), "External Shell Stops Soil Movement and Saves Tunnel", Civil Engineering, April, pg. 72.

Oakland, M. W. and Chameau, J. L. (1982). "Finite Element Analysis of Drilled Piers Used for Slope Stabilization", American Society of Testing and Materials Symposium on Laterally Loaded Piles and Pile Groups, Kansas City, June.

Offenberger, J.H. (1981), "Hillside Stabilization with Concrete Cylinder Pile Retaining Wall", Public Works, September, pp. 82-86.

Oteo, C. S. (1977), "Horizontally Loaded Piles, Deformation Influence", Proceedings Special Session 10, 9th International Conference Soil Mechanics and Foundation Engineering, Tokyo.

Palmer, L. A. and Thomson, S. B. (1948) "The Earth Pressure and Deflection Along the Embedded Lengths of Piles Subjected to Lateral Thrust", Proceedings, 2nd International Conference Soil Mechanics and Foundation Engineering, Rotterdam, Vol. 5, pp. 156-161.

Perloff, W. H. and Baron, W. (1976), "Soil Mechanics", John Wiley & Sons, Inc., New York.

Poulos, H. G. (1977) "Stresses and Displacements in an Elastic Layer Underlain by a Rough Rigid Base", Geotechnique, Vol. 17, No. 4, December, pp. 378-410.

Poulos, H. G. (1971), "Behavior of Laterally Loaded Piles: I - Single Piles", Proceedings Paper 8092, May, pp. 711-731.

Poulos, H. G. (1973), "Analysis of Piles in Soils Undergoing Lateral Movement", Journal of Soil Mechanics and Foundation Division, American Society of Civil Engineers, Vol. 99, SM5, pp. 391-406.

Poulos, H. G. and Davis, E. H. (1980) "Pile Foundation Analysis and Design", John Wiley and Sons, Inc.

Reese, L. C. and Cox, W. R. (1969) "Soil Behavior from Analysis of Tests on Uninstrumented Piles Under Lateral Loading", American Society of Testing and Materials, STP 444, pp. 160-176.

Reese, L. C. (1972) Program Documentation: Analysis of Laterally Loaded Piles by Computer, Univ. Texas Dept. Civil Engineering, Austin, July.

Rocha, M. (1970) "New Techniques in Deformability Testing of In Situ Rock Masses", Determination of the In Situ Modulus of Deformation of Rock, American Society of Testing and Materials, STP 477, pp. 39-57.

Root, A.W. (1958), "Prevention of Landslides, in Landslides and Engineering Practice", Ed. by E.B. Eckel, Highway Research Board, Special Report No. 29, pp. 113-149.

Rowe, R. K., Booker, J. R. and Balaam, N. P. (1978), "Application of the Initial Stress Method to Soil Structure Interaction", International Journal of Numerical Methods in Engineering, Vol. 12, No. 5.

Rowe, R. K. and Poulos, H. G. (1979). "A Method for Predicting the Effect of Piles on Slope Behavior", Proceedings, 3rd International Conference on Numerical Methods in Geomechanics, Vol. 3, Aachen, April.

SieGel, R. A. (1975), "Computer Analysis of general Slope Stability Problems", MSCE Thesis, Purdue University, West Lafayette, Indiana.

Taylor, D. W. (1937), "Stability of Earth Slopes", Journal of the Boston Society of Civil Engineers, Volume XXIV, Number 3, July, pp. 337-386.

Terzaghi, K. (1955) "Evaluation of Coefficients of Subgrade Reaction", Geotechnique, Vol. 5, No. 4, pp. 297-326.

Toms, A.H. and Bartlett, D.L. (1962), "Application of Soil Mechanics in the Design of Stabilizing Works for Embankments, Cuttings and Track Formations", Proceedings, Institute of Civil Engineers, Vol 21, pp. 705-732.

Vesic, A. B. (1961) "Bending of Beams Resting on Isotropic Elastic Solids", Journal of the Engineering Mechanics Division, American Society of Civil Engineers, Vol. 87, No. EM2, Proceedings Paper 2800, April, p. 35-53.

Vesic, A. S. (1965), "Ultimate Loads and Settlements of Deep Foundations in Sand", Proceedings, Symposium on Bearing Capacity and Settlement of Foundations, Duke.

Viggiani, C. (1981), "Ultimate Lateral Load on Piles Used to Stabilize Landslides", Proceedings, 10th Journal of Soil Mechanics and Foundation Engineering, Stockholm, Vol. 3, pp. 555-560.

Wallace, G. B., Slebir, E. J. and Anderson, F. A. (1970) "In Situ Methods for Determining Deformation Modulus Used by the Bureau of Reclamation", Determination of the In Situ Modulus of Deformation of Rock, American Society of Civil Engineers, STP 477, pp. 3-26.

Wans, M. G., Wu, A. H., and Scheessele, D. J., (1979), "Stress and Deformation in Single Piles Due to Lateral Movement of Surrounding Soils", Behavior of Deep Foundations, American Society of Testing and Materials, STP 670.

Welch (1972), "Lateral load behavior of Drilled Shafts", Ph.D. Thesis, University of Texas, Austin.

Winter, H., Schwarz, W., Gudehus, G. (1983), "Stabilization of Clay Slopes by Piles", Proceedings, 8th European Conference on Soil Mechanics and Foundation Engineering, Vol. 2, Helsinki, May, p. 545.

Yoshida, I. and Yoshinaka, R. (1972) "A Method to Estimate Modulus of Horizontal Subgrade Reaction for a Pile", Soils and Foundations, Vol. 12, No. 3, September, pp. 1-17.

Zaruba, Q. and Mencl, V. (1969), "Landslide and their Control", Elsevier, Amsterdam.

APPENDIX A

Determination of a Stability Number for the Reinforced Slope

Figure 9 in Chapter III is similar to the figure used by Taylor (1937) for the derivation of a stability number for an unreinforced slope. Assuming that the force F_p is known in magnitude and direction, and that its presence does not influence the point of action of P, a new stability number can be determined for the reinforced slope.

The following notation is used in the derivation (Figure 9):

W = weight of the sliding mass

C_r = cohesion required for equilibrium

P = resultant of the normal and frictional forces

F_p = pile reaction on the slope

d = moment arm of W

a = moment arm of C_r

OG = moment arm of F_p

H = height of the slope

i = slope angle

x = counterclockwise angle from the horizontal to the chord

2y = angle AOB

R = radius of the circle

Taylor (1937) derived the following expressions to arrive at a stability number. The cohesion force required for stability is:

$$C_r = c_r \overline{AB} = \frac{c_a}{F_c} \overline{AB} = \frac{2}{F_c} c_r R^{\bullet} \sin(y) \qquad (A\text{-}1)$$

where

c_r = unit cohesion required for equilibrium

c_a = unit cohesion available

$\overline{AB}$ = length of the chord

F_c = safety factor with respect to cohesion

The length OO′ is the moment arm of C_r and can be expressed as:

$$OO' = R \sin(\phi) \csc(u-v) \qquad (A\text{-}2)$$

The weight W is:

$$W = \gamma R^2 y - \gamma R^2 \sin(y) \cos(y) + \frac{\gamma H^2}{2} \{\cot(x) - \cot(i)\} \qquad (A\text{-}3)$$

The radius of the circle is:

$$R = \frac{H}{2} \csc(x) \csc(y) \qquad (A\text{-}4)$$

The moment of the weight with respect to the center of rotation, 0, is:

$$Wd = \frac{\gamma H^3}{12}\{1-2\cot^2(i)+3\cot(i)\cot(x)-3\cot(i)\cot(y) + 3\cot(x)\cot(y)\} \quad \text{(A-5)}$$

For the sake of simplicity, the expression inside the parenthesis will be replaced by E:

$$Wd = \frac{\gamma H^3}{12} E \quad \text{(A-6)}$$

Using the equations derived above and two equations of equilibrium (derived by summing moments around point 0 and summing forces in the x direction), an expression for the stability number is derived:

$$\frac{c_a}{F_c \gamma H} = \frac{\frac{1}{2}\csc^2(x)\{y\csc^2(y)-\cot(y)\}+\cot(x)-\cot(i)}{2\cot(x)\cot(v)+2} \quad \text{(A-7)}$$

where the angle v is obtained from the following relations:

$$\sin(u-v) = \frac{H}{2d}\sin(u)\csc(x)\csc(y)\sin(\phi) \quad \text{(A-8)}$$

with

$$\cot(u) = \frac{H}{2d} y \sec(x)\csc(x)\csc^2(y) - \tan(x) \quad \text{(A-9)}$$

and,

$$\frac{H}{2d} = \frac{\frac{1}{2}\csc^2(x)\{y\csc^2(y)-\cot(y)\}+\cot(x)-\cot(i)}{\frac{1}{3}\{1-2\cot^2(i)\}+\cot(i)\{\cot(x)-\cot(y)\}+\cot(x)\cot(y)} \qquad (A-10)$$

When a force F_p is inserted, the same relations can be used to define a new expression for the stability number.

Summation of forces in the direction of the x axis (Figure 3-11) gives

$$F_p \cos(CEO) + C_r \cos(x) = P\sin(v) \qquad (A-11)$$

Summation of moments around point 0 gives:

$$P\{R\sin(\phi)\} + C_r(OO') + F_p(OG) - W_d = 0 \qquad (A-12)$$

P is obtained from Equation (A-11):

$$P = \frac{F_p \cos(CEO) + C_r \cos(x)}{\sin(v)} \qquad (A-13)$$

Substitution of Equations (A-5), (A-6), and (A-13) in Equation (A-12) results in:

$$\left\{\frac{F_p \cos(CEO)+C_r \cos(x)}{\sin(v)}\right\}R\sin(\phi)+C_r\{R\sin(\phi)\csc(u-v)\}$$
$$+F_p(OG)-\frac{\gamma H^3}{12}E = 0 \qquad (A-14)$$

The new stability number for toe failure is obtained by substituting Equations (A-1) and (A-3) into this equation and simplifying:

$$\frac{c_a}{F_c \gamma H} = \frac{E - \frac{12\,F_p}{\gamma H^3}\left\{\frac{\cos(CEO)}{\sin(v)}\frac{H}{2}\csc(x)\csc(y)\sin(\phi)+OG\right\}}{6\csc^2(x)\csc(y)\sin(\phi)\left\{\frac{\cos x}{\sin v}+\csc(u-v)\cos(x-u)\right\}} \qquad \text{(A-15)}$$

with the angles u and v obtained from Equations A-8 and A-9.

If the failure surface extends below the toe of the slope:

$$Wd = \frac{\gamma H^3}{12} E + \frac{\gamma H^3}{4}\left\{2\eta^2 - 2\eta \sin(\phi) \csc(x) \csc(y)\right\} \qquad \text{(A-16)}$$

where η defines the distance from the toe of the slope to the point of the rupture surface on the ground as $AA' = \eta H$ (Figure 3-10 in Taylor, 1937):

$$\eta = \frac{1}{2}\left\{\cot(x)-\cot(y)-\cot(i)+\sin(\phi) \csc(x) \csc(y)\right\} \qquad \text{(A-17)}$$

With this expression of Wd the following stability number is obtained for failure below the toe:

$$\frac{c_a}{F_c \gamma H} = \frac{\left\{E+6\eta^2-6\eta\sin(\phi)\csc(x)\csc(y)\right\} - \frac{12F_p}{\gamma H^3} A}{6\csc^2(x)\csc(y)\sin(\phi)\left\{\frac{\cos(x)}{\sin(v)}+\csc(u-v)\cos(x-u)\right\}}$$

(A-18)

where

$$A = \frac{\cos(CEO)}{\sin(v)} \frac{H}{2} \csc(x)\csc(y)\sin(\phi) + OG \qquad (A\text{-}19)$$

If only a fraction of F_p is assumed mobilized, F_p is divided by the proper number in Equations (A-15) and (A-18).

APPENDIX B

Determination of the Pile Length Above the Failure Surface

Equations are derived to express the pile length above the critical surface, CE, in terms of the angles x and y defining the critical circle (Figure 9). Hence, each time a new potential critical surface is considered (defined by x and y), a new unit force, F_p, function of CE, is determined and used in the stability computations for that particular surface.

Figures 34 and 35 show the geometry of the slope. S′ is the horizontal distance between the toe and the center of the circle, and S is the horizontal distance between the toe and the pile. CE is the pile length above the failure surface. OG is the moment arm of the force F_p. x is the angle between the chord, AB, and the horizontal, and 2y is the angle AOB of the circle. The distance S is an input parameter since it defines the location of the pile upslope.

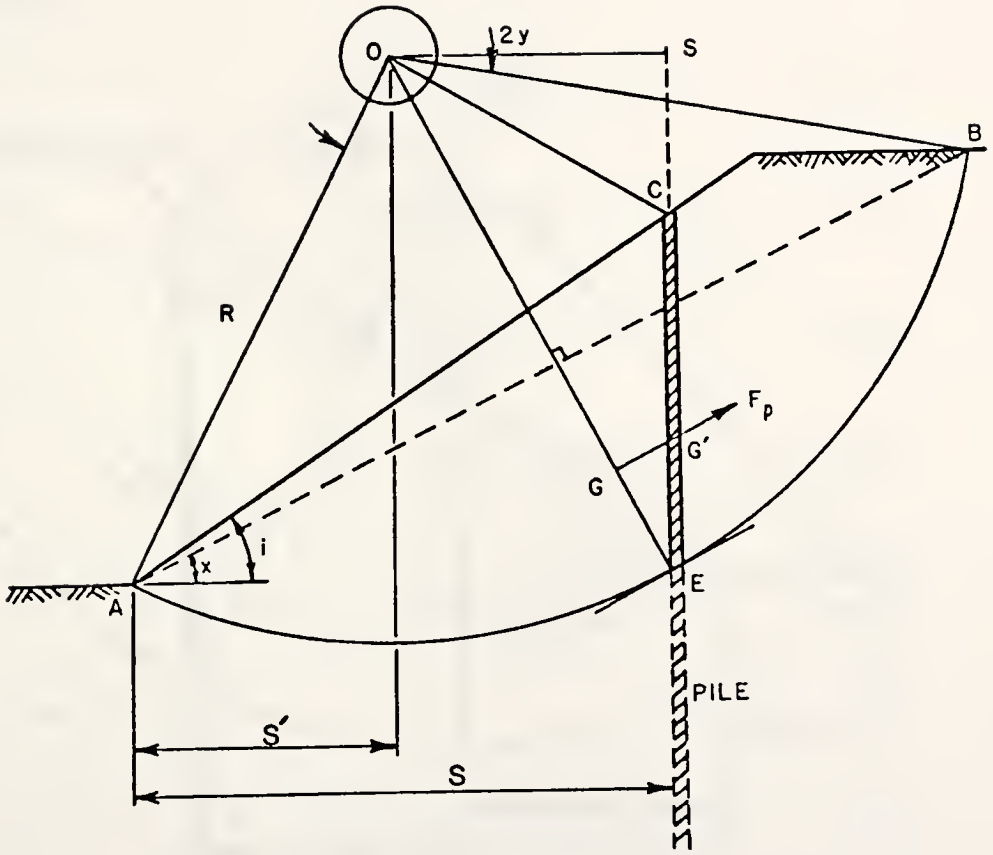

Figure 34 Toe Failure.

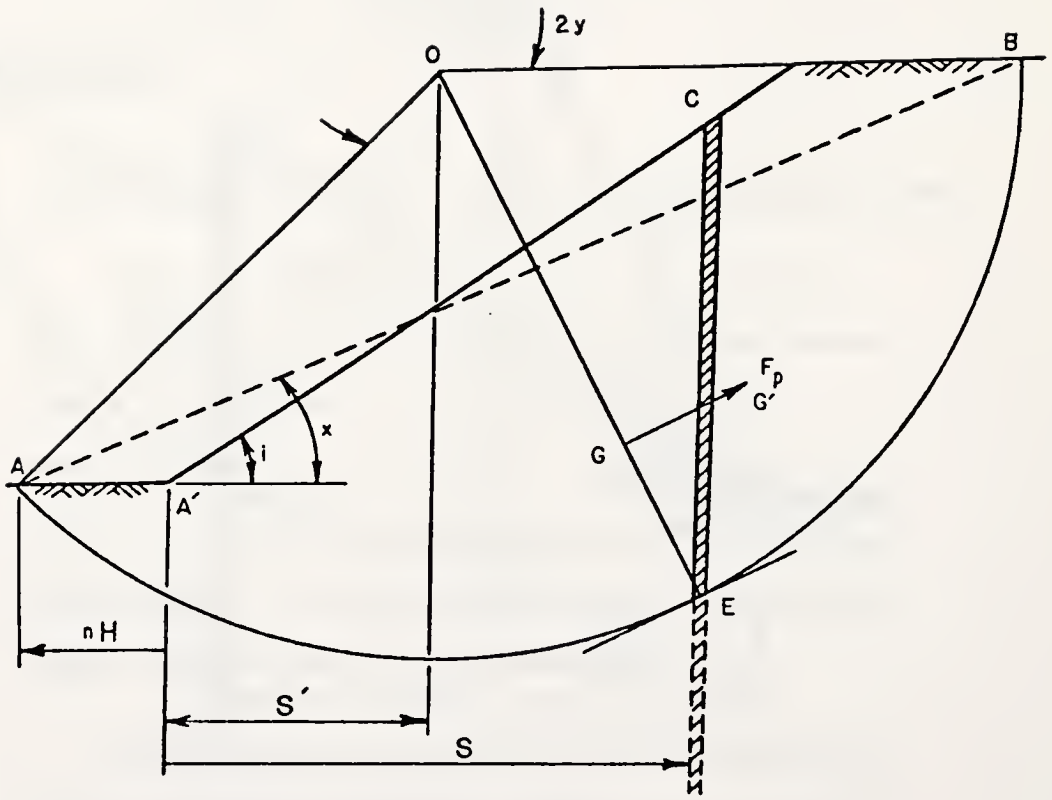

Figure 35 Failure below the Toe.

For a toe failure, the geometry of Figure 34 is considered. The following geometric relationships exist between the different segments and angles in this figure:

$$AC = \frac{D}{\cos(i)} \tag{B-1}$$

$$\hat{OAB} = \hat{OBA} = \frac{\pi}{2} y \tag{B-2}$$

$$S' = R \cos (\hat{OAB} + x) \tag{B-3}$$

$$\hat{OAC} = \hat{OAB} - (i-x) \tag{B-4}$$

$$\hat{OCA} = \cos^{-1} \left\{\frac{OC^2 - R^2 - AC^2}{-2AC(OC)}\right\} \tag{B-5}$$

and

$$\hat{OCE} = \hat{OCA} + 90 - i \tag{B-6}$$

Hence, using Equations (B-1) to (B-6), CE is obtained as:

$$CE = \frac{2(OC)\cos(\hat{OCE}) + \sqrt{\{2(OC)\cos(\hat{OCE})\}^2 - 4(OC^2 - R^2)}}{2} \tag{B-7}$$

If the pile is at the left of the origin, 0, the angle $\hat{OCE}$ is replaced in this equation by:

$$\hat{OCE} = \frac{3}{2}\pi + i - \hat{OCA} \tag{B-8}$$

For cases where the failure surface passes below the toe, the geometry of Figure 35 is considered. The following geometric relations exist:

$$AA' = \eta H \tag{B-9}$$

where $\eta = \frac{1}{2} \{\cot(x)-\cot(y)-\cot(i)+\sin(\phi) \csc(x) \csc(y)\}$ (B-10)

$$AC = D/\cos(i) \tag{B-11}$$

$$OAA' = OAB + x \tag{B-12}$$

$$OA'A = \cos^{-2} \{\frac{R^2 - OA'^2 - AA'^2}{-2AA' (OA')}\} \tag{B-13}$$

$$OA'C = \eta - OA'A - i \tag{B-14}$$

$$OCA' = \cos^{-2} \{\frac{OA'^2 - A'C^2 - OC^2}{-2 A'C (OC)}\} \tag{B-15}$$

and

$$OCE = OCA' + (\frac{\pi}{2} - i) \tag{B-16}$$

CE is then calculated by introducing the values obtained by Equations (B-8) to (B-16) in Equation (B-7). If the pile is at the left of the origin, the angle OCE is given by Equation (B-8).

The force F_p is assumed to act at the centroid of the pressure diagram in a direction parallel to the tangent to the circle at the point of intersection between the pile and the failure surface. Hence, the moment arm, OG, of this force is:

$$OG = R - G'E \cos (CEO) \qquad \text{(B-17)}$$

where G'E is the distance from the centroid of the pressure diagram to the failure surface and the angle CEO is given by:

$$CEO = \cos^{-1} \left\{ \frac{OC^2 - CE^2 - R^2}{-2CE(R)} \right\} \qquad \text{(B-18)}$$

APPENDIX C

Slope Stability Program

After reading the input data, the slope stability program performs the following steps.

1) Initializes an angle of friction ϕ

2) Computes the stability number for every possible surface through the slope

   If piles are used, the following additional steps are necessary for the calculation of a stability number

   a) The distance, measured along the length of the pile from the face of the slope to the surface under investigation, is computed
   b) The reaction,from the piles on the slope, is calculated
   c) The moment arm from the center of the phi-circle is found
   d) The stability number for the surface is calculated

3) Finds the critical stability number after all possible surfaces have been investigated

4) Uses the critical stability number to calculate a factor of safety with respect to cohesion

5) Checks for convergence
   If the difference between the factor of safety with respect to cohesion and the one with respect to friction is larger than the tolerance the program repeats steps 1 to 4. If the difference is less than the tolerance, it exits the itteration

6) Prints out the input and output

The following data is required for the design program. All input is free formated.

DATA CARDS

CARD 1	slope	slope angle in degrees
	h	height of slope
	s	horizontal distance from the toe of the slope to the piles
CARD 2	pilein	indicates the presence of piles
	nosur	indicates the type of analysis needed. For pilein=0 and nosur=0, the unreinforce slope is analyzed. For pilein=1 and nosur=0, the reinforced slope is analyzed and the new critical surface is found. For pilein=0 and nosur=1, the reinforced slope is analyzed assuming that the piles did not alter the original critical surface
CARD 3	phiav	friction angle for the soil, in degrees
	c	cohesion intercept of the soil
	gamma	unit weight of the soil
CARD 4	fphi	initial factor of safety with respect to friction; usually taken as 1.0
	sfdif	the difference between the safety factor with respect to friction and the one with respect to cohesion, used when checking for convergence. A difference of 0.001 is sufficient
CARD 5	d0	the pile diameter,b.
	d1	the center to center distance between the piles
CARD 6	fpar	degree of mobilization of Fp. For fpar=1, the total force, Fp, will be used. For Fp=0 the force will be divided by the factor of safety

```
c-------------------------------------------------------
c-------------------------------------------------------
c----------      DATA  INPUT      ----------------------
c-------------------------------------------------------
c-------------------------------------------------------
c
c   slope    = slope angle in degrees
c   h        = slope height
c   s        = the horizontal distance from the toe of
c              the slope to the piles
c   pilein   = The two quantities are used together to indi-
c   nosur      cate the presence of the pile and the type
c              of analysis needed.  When no piles are
c              present, both pilein=0, and nosur=0
c              When piles are present and they change the
c              critical surface, pilein=1, and nosur=0
c              When piles are present but are not expected
c              to change the critical surface, pilein=0, and
c              nosur=1
c   phiav    = friction angle of the soil in degrees
c   c        = cohesion of the soil
c   gamma    = unit weight of the soil
c   fphi     = initial factor of safety with respect to
c              friction
c   sdif     = difference between the safety factor with
c              respect to friction and the one with respect
c              to cohesion that will be used to check
c              convergence.  A difference of 0.001 will be
c              sufficient
c   d0       = pile diameter
c   d1       = center to center distance between the piles
c   fpar     = 0 if Fp is partially mobilized.  Otherwise,
c              it is equal to 1
c   dfac     = a parameter in subroutine phycir.  The max
c              depth of the failure surface measured from
c              the top of the slope is limited to dfac*h
c
c-------------------------------------------------------
c-------------------------------------------------------
c
c         MAIN PROGRAM
      parameter(pi=3.14159)
      common /all/ slope,h,csslp,cgch,oc,phi,xmax,ymax,
     1 nmax,dmax,tanslp,
     1 snmax,m,cotslp,sinphi,pilein,gamma,s,cosx,tanx,
     2  d,n,x,y,cscx,cscy,ge,fp,ce,ceo,og,r,oach,direc
      common /pres/ d0,d1,d2,tanphi,c,p(2),phiav
c
      common /phi/ cemax,fpmax,rmax,fc
       common /pc/ ii,jj,kk,ll,nosur,fpar
c
c
      real nmax
```

```
      integer  pilein,fpar
c
      read (5,*),slope,h,s
      read (5,*),pilein,nosur
      read (5,*),phiav,c,gamma
      read (5,*),d0,d1
      read (5,*),fpar
c
      d2=d1-d0
c
c In defining the different failure surfaces,
c x goes from 15 to m degrees and y goes
c from 25 to 50 degrees
c
      m=nint(slope)-1
       ii=25
       jj=50
       kk=15
       ll=m
      fc=1.0
c
      phiav=phiav*pi/180.
      slope=slope*pi/180.
      tanphi=tan(phiav)
      cosslp=cos(slope)
      cotslp=1./tan(slope)
      tanslp=tan(slope)
c
c a new critical surface is found after the addition
c of the piles
c
c initialize a friction angle
c
c
 100   phi =atan(tan(phiav)/fphi)
c
      sinphi=sin(phi)
c
c find the critical stability number
c
      call phicir
c     ==========
c
c:::::
c
      if (snmax.le.0.0) then
      print*,'You are overdesigning the slope'
      stop
      endif
c
c:::::
      fc=c/(snmax*gamma*h)
c
```

```
c  when phi is equal to zero
c
        if (phiav.le.0.0)  then
        fs=fc
        go to 05
        endif
c
c  check for convergence of the safety factors
c
       diff=abs(fc-fphi)
       if (diff.gt.sfdif) then
       fphi=(fphi+fc)/2.
       go to 100
       else
       fs=(fphi+fc)/2.
       endif
 05     continue
c
c one well defined surface that does not change with the
c presense of the piles
c
           if (nosur.eq.1.and.pilein.eq.0) then
c
            pilein=1
c
           ii=ymax*180/pi
           jj=ymax*180/pi
           kk=xmax*180/pi
           ll=xmax*180/pi
c
        fphi=1.
        fc=1.
c
c intialize a friction angle
c
 101    phi=atan(tan(phiav)/fphi)
        sinphi=sin(phi)
c
c find the critical stability number
c
        call phicir
c       ==========
c:::::
c
       if (snmax.le.0.0) then
       print*,'You are overdesigning the slope'
       stop
       endif
c
c:::::
        fc=c/(snmax*gamma*h)
c
c when phi is equal to zero
```

```
c
        if (phisv.le.0.0) then
        fs=fc
        go to 06
        endif
c
c check for convergence of the safety factors
c
        diff=abs(fc-fphi)
           if (diff.gt.sfdif) then
           fphi=(fphi+fc)/2.
           go to 101
           else
        fs=(fphi+fc)/2.
           endif
 06      continue
       endif
c
       slope=slope*180./pi
       phiav=phiav*180./pi
       xmax=xmax*180./pi
       ymax=ymax*180./pi
c
c
       write (6,440) slope,h,phisv,c,gamma
 440   format ('SLOPE CONFIGURATION'//
     1 5x,'Slope Angle = ',f5.1/
     1 5x,'Slope Height = ',f5.1//
     1 'SOIL PARAMETERS'//
     1 5x,'Friction Angle = ',f5.1/
     1 5x,'Cohesion = ',f6.1/
     1 5x,'Unit Weight = ',f6.1//)
c
            if (pilein.eq.0.and.nosur.eq.0) go to 450
       write (6,441) d0,dl,s
 441   format ('PILE DIMENSIONS'//
     1 5x,'Pile Diameter = ',f4.1/
     1 5x,'Center-to-Center Distance = ',f5.1/
     1 5x,'Distance Upslope = ',f5.1//)
c
            if (pilein.eq.1.and.nosur.eq.0) then
       write (6,442)
 442   format ('GEOMETRY OF THE CRITICAL SURFACE'//
     1 5x,'The critical surface of the slope changes'/
     1 5x,'with the insertion of the piles'//)
            else if (pilein.eq.0.and.nosur.eq.1) then
       write (6,443)
 443   format ('GEOMETRY OF THE CRITICAL SURFACE'//
     1 5x,'The critical surface of the slope does not change'/
     1 5x,'by the presence of the piles'//)
            endif
c
       write (6,444) xmax,ymax
```

```
 444   format (5x,'The angles that define the circle are:'/
     1 10x,'x= ',f5.1/
     1 10x,'y= ',f5.1//)
c
           if (nmax.lt.0.) then
       write (6,445)
 445   format (5x,'Toe failure'//)
           else if (nmax.gt.0) then
       hnmax=nmax*h
       write (6,446) hnmax
 446   format (5x,'Failure below the toe.   The critical surface'/
     1 5x,'intercepts the ground surface ',f7.2,'units left '/
     1 5x,'of the toe'//)
           endif
c
           if (fpar.eq.1) then
       write (6,447)
 447  format ('UNIT REACTION FORCE ON THE SLOPE EXERTED BY THE PILES'//
     1 5x,'Fp is assumed to be totally mobilized'//)
           else if (fpar.ne.1) then
       write (6,448)
 448  format ('UNIT REACTION FORCE ON THE SLOPE EXERTED BY THE PILES'//
     1 5x,'Fp is assumed to be partially mobilized,'/
     1 5x,'and is equal to Fp/FS'//)
           endif
c
c
       write (6,449) fpmax,cemax
 449   format (5x,'The unit reaction force on the slope provided'/
     1 5x,'by the piles is ',f7.0//
     1 5x,'The distance from the ground to the critical surface,'/
     1 5x,'CE, is 'f5.1//)
c
 450   write (6,451) sfdif, fs
 451   format ('FACTOR OF SAFETY'//
     1 5x,'The tolerable difference between Fc and Fphi'/
     1 5x,'is ',f7.4//
     1 5x,'The safety factor of the slope is  ',f5.2)
c
c
       stop
       end
c
c
c-------------------------------------------------------
       subroutine phicir
c-------------------------------------------------------
c
c subroutine that computes the critical surface and
c stability number
c
       real n,nmax,nfact
       common /all/ slope,h,csslp,cgch,oc,phi,xmax,ymax,
```

```
     1 nmax,dmax,tanslp,
     1 snmax,m,cotslp,sinphi,pilein,gamma,s,cosx,tanx,
     2 d,n,x,y,cscx,cscy,ge,fp,ce,ceo,og,r,oach,direc
c
      common /phi/ cemax,fpmax,rmax,fc
       common /pc/ ii,jj,kk,ll,nosur,fpar
c
       integer m,pilein,fpar
       parameter(pi=3.14159,dfac=8.50,nfact=169.)
c
c
c
          if (fc.le.1.0) f=1.0
          if (fc.gt.1.0) f=fc
          if (fpar.eq.1) f=1.0
c
c
       snmax=0.0
c
       do 20 numy=ii,jj
       do 10 numx=kk,ll
c
c
       x=numx*pi/180.
       y=numy*pi/180.
       cosx=cos(x)
       tanx=tan(x)
       cotx=1./tan(x)
       coty=1./tan(y)
       cscx=1./sin(x)
       cscy=1./sin(y)
       secx=1./cos(x)
       cosx=cos(x)
       siny=sin(y)
c
       d=0.5*(cscx*cscy-cotx*coty+1)
       n=0.5*(cotx-coty-cotslp+sinphi*cscx*cscy)
c
c
       if (n.le.0.0) then
c.....................................................
c  the  failure  surface  passes  through  the  toe
c.....................................................
       if (y.gt.x.and.d.ge.dfac) go to 20
c
c
         if (phi.le.0.0)go to 06
c
       h2dn=0.5*cscx**2*(y*cscy**2-coty)+cotx-cotslp
       h2dd=1./3.*(1.-2.*cotslp**2)+cotslp*(cotx-coty)+cotx*coty
       h2d =h2dn/h2dd
c
       cotu=h2d*y*secx*cscx*cscy**2-tan(x)
```

```
         u=atan(1./cotu)
       sinuv=h2d*sin(u)*cscx*cscy*sinphi
       cscuv=1./sinuv
c
       angl=asin(sinuv)
       v=u-angl
       sinv=sin(v)
c
 06    if (pilein.le.0) then
c
c  ***  without piles  ***
c
         if (phi.gt.0.0) then
       cfwhn=h2dn
       cfwhd=2.*cotx/tan(v)+2.
           else if (phi.le.0.0) then
       cfwhn=(1.-2*cotslp**2)/3.+cotx*coty+cotslp*(cotx-coty)
       cfwhd=2.*y*cscx**2*cscy**2
           endif
c
       sn=cfwhn/cfwhd
       else if (pilein.ne.0) then
c
c  ***  with piles  ***
c
       call momarm
c      ===========
       eq4=1.-(2.*cotslp**2)+(3.*cotslp*cotx)-(3.*cotslp*coty)
     1 +(3.*cotx*coty)
c
         if (phi.gt.0.0) then
       cfwhn=eq4-((12.*fp)/(f*gamma*h**3)*(cos(ceo)/sinv*h/2.*
     1 cscx*cscy*sinphi+og))
       cfwhd=6.*cscx**2*cscy**2*siny*sinphi*(cosx/sinv+
     1 cscuv)
         else if (phi.le.0.0) then
       cfwhn=eq4-12.*fp*og/(f*gamma*h**3)
       cfwhd=6.*y*cscx**2*cscy**2
         endif
c
       sn=cfwhn/cfwhd
       endif
c
       else
c.....................................................
c  the  failure  surface  passes  below  the  toe
c.....................................................
       if (n.gt.nfact) go to 20
       if (y.gt.x.and.d.ge.dfac) go to 20
c
c
         if (phi.le.0.0) go to 07
       h2dn=0.5*cscx**2*(y*cscy**2-coty)+cotx-cotslp-2.*n
```

```
      h2dd=1./3.*(1.-2.*cotslp**2)+cotslp*(cotx-coty)+cotx*coty
     1 +2.*n**2-2.*n*sinphi*cscx*cscy
      h2d=h2dn/h2dd
c
      cotu=h2d*y*secx*cscx*cscy**2-tan(x)
         u=atan(1./cotu)
      sinuv=h2d*sin(u)*cscx*cscy*sinphi
      cscuv=1./sinuv
      angl=asin(sinuv)
         v=u-angl
         sinv=sin(v)
c
 07   if (pilein.eq.0) then
c
c ***  without piles  ***
c
         if (phi.gt.0.0) then
      cfwhn=h2dn
      cfwhd=2.*cotx/tan(v)+2.
         else if (phi.le.0.0) then
      cfwhn=(1.-2.*cotslp**2)/3.+cotx*coty+cotslp*(cotx-coty)+2*n**2
      cfwhd=2.*y*cscx**2*cscy**2
         endif
      sn=cfwhn/cfwhd
      else if (pilein.ne.0) then
c
c  ***  with piles  ***
c
      call momarm
c     ===========
      if (oach.gt.r) go to 20
      eq4=1.-(2.*cotslp**2)+(3.*cotslp*cotx)-(3.*cotslp*coty)
     1 +(3.*cotx*coty)
         if (phi.gt.0.0) then
      cfwhn=(eq4+3.*(2.*n**2-2.*n*sinphi*cscx*cscy))-12.*fp/
     1 (f*gamma*h**3)*(cos(ceo)/sinv*h/2.*cscx*cscy*sinphi+og)
      cfwhd=6.*cscx**2*cscy**2*siny*sinphi*(cosx/sinv+cscuv)

         else if (phi.le.0.0) then
      cfwhn=eq4+6*n**2-12.*fp*og/(f*gamma*h**3)
      cfwhd=6.*y*cscx**2*cscy**2
         endif
      sn=cfwhn/cfwhd
      endif
c
      endif
c
c
c::::::::::::::::::::::::::::::::::::::::::::::::::::::::::::::
      if (sn.gt.snmax) then
      snmax=sn
      ymax=y
      xmax=x
```

```
      dmax=d
      nmax=n
      cemax=ce
      fpmax=fp
      rmax=r
c::::::::::::::::::::::::::::::::::::::::::::::::::::::::::::::
c
c
c
      endif
 10   continue
 20   continue
c
      return
      end
c
c
c-------------------------------------------------------------
      subroutine momarm
c-------------------------------------------------------------
c
c subroutine that calculates the moment arm of
c force Fp
c
      common /all/ slope,h,csslp,cgch,oc,phi,xmax,ymax,
     1 nmax,dmax,tanslp,
     1 snmax,m,cotslp,sinphi,pilein,gamma,s,cosx,tanx,
     2 d,n,x,y,cscx,cscy,ge,fp,ce,ceo,og,r,oach,direc
      real n
      parameter (pi=3.14159)
c
      r=h/2.*cscx*cscy
      oab=pi/2.-y
c
      if (n.lt.0.0) then
c.....................................................
c   the failure surface passes through the toe
c.....................................................
      ac=s/csslp
      oabx=oab+x
      sch=r*cos(oabx)
      oac=oab-slope+x
      oc=sqrt(r**2+ac**2-2.*r*ac*cos(oac))
      oca=acos((r**2-oc**2-ac**2)/((-2.)*ac*oc))
c
      if (sch.gt.s) then
c   pile to the left of origin
      oce=3./2.*pi+slope-oca
      else if (sch.lt.s) then
c   pile to the right of origin
      oce=pi/2.-slope+oca
      else if (sch.eq.s) then
c   pile underneath the origin
```

```
      ce=r-oc
      og=oc+cgch
      go to 111
      endif
c
      else if (n.gt.0.0) then
c.....................................................
c   the failure surface passes below the toe
c.....................................................
      aach=n*h
      achc=s/cosslp
      oaach=oab+x
      oach=sqrt(aach**2+r**2-2.*r*aach*cos(oaach))
      oacha=acos((r**2-oach**2-aach**2)/((-2.)*aach*oach))
      oachc=pi-slope-oacha
      oc=sqrt(oach**2+achc**2-2.*oach*achc*cos(oachc))
      ocach=acos((oach**2-achc**2-oc**2)/((-2.)*achc*oc))
      sch=oach*cos(pi-oacha)
c
      if (sch.gt.s) then
c   pile on left of origin
      oce=3./2.*pi+slope-ocach
      else if(sch.lt.s) then
c   pile to the right of origin
      oce=ocach+pi/2.-slope
      else if (sch.eq.s) then
c   pile underneath origin
      ce=r-oc
      og=oc+cgch
      go to 111
      endif
      endif
c
c
      ce=(2.*oc*cos(oce)+sqrt((2*oc*cos(oce))**2-4.*(oc**2
     1 -r**2)))/2.
c  cosc=cos(ceo)
      cosc=(oc**2-ce**2-r**2)/((-2.)*ce*r)
      ceo=acos(cosc)
c
      call presur
c     ===========
      gche=ce-cgch
      eg=gche*cosc
c     if (direc.eq.1) then
      og=r-eg
  111 continue
c
c
      return
      end
c
c
```

```
c-------------------------------------------------------
      subroutine presur
c-------------------------------------------------------
c
c subroutine that calcuates pressure Fp
c
      parameter (pi=3.14159)
      common /all/ slope,h,csslp,cgch,oc,phi,xmax,ymax,
     1 nmax,dmax,tanslp,
     1 snmax,m,cotslp,sinphi,pilein,gamma,s,cosx,tanx,
     2 d,n,x,y,cscx,cscy,ge,fp,ce,ceo,og,r,oach,direc
c
      common /pres/ d0,d1,d2,tanphi,c,p(2),phiav
      real nphi,nphi1,nphi2
c
c
c     equation in the form p=a+bz gives the pressure on the pile
c     as a function of depth z
c
      z=0.0
      do 10 i=1,2
      nphi=(tan(pi/4.+phiav/2.))**2
      nphi1=(nphi)**(.5)
      nphi2=(nphi)**(-.5)
      par1=(d1-d2)/d2*nphi*tan(pi/8.+phiav/4.)*tanphi
      par2=(2.*tanphi+2*nphi1+nphi2)/(nphi1*tanphi+nphi-1)
      par3=nphi1*tanphi+nphi-1
c
      if (c.le.0.0) then
c
c     cohesionless  soil
c
      p(i)=gamma*z/nphi*(d1*(d1/d2)**par3*exp((d1-d2)/d2*nphi*
     1 tanphi*tan(pi/8+phiav/4))-d2)
      else if (phiav.le.0.0) then
c
c     cohesive  soil
c
      p(i)=c*(d1*(3*alog10(d1/d2)+(d1-d2)/d2*tan(pi/8))
     1 -2*(d1-d2))+gamma*z*(d1-d2)
      else
c
c     c-phi  soil
c
      p(i)=c*d1*(d1/d2)**par3*(1/(nphi*tanphi)*(exp(par1)-2*nphi1
     1 *tanphi-1)+par2)-c*(d1*par2-2*d2*nphi2)+gamma*z/nphi*
     2 (d1*(d1/d2)**par3*exp(par1)-d2)
      endif
      z=ce
 10   continue
c
c     to find the force (ie.the area of the pressure diagram
c     and its center of action)
```

```
c
c
      a1=ce*p(1)
      a2=ce*(p(2)-p(1))/2.
      y1=ce/2.
      y2=2*ce/3.
      a1y1=a1*y1
      a2y2=a2*y2
      sum=a1y1+a2y2
      ftot=a1+a2
      y3=sum/ftot
      cgch=y3
      fp=ftot/dl
c
c
      return
      end
```

DATA

```
30.  45.   25.
1 0
10.  500.  125.
1.   .001
3.   7.5
0
```

RESULTS

SLOPE CONFIGURATION

Slope Angle = 30.0
Slope Height = 45.0

SOIL PARAMETERS

Friction Angle = 10.0
Cohesion = 500.0
Unit Weight = 125.0

PILE DIMENSIONS

Pile Diameter = 3.0
Center-to-Center Distance = 7.5
Distance Upslope = 25.0

GEOMETRY OF THE CRITICAL SURFACE

The critical surface of the slope changes with the insertion of the piles

The angles that define the circle are:
x= 23.0
y= 35.0

Toe failure

UNIT REACTION FORCE ON THE SLOPE EXERTED BY THE PILES

Fp is assumed to be partially mobilized, and is equal to Fp/FS

The unit reaction force on the slope provided by the piles is 21424.

The distance from the ground to the critical surface, CE, is 16.5

FACTOR OF SAFETY

The tolerable difference between Fc and Fphi is 0.0010

The safety factor of the slope is 1.33

APPENDIX D

Pile Analysis Program

After reading the input data, the pile analysis program performs the following steps.

1) Computes the force F_t on the pile

2) Constructs an array and solves the simultaneous equations produced by the finite difference method. The displacement of the pile below the critical surface is thus obtained

3) Calculates the slope, bending moment and shear force on the pile section below the critical surface

4) Calculates the displacement, slope bending moment, and shear force for the pile section above the failure surface, using a closed form solution

5) Prints out the input and output

The following data is required for the pile analysis program. All input is free formated.

DATA CARDS

CARD 1	phiav	friction angle for the soil, in degrees
	c	cohesion intercept for the soil
	gamma	unit weight of the soil
CARD 2	CE	depth from the slope face to the critical surface
	EL	depth of pile below the critical surface
	EB	depth of pile from the critical surface to the bedrock
	BD	depth of pile embedded in the bedrock. If bedrock is not present, the quantities EB and BD can be used to indicate the depth of two different layers of material below the critical surface. If the material below the critical surface is uniform, one of the two quantities can be set equal to zero.
CARD 3	MT	number of discretized points below the critical surface
CARD 4	d0	the pile diameter, b.
	d1	the center-to-center distance between the piles
	EI	pile stiffness
CARD 5	ks0	the coefficient of the horizontal subgrade reaction at the critical surface
	ks1	the coefficient of the horizontal subgrade reaction at the end of layer EB
	kr0	the coefficient of the horizontal subgrade reaction at the beginning of layer BD
	kr1	the coefficient of the horizontal subgrade reaction at the end of the pile
CARD 6	n1	index greater or equal to zero. Indicates the variation of ks with depth, for the layer EB. For example, if n1=0, ks is constant with depth. If n1=1, ks increases

		linearly with depth.
	n2	same index as nl. Indicates the variation of ks with depth for layer BD
CARD 7	bc	boundary condition at the top of the pile, equals to 1, 2, 3, or 4 (see Chapter 4)
	hr	Indicates the degree of hardness of layer BE. For hr=1, the layer is composed of hard rock (stiffer than the pile itself). For hr=0, this layer is composed of soft rock or soil
	kopt	gives the user the option to input ks for every single point of the discretized pile below the critical surface. For kopt=0, a total number of MT additional data cards (following card 7) are required.

```
c-------------------------------------------------------
c-------------------------------------------------------
c----------     DATA  INPUT     -------------------------
c-------------------------------------------------------
c-------------------------------------------------------
c
c    phiav   = friction angle of the soil in degrees
c    c       = cohesion of the soil
c    gamma   = unit weight of the soil
c    CE      = depth from the slope face to the critical
c              surface
c    EL      = depth of the pile below the critical surface
c    EB      = distance between the critical surface and
c              the bedrock
c    BD      = depth of the pile below the bedrock
c    mt      = number of points the pile will be descretized
c              to
c    d0      = pile diameter
c    dl      = center-to-center distance between the piles
c    ks0     = coefficient of subgrade reaction at the
c              critical surface
c    ksl     = coefficient of subgrade reaction at the end
c              of layer EB
c    kr0     = coefficiet of subgrade reaction at the beginning
c              of layer BD
c    krl     = coefficient of subgrade reaction at the end of
c              the pile
c    nl      = index that indicates the variation of ks with
c              depth.  For nl=0, ks is constant, for nl=1
c              ks increases linearly  (in layer EB)
c    n2      = same as nl, for layer BD
c    ei      = pile stiffness
c    bc      = boundary condition for the pile top (1, 2, 3, or 4)
c    hr      = for hr=1, layer BE is assumed to be hard rock
c              for hr=0, it is assumed to be soft rock or soil
c    kopt    = if kopt=0, a total number of mt additional data
c              cards are required to input the values of the
c              subgrade reaction along the pile
c
c-------------------------------------------------------
c-------------------------------------------------------
c
c            MAIN PROGRAM
      dimension a(85,86),g(85,86),h(85,86),y(86)
      dimension zl(86),z2(86),sl(86),s2(86)
      dimension ml(86),m2(86),vl(86),v2(86),yl(86)
      dimension ki(86)
c
      parameter (mtl=6,pi=3.14159)
c
       common /all/ ce,d0,dl,phiav,c,gamma,p(2)
c
      integer bc, r, hr
```

```
      real  n1,n2,  ks0,ks1,ks,  kr0,kr1,kr, m1,m2,  ki
c
      read(5,*) phiav,c,gamma
      read(5,*) ce,e1,eb,bd
      read(5,*) mt
      read(5,*) d0,d1,ei
      read(5,*) ks0,ks1,kr0,kr1
      read(5,*) n1,n2
      read(5,*) bc,hr,kopt
         if (kopt.le.0) then
      do 480 i=3,mt+3
      read(5,*) ki(i)
 480  continue
         endif
c
c
      write (6,460) phiav,c,gamma
 460  format ('SOIL PARAMETERS'//
     1 5x,'Above The Critical Surface'//
     1 10x,'Friction Angle = ',f4.1,' degrees'/
     1 10x,'Cohesion = ',f6.1/
     1 10x,'Unit Weight = ',f6.1//
     1 5x, 'Below The Critical Surface'//)
c
        if (kopt.ne.0) then
      write (6,461) ks0,ks1,kr0,kr1,kopt
 461  format (10x,'Coefficients of Subgrade Reaction'//
     1 20x,'ks0 = ',e10.3/
     1 20x,'ks1 = ',e10.3/
     1 20x,'kr0 = ',e10.3/
     1 20x,'kr1 = ',e10.3//
     1 10x,'kopt = ',I2//)
c
        else if (kopt.eq.0) then
      write (6,462)
 462  format (10x,'Coefficients of Subgrade Reaction'//)
        do 463 i=3,mt+3
      write (6,464) ki(i)
 464  format (20x,e10.3)
 463  continue
      write (6,465) kopt
 465  format (10x,/
     1 10x,'kopt = ',i2//)
c
        endif
c
      write (6,466) n1,n2
 466  format (10x,'Variation of the subgrade reaction coefficients'//
     1 20x,'n1 = ',f3.1/
     1 20x,'n2 = ',f3.1//)
c
      write (6,467) ce,e1,eb,bd,d0,d1,ei,mt
 467  format ('PILE DIMENSIONS'//
```

```
     1 5x,'Length of pile above the critical surface = ',f4.1/
     1 5x,'Length below the critical surface = ',f4.1/
     1 10x,'Distance between the critical surface and the'/
     1 10x,'bedrock (or hard soil layer) = ',f4.1/
     1 10x,'Length of pile embedded in the bedrock = ',f4.1//
     1 5x,'Pile Diameter = ',f4.1/
     1 5x,'Center-to-Center Distance = ',f4.1/
     1 5x,'Stiffness = 'e10.3//
     1 5x,'Number of points that the pile length below the'/
     1 5x,'critical surface is discretized to = ',i3//)
c
       if (bc.eq.1) print*,'Boundary Condition--Free Head'
       if (bc.eq.2) print*,'Boundary Condition--Unrotated Head'
       if (bc.eq.3) print*,'Boundary Condition--Hinged Head'
       if (bc.eq.4) print*,'Boundary Condition--Fixed Head'
c
c
c
        phiav=phiav*pi/180.
         call presur
         p1=p(1)
         p2=p(2)
         write (6,469) p(1),p(2)
 469     format (5x,/
     1   5x,'Force Diagram'/
     1   10x,'force on the pile head = 'f7.0/
     1   10x,'force acting on the pile at the critical'/
     1   10x,'surface = 'f7.0//)
c
         write (6,470)
 470     format (5x,'Z',8x,'DISPL(Y)',7x,'SLOPE(S)',7x,'MOMENT(M)',
     1   6x,'SHEAR(V)'//)
c
       b=d0
c
        ks=ks1-ks0
        kr=kr1-kr0
       q=el/mt
       a3=q**4/ei
        f1=p2
        f2=(p2-p1)/ce
c
c*************************************************************
c Finite difference solution for the pile section below
c the failure surface --solving the simultaneous equations
c*************************************************************
c
c.............................................................
c Constructing the array
c.............................................................
c
c     zero array
              do 2 i=1,85
```

```
            do 3 j=1,86
       a(i,j)=0.
 3          continue
 2          continue
c
c
c      read first two boundary conditions
c
      if (bc.eq.1.or.bc.eq.3) then
       a(1,1)=ce
       a(1,2)=2.*q-2.*ce
       a(1,3)=-4.*q
       a(1,4)=2.*q+2.*ce
       a(1,5)=-ce
       a(1,mt+6)=2*q**3*(f2/(6*ei)*ce**3-f1/(2*ei)*ce**2)
      endif
      if (bc.eq.1.or.bc.eq.2) then
       a(2,1)=-1.
       a(2,2)=2.
       a(2,4)=-2.
       a(2,5)=1.
       a(2,mt+6)=2*q**3*(f1/ei*ce-f2/(2*ei)*ce**2)
      endif
      if (bc.eq.2.or.bc.eq.4) then
       a(1,1)=-(ce**2)
       a(1,2)=2*ce**2-4*q*ce-2*q**2
       a(1,3)=8*q*ce
       a(1,4)=-2*ce**2-4*q*ce+2*q**2
       a(1,5)=ce**2
       a(1,mt+6)=4*q**3*(f1/(6*ei)*ce**3-f2/(24*ei)*ce**4)
      endif
      if (bc.eq.3.or.bc.eq.4) then
       a(2,1)=ce**3
       a(2,2)=6*q**2*ce+6*q*ce**2-2*ce**3
       a(2,3)=12.*q*(q**2-ce**2)
       a(2,4)=6*q*ce**2-6*q**2*ce+2*ce**3
       a(2,5)=-ce**3
       a(2,mt+6)=12*q**3*(f2/(120*ei)*ce**5-f1/(24*ei)*ce**4)
      endif
c
c      inputing rest of array
c
            do 30 i=3,mt+3
          j=i-2
       a(i,j)=1.
          j=i-1
       a(i,j)=-4.
          j=i
       m=i-3
       z=m*q
c
       if (kopt.ge.1) then
c
```

```
      if (z.le.eb) then
       a(i,j)=6.+a3*b*(ks0+ks*(z/eb)**n1)
      elseif (z.gt.eb) then
       a(i,j)=6+a3*b*(kr0+kr*((z-eb)/bd)**n2)
       endif
c
       elseif (kopt.le.0) then
c
       a(i,j)=6.+a3*b*ki(i)
c
       endif
           j=i+1
       a(i,j)=-4.
           j=i+2
       a(i,j)=1.
 30            continue
c
c       inputing last boundary conditions
c
c
         if (hr.le.0) then
c Soft Rock, Shear and Moment equal zero at EL
c
c
           i=mt+5
       a(i,mt+1)=-1.
       a(i,mt+2)=2.
       a(i,mt+4)=-2.
       a(i,mt+5)=1.
c
           i=mt+4
       a(i,mt+2)=1.
       a(i,mt+3)=-2.
       a(i,mt+4)=1.
c
         elseif (hr.ge.1) then
c Hard rock, displacement and  rotation equal zero at EL
c
c
            i=mt+5
       a(i,mt+1)=1.
       a(i,mt+2)=-4.
       a(i,mt+3)=a(mt+3,mt+3)
       a(i,mt+4)=-4.
       a(i,mt+5)=1.
c
           i=mt+4
       a(i,mt+2)=-1.
       a(i,mt+4)=1.
c
           i=mt+3
       a(i,mt+1)=0.
       a(i,mt+2)=0.
```

```
       a(i,mt+3)=1.
       a(i,mt+4)=0.
       a(i,mt+5)=0.
c
        endif
       do 70 i=1,mt+5
       do 80 j=1,mt+6
c         print*, a(i,j)
 80    continue
 70    continue
c
c.....................................................
c      calculating the auxiliary quantities
c.....................................................
c
       sum1=0.
       sum2=0.
       do 111 l=1,mt+5
       do 222 k=1,mt+5
      if (l.le.1) go to 12
       do 22 r=1,l-1
         sum1=sum1+g(k,l-r)*h(l-r,l)
 22    continue
 12      g(k,l)=a(k,l)-sum1
       sum1=0.
 222   continue
c
       i=1
       do 333 j=i+1,mt+6
       m=i
      if (l.le.1) go to 13
       do 32 r=1,i-1
          sum2=sum2+g(i,i-r)*h(i-r,j)
 32    continue
 13       h(i,j)=(a(i,j)-sum2)/g(i,m)
       sum2=0.
 333   continue
 111   continue
c
       do 989 i=1,mt+5
       do 898 j=1,mt+6
 898   continue
 989   continue
c
c.....................................................
c      solving for the unknown displacements y
c.....................................................
c
       sum3=0.
       do 555 l=1,mt+5
        m=mt+6-l
       if (l.le.1) go to 55
      do 65 r=1,l-1
```

```
      sum3=sum3+h(m,m+r)*y(m+r)
 65   continue
 55    y(m)=h(m,mt+6)-sum3
       sum3=0.
         z=(m-3)*q
       if (z.gt.el) go to 555
 555   continue
c
c.....................................................
c       calculating slope s, moment m, and shear v  for
c       z>0.
c.....................................................
c
       do 666 m=3,mt+3
        z2(m)=(m-3)*q
       s2(m)=(y(m+1)-y(m-1))/(2*q)
       m2(m)=-ei*(y(m+1)-2*y(m)+y(m-1))/q**2
       v2(m)=-ei*(y(m+2)-2*y(m+1)+2*y(m-1)-y(m-2))/(2*q**3)
 666   continue
c
c*******************************************************
c Close form solution of the pile section above the
c failure surface
c*******************************************************
c
c.....................................................
c      calculating deflection y, slope s, moment m, and
c      shear v for z<0
c.....................................................
c
       a0=y(3)
       a1=(y(4)-y(2))/(2*q)
       a2=(y(4)-2*y(3)+y(2))/(2*q**2)
       a3=(y(5)-2*y(4)+2*y(2)-y(1))/(12*q**3)
c
       do 777 i=1,mt1+1
       q1=ce/mt1
       z1(i)=-(i-1)*q1
c
       y1(i)=a0+a1*z1(i)+a2*z1(i)**2+a3*z1(i)**3+f1/(24*ei)*z1(i)**4+f2/
     1 (120*ei)*z1(i)**5
       s1(i)=a1+2*a2*z1(i)+3*a3*z1(i)**2+f1/(6*ei)*z1(i)**3+f2/(24*ei)*
     1 z1(i)**4
       m1(i)=-ei*(2*a2+6*a3*z1(i)+f1/(2*ei)*z1(i)**2+f2/(6*ei)*z1(i)**3)
       v1(i)=-ei*(6*a3+f1/ei*z1(i)+f2/(2*ei)*z1(i)**2)
c
 777   continue
c
       i=mt1+1
 442   write (6,440) z1(i),y1(i),s1(i),m1(i),v1(i)
 440   format (2x,f5.1,5x,e10.3,5x,e10.3,5x,e10.3,5x,e10.3)
       i=i-1
          if (i.lt.2) go to 441
```

```
      go to 442
 441  continue
c
      do 443 m=3,mt+3
      write (6,444) z2(m),y(m),s2(m),m2(m),v2(m)
 444  format (2x,f5.1,5x,e10.3,5x,e10.3,5x,e10.3,5x,e10.3)
 443  continue
c
      stop
      end
c
c
c-------------------------------------------------------
      subroutine presur
c-------------------------------------------------------
c
c subroutine that calcultes the force Fp
c
      parameter (pi=3.14159)
      common /all/ ce,d0,dl,phiav,c,gamma,p(2)
c
      real nphi,nphil,nphi2
c
c
c     equation in the form p=a+bz gives the pressure on the pile
c     as a function of depth z
c
         d2=dl-d0
         tanphi=tan(phiav)
c
c
      z=0.0
      do 10 i=1,2
      nphi=(tan(pi/4.+phiav/2.))**2
      nphil=(nphi)**(.5)
      nphi2=(nphi)**(-.5)
      par1=(dl-d2)/d2*nphi*tan(pi/8.+phiav/4.)*tanphi
      par2=(2.*tanphi+2*nphil+nphi2)/(nphil*tanphi+nphi-1)
      par3=nphil*tanphi+nphi-1
c
      if (c.le.0.0) then
c     cohesionless  soil
      p(i)=gamma*z/nphi*(dl*(dl/d2)**par3*exp((dl-d2)/d2*nphi*
     1 tanphi*tan(pi/8+phiav/4))-d2)
      else if (phiav.le.0.0) then
c     cohesive  soil
      p(i)=c*(dl*(3*alog10(dl/d2)+(dl-d2)/d2*tan(pi/8))
     1 -2*(dl-d2))+gamma*z*(dl-d2)
      else
c     c-phi  soil
      p(i)=c*dl*(dl/d2)**par3*(1/(nphi*tanphi)*(exp(par1)-2*nphil
     1 *tanphi-1)+par2)-c*(dl*par2-2*d2*nphi2)+gamma*z/nphi*
     2 (dl*(dl/d2)**par3*exp(par1)-d2)
```

```
      endif
      z=ce
 10   continue
c
      return
      end
```

```
      DATA

10.  500.  125.
16.5  40.  10.  30.
30
3.  7.5  2.e+09
5.e+04  5.e+04  4.e+08  4.e+08
0.  0.
3 1 3
```

RESULTS

SOIL PARAMETERS

Above The Critical Surface

Friction Angle = 10.0 degrees
Cohesion = 500.0
Unit Weight = 125.0

Below The Critical Surface

Coefficients of Subgrade Reaction

ks0 = 0.500e+05
ks1 = 0.500e+05
kr0 = 0.400e+09
kr1 = 0.400e+09

kopt = 3

Variation of the subgrade reaction coefficients

n1 = 0.
n2 = 0.

PILE DIMENSIONS

Length of pile above the critical surface = 16.5
Length below the critical surface = 40.0
Distance between the critical surface and the bedrock (or hard soil layer) = 10.0
Length of pile embedded in the bedrock = 30.0

Pile Diameter = 3.0
Center-to-Center Distance = 7.5
Stiffness = 0.200e+10

Number of points that the pile length below the critical surface is discretized to = 30

Boundary Condition--Hinged Head

Force Diagram
force on the pile head = 4845.
force acting on the pile at the critical surface = 14556.

Z	DISPL(Y)	SLOPE(S)	MOMENT(M)	SHEAR(V)
-16.5	0.439e-06	0.191e-02	-0.300e+01	0.827e+05
-13.8	0.511e-02	0.176e-02	0.207e+06	0.671e+05
-11.0	0.944e-02	0.136e-02	0.365e+06	0.471e+05
-8.3	0.124e-01	0.783e-03	0.462e+06	0.227e+05
-5.5	0.137e-01	0.122e-03	0.486e+06	-0.621e+04
-2.8	0.131e-01	-0.514e-03	0.424e+06	-0.396e+05
0.	0.110e-01	-0.999e-03	0.264e+06	-0.774e+05
1.3	0.953e-02	-0.114e-02	0.162e+06	-0.753e+05
2.7	0.794e-02	-0.122e-02	0.633e+05	-0.736e+05
4.0	0.629e-02	-0.123e-02	-0.337e+05	-0.722e+05
5.3	0.467e-02	-0.117e-02	-0.129e+06	-0.711e+05
6.7	0.317e-02	-0.105e-02	-0.223e+06	-0.703e+05
8.0	0.186e-02	-0.875e-03	-0.317e+06	-0.698e+05
9.3	0.833e-03	-0.633e-03	-0.409e+06	-0.695e+05
10.7	0.172e-03	-0.329e-03	-0.502e+06	0.679e+05
12.0	-0.439e-04	-0.855e-04	-0.228e+06	0.170e+06
13.3	-0.564e-04	0.668e-05	-0.483e+05	0.898e+05
14.7	-0.261e-04	0.190e-04	0.112e+05	0.238e+05
16.0	-0.566e-05	0.102e-04	0.152e+05	-0.154e+04
17.3	0.120e-05	0.276e-05	0.713e+04	-0.511e+04
18.7	0.171e-05	-0.143e-06	0.159e+04	-0.279e+04
20.0	0.814e-06	-0.572e-06	-0.303e+03	-0.769e+03
21.3	0.186e-06	-0.317e-06	-0.461e+03	0.303e+02
22.7	-0.319e-07	-0.891e-07	-0.223e+03	0.153e+03
24.0	-0.518e-07	0.246e-08	-0.521e+02	0.865e+02
25.3	-0.254e-07	0.171e-07	0.800e+01	0.248e+02
26.7	-0.607e-08	0.983e-08	0.139e+02	-0.400e+00
28.0	0.830e-09	0.286e-08	0.694e+01	-0.459e+01
29.3	0.156e-08	-0.148e-10	0.170e+01	-0.268e+01
30.7	0.790e-09	-0.513e-09	-0.204e+00	-0.795e+00
32.0	0.198e-09	-0.304e-09	-0.421e+00	-0.430e-02
33.3	-0.207e-10	-0.918e-10	-0.216e+00	0.137e+00
34.7	-0.471e-10	-0.143e-11	-0.551e-01	0.829e-01
36.0	-0.246e-10	0.152e-10	0.517e-02	0.256e-01
37.3	-0.657e-11	0.914e-11	0.131e-01	0.670e-03
38.7	-0.192e-12	0.246e-11	0.695e-02	-0.474e-02
40.0	0. e+00	0. e+00	0.433e-03	-0.489e-02

COVER DESIGN BY ALDO GIORGINI